This is to certify that the
thesis entitled

UNDERSTANDING THE STRUCTURE OF YSCF, THE TYPE III SECRETION PROTEIN FROM *YERSINIA* AND HOW IT FORMS PILI

presented by

Joel Sanya Lwande

has been accepted towards fulfillment
of the requirements for the

Ph.D degree in Biochemistry and Molecular Biology

William J. Wedemeyer
Major Professor's Signature

13 August 2010
Date

MSU is an Affirmative Action/Equal Opportunity Employer

UNDERSTANDING THE STRUCTURE OF YSCF, A TYPE III SECRETION PROTEIN FROM *YERSINIA* AND HOW IT FORMS PILI

By

Joel Sanya Lwande

A DISSERTATION

Submitted to
Michigan State University
in partial fulfillment of the requirements
for the degree of

DOCTOR OF PHILOSOPHY

Biochemistry and Molecular Biology

2010

ABSTRACT

UNDERSTANDING THE STRUCTURE OF YSCF, A TYPE III SECRETION PROTEIN FROM *YERSINIA* AND HOW IT FORMS PILI

By

Joel Sanya Lwande

Pathogenic bacteria of the genus *Yersinia* inject effector proteins into mammalian host cells to interfere with the host immune response, thereby enabling the pathogens to thrive. The effector proteins are translocated through an extracellular, hollow needle structure that forms part of the Type III Secretion System (T3SS). The needle is made up of many copies of a single protein called YscF. The needle is anchored by interactions with the T3SS base, which is embedded in the inner and outer bacterial membranes.

In this thesis, we look for YscF residues that are likely to interact between the needle and the base in *Y. pseudotuberculosis*. We used multiple sequence alignment, secondary-structure prediction, homology modeling, and the crystal structures of YscF, in complex with YscE and YscG, and homologous proteins BsaL, MxiH, and PrgI. We identified the YscF residues Y65, N66, K76, D77, I82, Q84 and F86 as potential residues interacting with the base in *Y. pseudotuberculosis*. We used site-directed mutagenesis, circular dichroism spectroscopy and transmission electron microscopy to analyze the role of these residues in YscF structure and needle assembly *in vitro*. This work also analyzed the role of the 19 N-terminal residues in YscF needle assembly. Finally, we used a GFP-YopQ hybrid protein to analyze the role of these residues in YopQ secretion, both in a YscF knockout strain and in wild-type *Y. pseudotuberculosis*.

Our results show that the 19 N-terminal residues of YscF are not required for needle assembly. Circular dichroism spectroscopy shows that seven YscF variants (Y65A, N66A, K76A, D77A, I82A, Q84A and F86A) are α-helical, whereas Y65F seems to be unstructured. Our results also show that the YscF mutations resulting in N66A and Y65F abolish needle assembly *in vitro*, whereas the mutations resulting in K76A, D77A, I82A, Q84A and F86A have little effect. The rate of needle assembly in Y65A is very slow compared to that of wild-type. Three YscF variants (Y65A, Y65F and I82A) did not reconstitute GFP-YopQ secretion in the YscF knockout strain; however, the remaining mutants reconstituted secretion in the knockout strain. Our secretion assays also show that mutations resulting in variants Y65A and Y65F have a dominant-negative phenotype for secretion; the Y65A and Y65F variant proteins inhibit secretion of GFP-YopQ in wild-type *Y. pseudotuberculosis*. Based on these results, residues Y65 and N66 are likely to be involved in the pilin-pilin interactions, although it seems likely that the pilin-pilin interactions are less disrupted by mutations of N66 than by mutations of Y65. The YscF residue I82 is likely to be nonessential in YscF monomer folding and pilus assembly (pilin-pilin interactions) because the I82A mutation has little effect on needle assembly. However, since the I82A variant inhibits GFP-YopQ53 secretion and I82 is strictly conserved, this residue likely makes a critical interaction for secretion and, in particular, may be involved in the needle-base interface.

ACKNOWLEDGEMENTS

This work is a result of great effort and dedication that would not have been possible without support from people who surrounded me. I thank my wife Jane for helping me throughout the difficult moments I encountered in the course of my research. I express my heartfelt gratitude to my mentor Dr. William Wedemeyer who guided and supported me until completion of this project. His patience and dedication kept me focused even in times of immense pressure. It was a great privilege to work in your lab. I was lucky to work with great lab mates and friends: Terry, Kai-Chun, Amy, Kelly, and Jason. I will forever cherish the comfort and happiness you provided in that lab environment. I also thank my uncle Dr. Wilber Lwande for helping me follow this direction in life. Thank you for believing in me and providing me with the opportunity to pursue my dream.

My sincere thanks go to my guidance committee members: Dr. Dean DellaPenna, Dr. Leslie Kuhn, Dr. Honggao Yan and Dr. Michael Bagdasarian for providing me with great support. I give special thanks to Dr. Michael Bagdasarian for helping me with research facilities and teaching me a lot of microbiology work. I thank Dr. Alicia Pastor-Lecha for teaching me Transmission Electron Microscopy. I appreciate the help I got from the department of Biochemistry at MSU and thank the graduate director, Dr. Jon Kaguni and chair, Dr. Tom Shakey for their support.

Finally, I thank my special friends and family: Peter Sande, Betty Okwako, David Maina, and Salmon Aguko

TABLE OF CONTENTS

Images in this dissertation are presented in color

LIST OF TABLES

LIST OF FIGURES

ABBREVIATIONS

ATP	adenosine triphosphate
BHI	brain-heart infusion
BsaL	type III secretion system pilin from *Burkholderia*
CD	Circular dichroism
Δ19YscFΔ4	YscFΔ4 with 19 N-terminal residue truncation
EDTA	Ethylenediaminetetraacetic acid
EGTA	ethylene glycol tetraacetic acid
FLP	Flippase recombinase
FRT	FLP recognition target
GFP-YopQ18	Green Fluorescent Protein-YopQ18 hybrid protein
GFP-YopQ53	Green Fluorescent Protein-YopQ53 hybrid protein
GnHCl	guanidine hydrochloride
His_6-tag	Histidine tag
IPTG	isopropyl-β-D-thiogalactopyranoside
MALDI-TOF	Matrix-assisted laser desorption/ionization – time of flight
MxiH	type III secretion system pilin from *Shigella*
NIAID	National Institute of Allergy and Infectious Diseases
PCR	Polymerase Chain Reaction
PDB	Protein Data Bank
PrgI	type III secretion system pilin from *Salmonella*
pYscFΔ4	pET22b containing the YscFΔ4 gene

SDS-PAGE	sodium dodecyl sulfate polyacrylamide gel electrophoresis
T3SS	type III secretion system
TCA	Trichloroacetic acid
TEM	transmission electron microscopy
TPR	tetratrico peptide repeat
Yops	*Yersinia* outer proteins
Ysc	Yop secretion
YscF	type III secretion system pilin from *Yersinia*
YscFΔ4	YscF with 4 C-terminal residue truncation
YscEFG	YscF in complex with YscE and YscG chaperones

Chapter 1

Introduction

INTRODUCTION TO *YERSINIA PESTIS* AND PLAGUE

Y. pestis is a Gram-negative bacterium that causes bubonic, pneumonic and septicemic plague and is classified as a Category A priority pathogen by the National Institute of Allergy and Infectious Diseases (NIAID). During the Middle Ages, the plague was pandemic from Europe to China and killed approximately one-third of Europe's population (~25 million) within a five-year span (1347-1351) (1). *Y. pestis* is still found in the developing world and is a potential weapon of bioterrorism and biowarfare (2). Although *Y. pestis* is generally susceptible to antibiotics such as streptomycin and chloramphenicol, partially resistant strains have been isolated from nature (3) and fully resistant strains may be developed by design. Hence, there is an urgent need to identify drug targets that are necessary for pathogenesis and against which the bacterium will be unlikely to develop resistance. Other bacterial species closely related to *Yersinia* within the family *Enterobacteriaceae* include well-known pathogens such as *Shigella dysenteriae*, *Salmonella typhi* and *Eschericia coli*.

Yersinia is an eleven-species genus in the family Enterobacteriaceae. Only 3 of the 11 *Yersinia* species are human pathogens: *Y. pestis, Y. pseudotuberculosis* and *Y. enterocolitica* (4). *Y. pestis,* and *Y. pseudotuberculosis* are closely related to each other based on their chromosomal DNA sequence, but not as closely related to *Y. enterocolitica* (5, 6). Earlier suggestions were raised to classify *Y. pestis* as a subspecies of *Y. pseudotuberculosis,* but this has not been implemented because of public health

safety and unique laboratory and historical considerations linked with plague (5, 7).

Historically, the global pandemic caused by both bubonic and pneumonic plague is much greater than other infectious diseases (4). Throughout recorded history, almost 200 million deaths have been attributed to plague (8). The disease can occur in any one of the three primary forms: bubonic, septicemic or pneumonic (4). The classic form of plague is bubonic and is characterized by many symptoms including fever, headache, chills, swollen and extremely tender lymph nodes (buboes) within 2-6 days of infection (4). These infections can be treated successfully with antibiotics, especially streptomycin (9). There have been attempts to develop vaccines, but some of the existing vaccines cause an adverse reaction in significant percentage of vaccinees and sometimes the reactions can be severe (10). Experimental evidence has shown that the plague vaccine does not protect against pneumonic plague (11). The plague has a complex life cycle that makes it extremely difficult to eradicate (4).

Three major pandemics have occurred, causing major calamities. The first, second and third pandemics occurred in A.D. 541 – 544 (12, 8, 13), A.D. 1347 – 1351 (1, 14) and 1855 – 1918 (15, 16, 8, 17) respectively. The mortality rates and outbreaks have since reduced because of good public-health measures and antibiotics (4). Plague affects rodents primarily, but the *Y. pestis* pathogen can be transmitted between rodents and humans by fleas that acquire it from an infected blood meal (4). Following ingestion of an infected blood meal, bacteria may grow into masses that block the gut of the flea after 3-9 days. This

prevents ingested blood from reaching the stomach (18, 19, 20, 21, 22, 23). During feeding, the blood sucked from the host can mix with the pathogen and is then regurgitated into the host (19, 22). Although not all blocked fleas transmit the disease, blockage is central to successful transmission (24, 22, 25). The pathogen moves from the site of the bite to local lymph nodes, thereby multiplying and leading to formation of bubo (swollen lymph nodes) (4). The infection enters the bloodstream, at which point some pathogens are removed in the spleen and liver; however, the bacteria continue to grow and spread in the blood and other organs (4). Bubonic plague can then lead to secondary pneumonic plague, which becomes highly contagious due to respiratory droplets. This scenario can trigger an epidemic because of the human-human transmission (26, 17).

1. The type III secretion system (T3SS)

1.1 Yersinia type III secretion system

The type three secretion system (T3SS) (Figure 1.1) is a unique device known as the injectisome. The injectisome is used by many Gram-negative bacteria to translocate proteins across lipid membranes and also deliver effector proteins into the cytosol of the host cells (27). Following their delivery into host cells, these Yops affect signal transduction pathways that control phagocytosis, apoptosis, the actin cytoskeleton, and the inflammatory response, thereby helping the pathogen to survive (28). A properly assembled injectisome consists of approximately 25 proteins. Although the functions and positions of some of

these proteins have been determined, most of them are yet to be defined (27). The genes encoding the secretion machinery are organized in three operons, *virA* (*lcrDR* genes), *virB* (*yscNOPQRSTU* genes) and *virC* (*yscABCDEFGHIJKL* genes) (29). The T3SS can be divided into three different regions: (i) the translocon, (ii) the needle, and (iii) the base.

1.2 The translocon

The T3SS is used by many Gram-negative bacteria like *Yersinia* spp., *Burkholderia* spp., and *Shigella* spp. to translocate effector proteins into host cells (30, 31, 27). The delivery of *Yersinia* outer proteins (Yops) into host cells involves two processes aimed at overcoming the membrane barriers: (a) secretion involving extracellular release of Yops through the bacterial membrane barrier and (b) translocation involving delivery of Yops into the host cell cytosol through the host cell membrane barrier (32, 33). The three structural parts of the T3SS work in a well-coordinated fashion to accomplish the task (34).

Effector proteins are released when the pathogen comes into contact with a host cell in a well-regulated way at the translocon (34). Secretion can also occur *in vitro* under conditions that resemble the host environment. In *Yersinia*, many proteins play a role in this kind of regulation by enabling the pathogen-host cell contact. Some of the *Yersinia* regulatory factors involved in this process include: SycN, YscB, LcrG, YopN, and TyeA (35-39). It has been suggested that these regulation occurs in the bacterial cytosol because only two (YopN and LcrG) of these regulatory proteins are secreted (40, 41). Due to the regulatory

role played by these proteins, uncontrolled secretion occurs when regulatory proteins are mutated (42, 37).

In *Yersinia,* a translocon is a pore that is formed by the pathogen in the host cell membrane to enable delivery of Yops to the host-cell cytoplasm. This pore is made by three proteins: LcrV, YopB, and YopD under the control of the translocation regulatory proteins called the translocators (43-48). LcrV is hydrophilic and located at the tip of the needle where it forms a multi-subunit complex (49) required for the translocon build-up. Unlike LcrV, YopB, and YopD are hydrophobic and embedded in the host cell membrane where they form the translocon (50, 51). Translocation of Yops into host cell cytosol cannot occur without these three proteins (47, 52, 53), although extracellullar release of the effector proteins can still occur without them. In their work, Davis *et al.* (34) identified *yscF* mutants that were specifically altered in translocation but not in Yop secretion or needle assembly. Their results showed that YscF functions in Yop secretion and translocation can be genetically separated.

1.3 The base

The *Yersinia* T3SS is made up of Ysc (Yop secretion) injectisome involved in Yop secretion and translocation (54). The genes encoding the Yops and the secretion system are located on a large virulence plasmid, known as pYV (55). A total of 27 Ysc proteins make up this complex of two pairs of rings. The first ring is embedded in the inner bacterial membrane while the other is in the outer bacterial membrane. This pair of rings forms the base of the T3SS complex. The

two rings are linked by a hollow needle of 10 nm diameter and 60 nm length that protrudes on the outside of the bacterial membrane (56-58). The function of some Ysc proteins in the base has been defined, although much is still unknown.

The length of the *Yersinia* needle is determined by YscP (59), a protein that belongs to the base of the injectisome complex. It was proposed that YscP acts as a molecular ruler during the stepwise assembly of the injectisome (60). They hypothesized that one end of YscP is attached to the basal body while the other end is connected to the growing tip of the needle. The needle grows by addition of YscF at the tip. When the needle reaches its mature length, YscP would be fully stretched and signal, via its internal anchor, to the secretion apparatus, which would stop exporting YscF and switch to other substrates (59). As part of the base, the YscR/S/T group of proteins resembles flagellar proteins FliP/Q/R that form a membrane channeling structure (60). These three proteins are embedded in the inner bacterial membrane (61). Two other proteins, LcrD and YscU in the *Yersinia* injectisome play a role in rod formation. YscU is in the inner bacterial membrane just like YscR/S/T. The rod is thought to act as a link between proteins in the two bacterial membranes just like the P rod in flagellum structure (61). YscJ is a lipoprotein involved in the *Yersinia* T3SS-dependent secretion. It is also connected to other proteins in both the inner and outer bacterial membranes (61). Like YscP, YscU plays a role in regulation of effector and YscF secretion and is located in the inner bacterial membrane (61). The injectisome also has a cytoplasmic protein YscN with an ATP binding motif resembling the ß-subunit of F_0F_1-ATPase (61). This is the energy source for the

apparatus (27). Another protein required for effector secretion is YscO and it is a mobile component of the T3SS (61). YscQ is a peripheral cytoplasmic protein that interacts with YscK and YscL (61).

YscC is an outer membrane protein that exists as a stable oligomeric complex in the outer membrane of the bacterium (55). The YscC protein of *Y. enterocolitica* was isolated as a stable multimeric complex with an apparent molecular weight of 600 kDa in the outer membrane (55). They showed the YscC complex in a ring-shaped structure of ~ 20 nm with an apparent central pore. The study also showed that YscC plays a central role in the export of the Yop proteins. It is an outer membrane component of the Yop secretion machinery of *Yersinia*. YcsC seems to be in clear contact with the needle protein (YscF). The *virG* gene also results in products that improve the overall response and speed of the secretion process (62). It has been suggested that the VirG lipoprotein interacts with YscC in the bacterial outer membrane (62).

1.4 The needle

The needle is a hollow tube protruding from the injectisome base in the bacterial membrane to the exterior. In *Yersinia,* the needle is a result of polymerization of a major subunit called YscF (63). The needle length is between 45 and 80 nm depending on the *Yersinia* species, but the interior diameter is 2.5 nm (27). Extension of the needle length in *Yersinia* is controlled by YscP, as described above (59).

2. *Yersinia* outer protein secretion (Yop secretion)

2.1 T3SS chaperones

Some of the T3SS proteins act as chaperones to prevent premature folding or the wrong protein-protein interaction. The hydrophilic translocator LcrV acts as an extracellular chaperone that guides the two hydrophobic translocators, YopB and YopD, to integrate in the eukaryotic plasma membrane (64, 65). Secretion of some, but not all, T3S substrates requires the assistance in the bacterial cytoplasm of a particular type of chaperones (65). These chaperones are mostly acidic proteins with low molecular mass ~ 15 kDa. Each chaperone enables proper secretion of its cognate substrate (65). SycE (66) is one such chaperone and it binds YopE. In absence of the chaperone, YopE is unstable and is rapidly degraded. SycE masks an aggregation-prone region of YopE (67) and was also shown to be necessary for YopE recognition by the secretion system (68, 69). As "chaperones", YscG and YscE interact with YscF to prevent it from premature polymerization in the cytosol of the bacterium prior to assembly of the needle (70).

3. T3SS needle protein structures

3.1 MxiH and BsaL

Structural determination of T3SS needle proteins has remained difficult because they tend to readily polymerize into much larger structures. Only three structures have been solved including MxiH (Figure 1.2), BsaL (Figure 1.3), and PrgI (Figure 1.4) (71, 72 and 73), although the YscF structure has also been

solved in complex with the heterodimeric chaperone YscE/YscG (Figure 1.5). Determination of MxiH, BsaL and PrgI structures involved some modifications in form of truncation of the last five C-terminal residues and addition of a His_6-tag to the C-terminus. These modifications increased the solubility of those proteins while preventing their self-oligomerization. The reported crystal structure of the *Shigella flexneri* T3SS needle subunit MxiH (Figure 1.2) (71) and the nuclear magnetic resonance structure of *Burkholderia pseudomallei* T3SS needle subunit BsaL (1.3) (72) have contributed important information towards further understanding of the T3SS. Both MxiH and BsaL are YscF homologs based on the multiple sequence alignment with each having a 30% sequence identity to YscF. This thesis predicts YscF secondary structure using four different programs (namely PsiPRED, SAM, PROFsec and SABLE2). The results suggest the possibility of four α-helices which we will denote here as α_1, α_2, α_3 and α_4 (Figure 1.6).

Two of the four predicted YscF helices (α_2 and α_3) align well with the two reported core helices in both MxiH (Figure 1.2) and BsaL (Figure 1.3). The structure of MxiH consists of two long anti-parallel helices (corresponding to our predicted α_2, α_3 and α_4 helices of YscF) connected by a short Pro-Ser-Asn-Pro (PSNP) turn. The structure of BsaL has a similar helix-turn-helix core domain with two well-defined α-helices that are joined by a PSDP linker. The two helices also correspond to our predicted α_2 and α_3 helices of YscF. The tetrapeptide P-(S/D)-(D/N)-P is conserved among four YscF homologs (71) namely, BsaL, MxiH, PrgI (*S. typhimurium*) and EprI (*E. coli*) with YscF having Pro-Asp-Asn-Pro

(PDNP). Thus, there is a high probability that YscF forms an α-helical hairpin centered on this tetrapeptide.

Although MxiH had been strongly predicted to form a helix α_1 at the N-terminus (74), this prediction disagreed with the crystal structure in which the N-terminus is disordered. Two possible explanations (71) were suggested for this outcome: the truncated C-terminal residues might be essential for N-terminal helix formation; or this region becomes folded only within the intact needle, possibly in response to environmental factors. Based on these findings, Deane *et al.* (71) generated a model of the *Shigella* T3SS needle by docking the crystal structure for MxiH into the 16 Å density map from their earlier three-dimensional EM reconstruction of the needle (75). This study shows that the C-terminal helix forms the outer shell of the needle core, whereas the PSNP loop directs the N-terminal helix to line the inner wall of the needle channel. Their model shows that the C terminus of MxiH is involved in extensive inter-subunit contacts. They also suggested that this interaction is important for needle stability because polymerization was blocked following truncation of the last 5 residues of MxiH. In their analysis of the interface between two subunits, the patch of the α_2 residues L30, L34, A38, and Y50 on the head of one subunit contacts the patch of the α_4 residues D73, D75, I78, I79, and Q80 on the tail of another subunit.

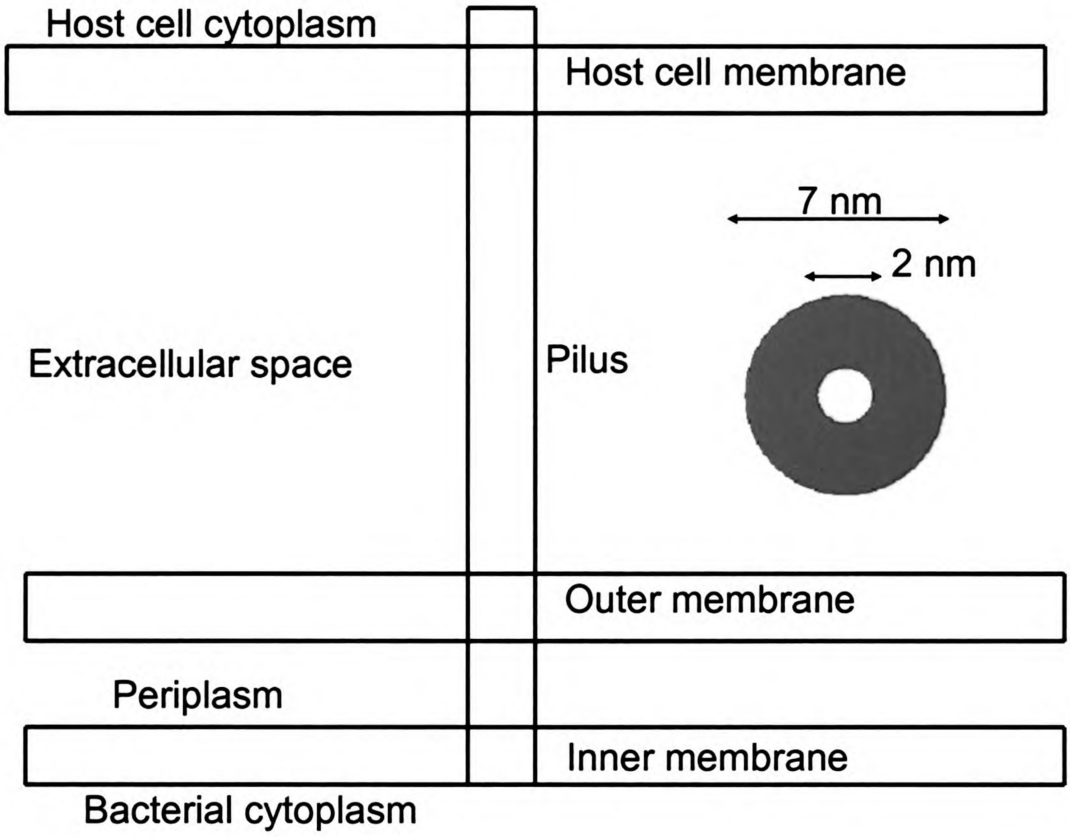

Figure 1.1. A schematic diagram of a type III secretion apparatus showing the width of the hollow needle and the membranes of the bacterium and the host cell.

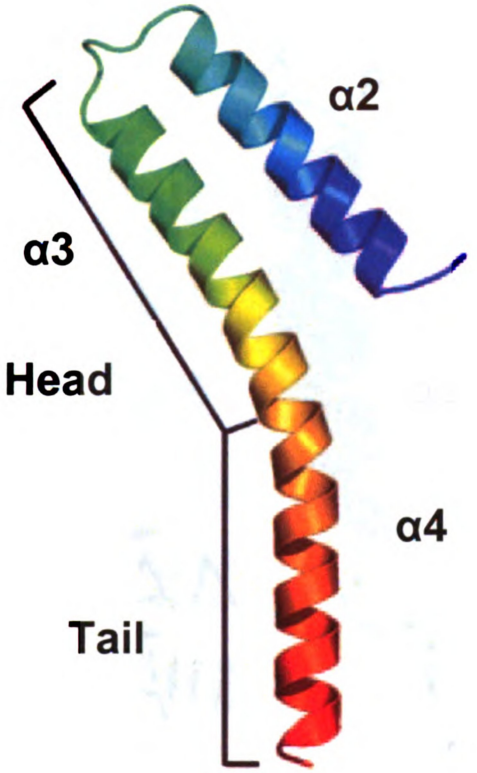

Figure 1.2. The crystal structure of the MxiH monomer. Two long anti-parallel helices connected by a short Pro-Ser-Asn-Pro (PSNP) turn. (Deane *et al.*) (71).

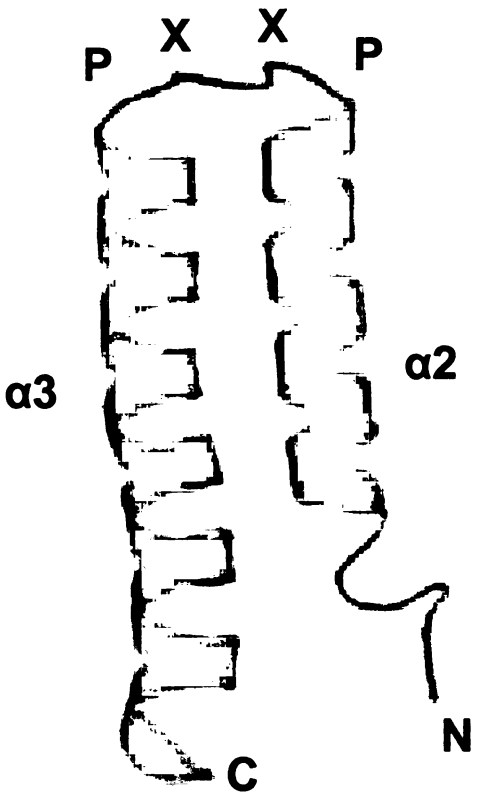

Figure 1.3. The NMR structure of BsaL showing the helix-turn-helix core domain with two well-defined α-helices that are joined by a PSDP linker (Zhang *et al.*) (72).

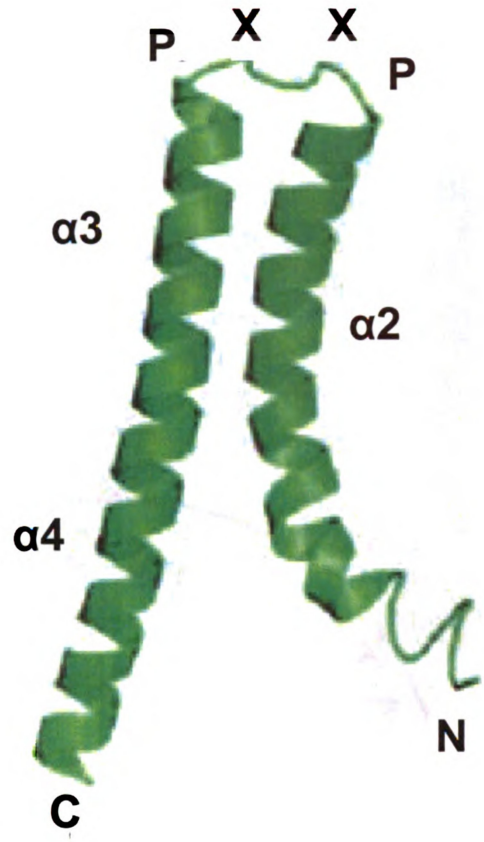

Figure 1.4. PrgICΔ5 forms a two helix bundle stabilized by hydrophobic contacts at the helix α2- α3 interface. (Wang *et al.*) (73).

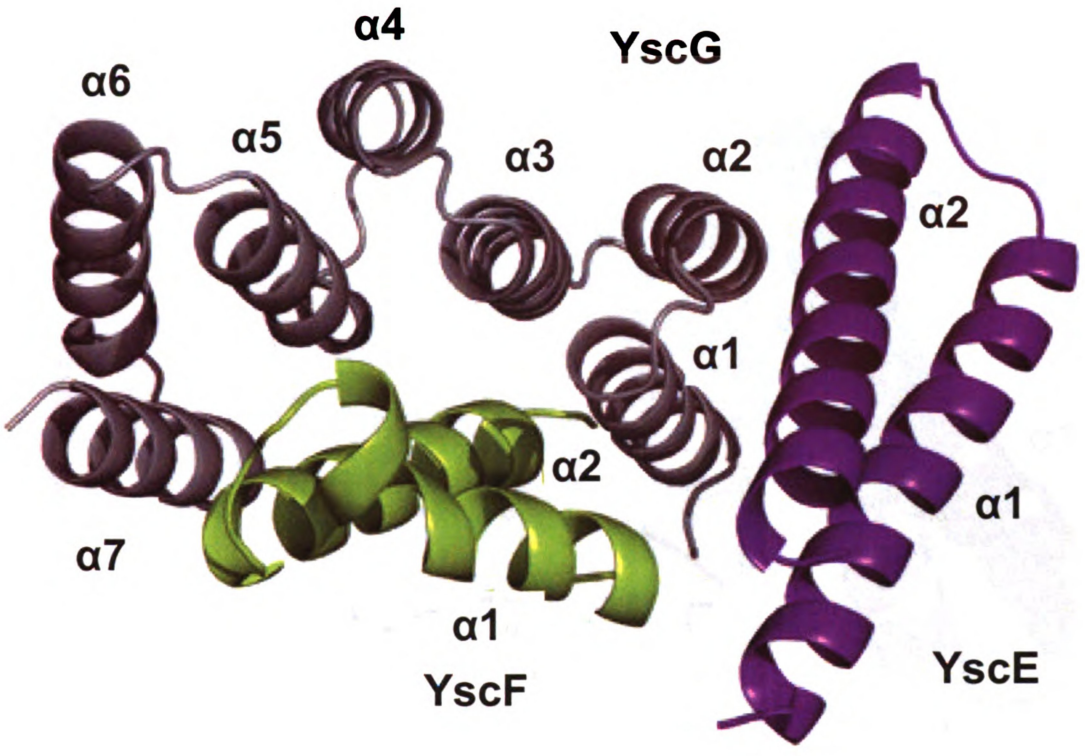

a

Figure1.5. (a) Ribbon representation of the overall structure of the YscEFG complex. YscE, YscF and YscG are colored purple, lime and grey, respectively. (b) Ribbon representation of the overall structure of the YscEFG complex after a 90° rotation. (Sun *et al.*) (76).

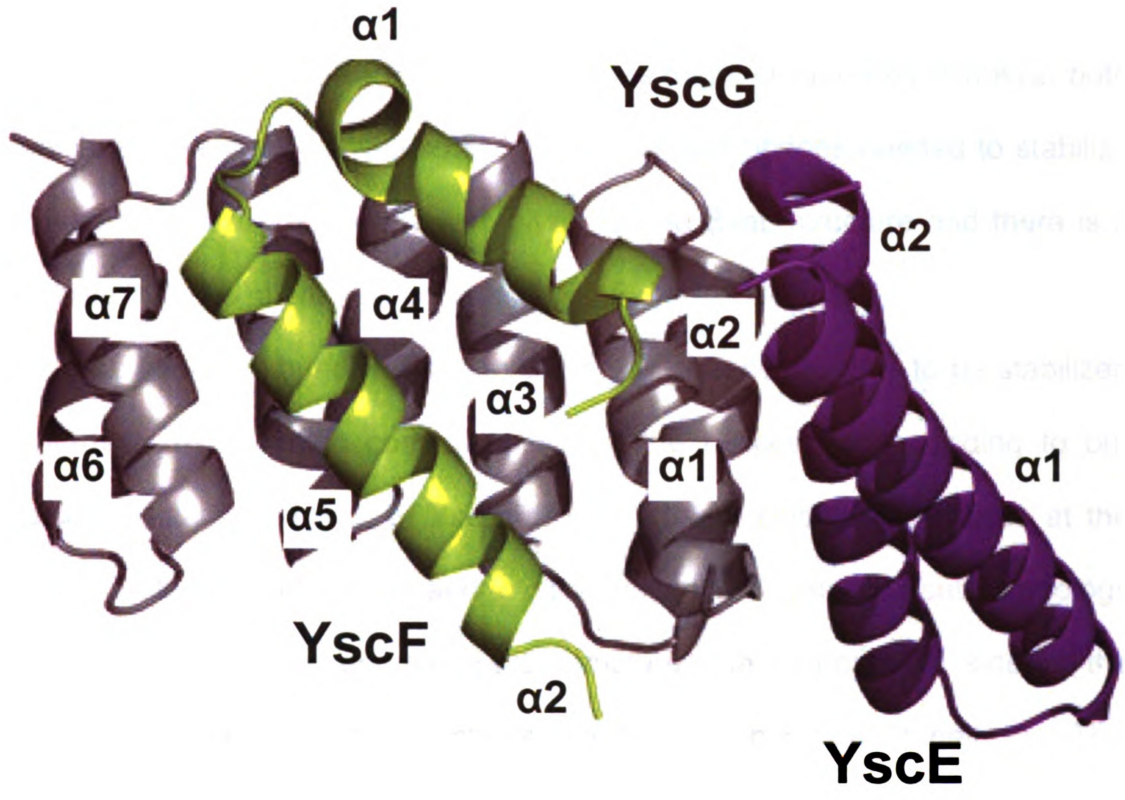

b

Figure 1.5 (cont'd)

The tail region (residues 58 to 83 of α_4) of MxiH has well conserved hydrophobic and polar residues namely, L59, Y60, A63, T67, V68, V74, I78, I79, F82 (hydrophobic) and N62, Q64, S65, K69, K72, D73, Q80, N81 (polar). This part of the C-terminal helix does not participate in the α_2-α_3 interhelix interactions, meaning that the hydrophobic residues listed above are exposed in monomeric MxiH. There is a high possibility that these residues are buried (shielded from the solvent) during needle formation. Only D73, I78, I79, and Q80 are reported to participate in MxiH-MxiH (tail to head) interaction. While some of these residues might be involved in lateral MxiH-MxiH interaction during needle formation,

others are presumably involved in interactions at the interface between MxiH and other proteins in the T3SS base. Such residues might include K69 and K72, both of which are likely to be involved in formation of salt bridges needed to stabilize the needle. This explanation is also given for the BsaL structure and there is a possibility that this might also be true for YscF.

The two-helix bundle structure of BsaL was reported (72) to be stabilized by interhelix hydrophobic contacts between the helices corresponding to our predicted α_2 and α_3 helices of YscF. In BsaL, these stabilizing residues at the interface between helices α_2 and α_3 are conserved among BsaL homologs including YscF. In the reported BsaL structure, the hydrophobic side of the amphipathic helix α_2 directly contacts the hydrophobic side of helix α_3. This interface involves interactions of Leu32, Leu36, Ala39, and Leu43 of helix α_2 with Tyr63, Met60, Ile59, Tyr56, Leu53, and Ala52 of helix α_3. In their paper, Zhang *et al.* reported that Asn 68 is conserved among needle proteins including YscF, but does not participate in contacts at the helix α_2-α_3 interface. They suggested that this residue might be involved in functions other than stabilizing the core domain, such as the interaction between BsaL and other T3SS proteins of the base. This residue corresponds to N66 in YscF. There is a possibility that N66 of YscF participates in the interactions at the needle-base interface. Based on chemical shifts, the first seven residues of BsaL were reported to be unstructured while the regions flanking the well-defined core domain (Ala10 to Gly28 at the N terminus and Ser71 to Ile84 at the C terminus) are in partial-helical conformations.

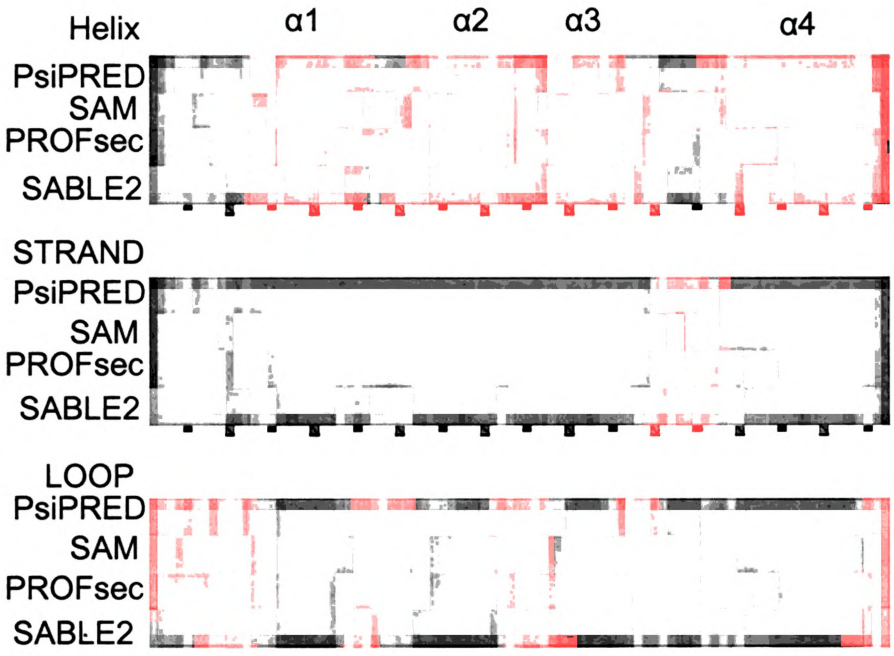

Figure 1.6. Secondary structure predictions for YscF by four different methods, PsiPRED, SAM, PROFsec and SABLE2. Four helices are predicted (structured regions of the sequence are highlighted in red).

3.2 YscEFG complex

The recently determined crystal structure of the YscEFG protein complex (Figure 1.5) (76) shows that YscG binds tightly to the C-terminal half of YscF, implying that it is this region of YscF that controls its polymerization into the needle structure (76). The structure shows that YscE interacts with YscG, but makes very little direct contact with YscF. In the crystal structure, they could not observe electron density for the N-terminal 49 residues of YscF. This and additional evidence from their study suggest that the N-terminal region of YscF is disordered in the complex with YscE and YscG.

The structure shows that conserved residues in the C-terminal half of YscF mediate important intra- and inter-molecular interactions in the complex. The final YscEFG model consists of 204 amino acids, including residues 10–63 of YscE, 50–87 of YscF and 3–114 of YscG. YscF is bound within the hydrophobic groove of YscG generated by nonpolar residues. The crystal structure shows hydrophobic residues on the concave surface of YscG (Val7, Ala10, Leu14, Ala40, Leu43, Leu70, Pro72, Trp73, Leu76, Tyr79, Met109, and Phe105) interacting with hydrophobic residues on YscF (Asn66, Ile71, Met75, Met78, Met79, Ile82, Leu83, and Phe86). In the complex, YscF is reported to have two α-helices connected by a 5 residue loop (Ile64-Asn68). In addition to the numerous hydrophobic interactions between YscF and YscG described in their findings, hydrophilic interactions also seem to play an important role in maintaining the conformation of YscF within the complex.

The loop in YscF is well-ordered and stabilized by a hydrogen bond with YscG. Additionally, the side chains of Tyr79 and Arg80 from the 3rd TPR (tetratrico peptide repeat) motif of YscG and that of Gln112 from the C-terminal α-helix of YscG form hydrogen bonds with the main chain constituents of the loop residues in YscF. The side chain of YscF residue Asn68 forms a hydrogen bond with Gly108 of YscG. They also show that the hairpin loop between the two α-helices in YscF is further stabilized by intramolecular hydrogen bonds between Oε of Gln55 and Nζ of Lys76, Nε of Gln55 and Oδ of Asn59, and Nζ of Lys76 and Oε of Gln80. Based on the structure, they suggest that intramolecular hydrogen bond "bridge" between highly conserved Gln55 and Lys76 in YscF may play an

important role in maintaining the helical hairpin fold of YscF. They concluded that the α-helical hairpin conformation of YscF in the YscEFG complex may be an accurate representation of the biologically relevant structure. Several experiments in the report showed that the N-terminal 49 residues of YscF are present and disordered in the structure of the heterotrimer.

3.3 YscF

In this work, we modeled YscF (Figure 1.7) based on the crystal structure of MxiH. We compared the YscF model to the three T3SS needle structures (MxiH, BsaL and PrgI) and the YscEFG complex. The following is a list of selected YscF residues located in the predicted tail region (α_4 helix in our model): V63, I64, Y65, N66, S69, R73, K76, D77, I82, L83, Q84 and F86. Conserved residues in YscF play different roles that together contribute to the proper functional mechanism of T3SS in *Yersinia*. These conserved residues are likely to fall under three different categories. The first category comprises residues that are likely to be important for the folding stability of YscF protein. These may include A30, S37 and L41 of helix α_2 and L50, L51, S57, I58 and W61 of helix α_3 likely to form the $\alpha_2 - \alpha_3$ interaction interface of the predicted structure. The second category could be crucial for the self oligomerization of the protein leading to the formation of the needle. These may include V34, I38, K42, D53, L54, and L83. Although four out of the six residues are hydrophobic, the polar residues K42 and D53 may also be necessary for "indexing" the two subunits relative to one another. A specific polar interaction is often observed in protein-

protein interface, since purely hydrophobic interfaces are "greasy" and tend to slide upon each other. The third category of the conserved residues is likely to be important for interaction at the needle-base interface. This interaction is likely to be important for proper linkage between the needle and the base. In this category, we predict a mixture of hydrophobic and polar residues. The polar residues may help in "indexing" the interface (keeping the interacting hydrophobic residues in place).

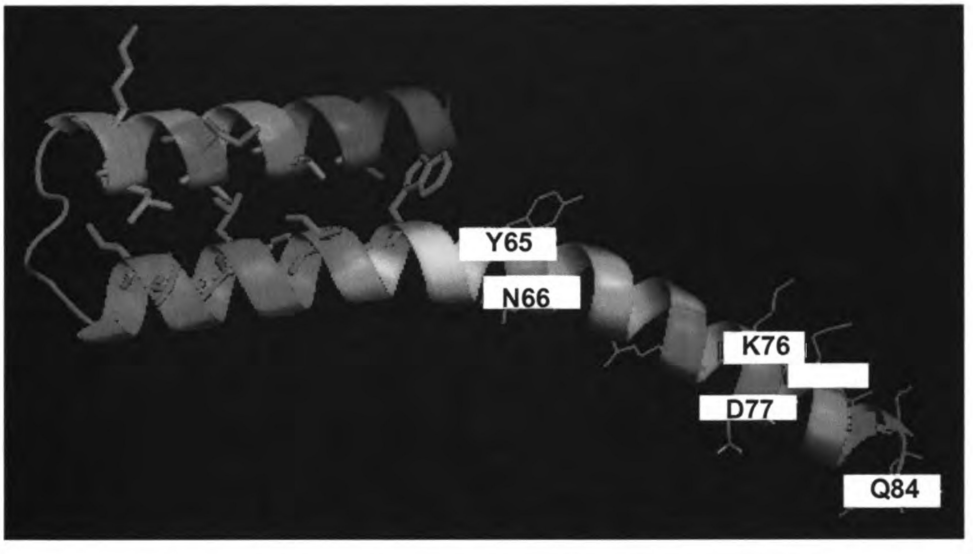

Figure 1.7. YscF homology model based on the MxiH crystal structure. Some of the selected conserved residues are shown on predicted α_2 and α3-α4 helices. Blue represents N terminus while red represents C terminus. Some of the residues are involved in $\alpha_2 - \alpha_3$ hydrophobic interactions to keep the two core helices close to each other.

CONCLUSIONS AND REMAINING QUESTIONS

A previous study (77) examined the effect of individual amino acid substitutions on the regulation of type III secretion by YscF. They targeted conserved residues for replacement by alanine. Alanine substitutions at two positions (Asp77 and Ile82) abolished the secretion of YscF. Based on the YscEFG structure (76), Sun *et al.* suggested that the highly conserved Ile82 residue is located at the interface between YscG and YscF and the mutant may therefore destabilize the interaction between them. They also concluded that Asp77 is a solvent-accessible residue on the outer surface of YscF in the heterotrimeric complex. Therefore, the secretion defect exhibited by this mutant is not the result of the failure to properly interact with its chaperones YscE/G in cytosol. Instead, most likely, mutation in D77 will influence the architecture between needle monomers. In this work, we suggest that these two residues (Ile82 and D77) might be important for interactions at the interface between YscF and YscC.

In the base of the *Yersinia* T3SS, YscC forms a ring in the outer membrane that seems to interact with the needle (78). This outer ring of the base is almost exclusively made of YscC. Indeed the *Yersinia* base has very few other proteins embedded in the outer membrane other than YscC. Almost all the other mentioned membrane proteins are embedded in the inner membrane of the base and two in the translocon. The presence of another structure called the rod linking the outer ring to the inner ring means that the needle originates from the outer ring (YscC) where it makes the needle-base interactions.

The aim of this work is to identify some conserved YscF residues that are likely to participate in the interaction at the needle-base interface. During needle formation, it is likely that YscF is released from the YscEFG complex enabling it to participate in new hydrophobic and hydrophilic interactions. The new interactions bury the interacting hydrophobic residues while maintaining the hydrogen bonding to form a stable needle structure. Some interactions are between YscF monomers (forming the needle) while others are between YscF and proteins in the base (linking the needle to the base).

We have carried out a study to show that individual replacement of some of the interacting residues (both hydrophilic and hydrophobic) with alanine does not prevent *in vitro* needle formation. While previous studies have focused mainly on secretion analysis, our study goes a step further by looking at both the *in vitro* needle formation and *in vivo* YopQ secretion by the mutated YscF. If a given mutant is able to form needles *in vitro* but prevents Yop secretion and *in vivo* needle formation, then we propose that such a residue participates in linking the needle to the base. We have used the information from the four available T3SS structures (71, 72, 73, and 76) and our preliminary *in vitro* needle assembly results to identify 7 YscF residues that are likely to be important for the interactions between the needle and the base. These residues include: Y65, N66, K76, D77, I82, Q84 and F86. All 7 amino acid residues in this study are within the C-terminal half of YscF and are within the reported YscEFG crystal structure.

REFERENCES

1. Gottfried, R. S. (1983) The Black Death. Natural and Human Disaster in medieval Europe. The Free Press, New York, N.Y.

2. Greenfield, R. A., Drevets, D. A., Machado, L. J., Voskuhl, G. W., Cornea, P., and Bronze, M. S. (2002) Bacterial Pathogens as Biological Weapons and Agents of Bioterrorism. *Am J Med Sci* **323,** 299-315.

3. Galimand, M., Guiyoule, A., Gerbaud, G., Rasoamanana, B., Chanteau, S., Carniel, E., and Courvalin, P. (1997) Multidrug Resistance in *Yersinia pestis* Mediated by a Transferable Plasmid. *N Engl J Med* **337,** 677-681.

4. Perry, D. R., and Fetherston, D. J. (1997) *Yersinia pestis*-Etiologic Agent of Plague. *Clin Microbiol Rev* **10,** 35-66.

5. Bercovier, H., Mollaret, H. H., Alonso, J. M., Brault, J., Fanning, G. R., Steigerwalt, A. G., and Brenner, D. J. (1980) Intra- and interspecies relatedness of *Yersinia pestis* by DNA hybridization and its relationship to *Yersinia pseudotuberculosis*. *Curr Microbiol* **4,** 225-229.

6. Brubaker, R. R. (1991) Factors promoting acute and chronic disease caused by yersiniae. *Clin Microbiol Rev* **4,** 309-324.

7. Wayne, L. G. (1986) Actions of the Judicial Commission of the International Committee on Systematic Bacteriology on requests for opinions published in 1983 and 1984. *Int J Syst Bacteriol* **36,** 357-358.

8. Duplaix, N. (1988) Fleas—the lethal leapers. *Natl Geogr* **173,** 672-694.

9. Meyer, K. F. (1950) Modern therapy of plague. *JAMA* **144,** 982-985.

10. Marshall, J. D., Jr., Bartelloni, P. J., Cavanaugh, D. C., Kadull, P. J., and Meyer, K. F. (1974) Plague immunization. II. Relation of adverse clinical reactions to multiple immunizations with killed vaccine. *J Infect Dis* **129,** (Suppl.):S19-S25.

11. Cohen, R. J., and Stockard, J. L. (1967) Pneumonic plague in an untreated plague-vaccinated individual. *JAMA* **202,** 365-366.

12. Biraben, J.-N., and Le Goff, J. (1975) The plague in the early middle ages, p. 48-80. In R. Forster and O. Ranum (ed.), Biology of man in history. The Johns Hopkins University Press, Baltimore, Md.

13. Russell, J. C. (1968) That earlier plague. *Demography* **5,** 174-184.

14. Ziegler, P. (1991) The black death. Alan Sutton Publishing Inc., Wolfeboro Falls, NH.

15. Barnes, A. M., and Quan T. J. (1992) Plague, p. 1285-1291. *In* S. L. Gorbach, Bartlett, J. G., and Blacklow, N. R. (ed.), Infectious diseases. The W. B. Saunders Co., Philadelphia, PA.

16. Butler, T. (1983) Plague and other *Yersinia* infections. Plenum Press, New York, N.Y.

17. Poland, J. D., Quan, T. J., and Barnes, A. M. (1994) Plague, p. 93-112. *In* G. W. Beran (ed.), Handbook of zoonoses. Section A. Bacterial, rickettsial, chlamydial, and mycotic, 2nd ed. CRC Press, Inc., Ann Arbor, MI.

18. Bacot, A. W. (1915) Further notes on the mechanism of the transmission of plague by fleas. *J Hyg* **14,** 774-776.

19. Bacot, A. W., and Martin, C. J. (1914) Observations on the mechanism of the transmission of plague by fleas. *J Hyg* **13,** 423-439.

20. Bahmanyar, M., and Cavanaugh, D. C. (1976) Plague manual. World Health Organization, Geneva, Switzerland.

21. Bibikova, V. A. (1977) Contemporary views on the interrelationships between fleas and the pathogens of human and animal diseases. *Annu Rev Entomol* **22,** 23-32.

22. Cavanaugh, D. C. (1971) Specific effect of temperature upon transmission of the plague bacillus by the oriental rat flea, *Xenopsylla cheopis*. *Am J TropMed Hyg* **20,** 264-272.

23. Wheeler, C. M., Suyemoto, W., Cavanaugh, D. C., Shimada, T., and Yamakawa, Y. (1956) Studies on *Pasteurella pestis* in various flea species. II. Simplified method for the experimental infection of fleas. *J Infect Dis* **98,** 107-111.

24. Burroughs, A. L. (1947) Sylvatic plague studies. The vector efficiency of nine species of fleas compared with *Xenopsylla cheopis*. *J Hyg* **45,** 371-396.

25. Kartman, L. (1969) Effect of differences in ambient temperature upon the fate of *Pasteurella pestis* in *Xenopsylla cheopis*. *Trans R Soc Trop Med Hyg* **63,** 71-75.

26. Poland, J. D., and Barnes, A. M. (1979) Plague, p. 515-559. *In* J. H. Steele (ed), CRC handbook series in zoonoses. Section A. Bacterial, rickettsial, and mycotic diseases, vol. I. CRC Press, Inc., Boca Raton, Fla.

27. Mota 1, L. J., Sorg, I., Cornelis, G. R. (2005) Type III secretion: The bacteria-eukaryotic cell express, *FEMS Microbiol Lett* **252,** 1-10.

28. Navarro, L., Alto N. M., Dixon, J. E. (2005) Functions of the Yersinia effector proteins in inhibiting host immune responses. *Curr Opin Microbiol* **8,** 21-27.

29. Koster, M., Bitter, W., de Cock, H., Allaoui, A., Cornelis, G. R., and Tommassen, J. (1997) The outer membrane component, YscC, of the Yop secretion machinery of *Yersinia enterocolitica* forms a ring-shaped multimeric complex. *Mol Microbiol* **26,** 789-797.

30. Ghosh, P. (2004) Process of protein transport by the type III secretion system. *Microbiol. Mol Biol Rev* **68,** 771-795.

31. He, S. Y., Nomura, K., and Whittam, T. S. (2004) Type III protein secretion mechanism in mammalian and plant pathogens. *Biochim Biophys Acta* **1694,** 181-206.

32. Rosqvist, R., Magnusson, K. E., and Wolf-Watz., H. (1994) Target cell contact triggers expression and polarized transfer of *Yersinia* YopE cytotoxin into mammalian cells. *EMBO J* **13,** 964-972.

33. Sory, M. P., and Cornelis, G. R. (1994). Translocation of a hybrid YopEadenylate cyclase from Yersinia enterocolitica into HeLa cells. *Mol Microbiol* **14,** 583-594.

34. Davis, A. J., and Mecsas, J. (2007) Mutations in the *Yersinia pseudotuberculosis* type III secretion system needle protein, YscF, that specifically abrogate effector translocation into host cells. *J Bacteriol* **189,** 83-97.

35. Iriarte, M., Sory, M. P., Boland, A., Boyd, A. P., Mills, S. D., Lambermont, I., and Cornelis, G. R. (1998) TyeA, a protein involved in control of Yop release and in translocation of Yersinia Yop effectors. *EMBO J* **17,** 1907-1918.

36. Jackson, M. W., Day, J. B., and Plano, G. V. (1998) YscB of *Yersinia pestis* functions as a specific chaperone for YopN. *J Bacteriol* **180,** 4912-4921.

37. Yother, J., and Goguen J. D. (1985) Isolation and characterization of Ca^{2+}-blind mutants of *Yersinia pestis*. *J Bacteriol* **164,** 704-711.

38. DeBord, K. L., Lee, V. T., and Schneewind, O. (2001) Roles of LcrG and LcrV during type III targeting of effector Yops by *Yersinia enterocolitica*. *J Bacteriol* **183,** 4588-4598.

39. Iriarte, M., and Cornelis, G. R. (1999) Identification of SycN, YscX, and YscY, three new elements of the *Yersinia* Yop virulon. *J Bacteriol* **181,** 675-680.

40. Ferracci, F., Schubot, F. D., Waugh, D. S., and Plano, G. V. (2005) Selection and characterization of *Yersinia pestis* YopN mutants that constitutively block Yop secretion. *Mol Microbiol* **57,** 970-987.

41. Nilles, M. L., Williams, A. W., Skrzypek, E., and Straley, S. C. (1997) *Yersinia pestis* LcrV forms a stable complex with LcrG and may have a secretion related regulatory role in the low-Ca^{2+} response. *J Bacteriol* **179,** 1307-1316.

42. Forsberg, A., Viitanen, A. M., Skurnik, M., and Wolf-Watz, H. (1991) The surface-located YopN protein is involved in calcium signal transduction in *Yersinia pseudotuberculosis*. *Mol Microbiol* **5,** 977-986.

43. Boland, A., Sory, M. P., Iriarte, M., Kerbourch, C., Wattiau, P., and Cornelis, G. R. (1996) Status of YopM and YopN in the *Yersinia* Yop virulon:YopM of Y. enterocolitica is internalized inside the cytosol of PU5-1.8 macrophages by the YopB, D, N delivery apparatus. *EMBO J* **15,** 5191-5201.

44. Hakansson, S., Schesser, K., Persson, C., Galyov, E. E., Rosqvist, R., Homble, F., and Wolf-Watz, H. (1996) The YopB protein of *Yersinia pseudotuberculosis* is essential for the translocation of Yop effector proteins across the target cell plasma membrane and displays a contact-dependent membrane disrupting activity. *EMBO J* **15,** 5812-5823.

45. Lee, V. T., Tam, C., and Schneewind, O. (2000) LcrV, a substrate for *Yersinia enterocolitica* type III secretion, is required for toxin targeting into the cytosol of HeLa cells. *J Biol Chem* **275,** 36869-36875.

46. Nordfelth, R., and Wolf-Watz, H. (2001) YopB of *Yersinia enterocolitica* is essential for YopE translocation. *Infect Immun* **69,** 3516-3518.

47. Pettersson, J., Holmstrom, A., Hill, J., Leary, S., Frithz-Lindsten, E., von Euler-Matell, A., Carlsson, E., Titball, R., Forsberg, A., and Wolf-Watz, H. (1999) The V-antigen of Yersinia is surface exposed before target cell contact and involved in virulence protein translocation. *Mol Microbiol* **32,** 961-976.

48. Rosqvist, R., Forsberg, A., and Wolf-Watz, H. (1991) Intracellular targeting of the *Yersinia* YopE cytotoxin in mammalian cells induces actin microfilament disruption. *Infect Immun* **59,** 4562-4569.

49. Mueller, C. A., Broz, P., Muller, S. A., Ringler, P., Erne-Brand, F., Sorg, I., Kuhn, M., Engel, A., and Cornelis, G. R. (2005) The V-antigen of Yersinia forms a distinct structure at the tip of injectisome needles. *Science* **310,** 674-676.

50. Neyt, C., and Cornelis, G. R. (1999) Insertion of a Yop translocation pore into the macrophage plasma membrane by *Yersinia enterocolitica*: requirement for translocators YopB and YopD, but not LcrG. *Mol Microbiol* **33,** 971-981.

51. Tardy, F., Homble, F., Neyt, C., Wattiez, R., Cornelis, G. R., Ruysschaert, J. M., and Cabiaux, V. (1999) Yersinia enterocolitica type III secretion-translocation system: channel formation by secreted Yops. *EMBO J* **18,** 6793-6799.

52. Fields, K. A., Nilles, M. L., Cowan, C., and Straley, S. C. (1999) Virulence role of V antigen of *Yersinia pestis* at the bacterial surface. *Infect Immun* **67,** 5395-5408.

53. Lee, V. T., and Schneewind, O. (1999) Type III machines of pathogenic yersiniae secrete virulence factors into the extracellular milieu. *Mol Microbiol* **31,** 1619-1629.

54. Cornelis, G. R. (2002) The Yersinia Ysc–Yop 'Type III' weaponry. *Nature Rev Mol Cell Biol* **3,** 742.

55. Koster, M., Bitter, W., de Cock, H., Allaoui, A., Cornelis, G. R., and Tommassen, J. (1997) The outer membrane component, YscC, of the Yop secretion machinery of Yersinia enterocolitica forms a ring-shaped multimeric complex. *Mol Microbiol* **26** (4), 789-797.

56. Kubori, T., Sukhan, A., Aizawa, S., and Gala´n, J. E. (2000) Molecular characterization and assembly of the needle complex of the Salmonella typhimurium type III protein secretion system. *PNAS* **97**(18), 10225-10230.

57. Kimbrough, T. G., and Miller, S. I. (2000) Contribution of Salmonella typhimurium type III secretion components to needle complex formation. *PNAS* **97**(20) 11008-11013.

58. Blocker, A., Jouihri, N., Larquet, E., Gounon, P., Ebel, F., Parsot, C., Sansonetti, P., and Allaoui, A. (2001) Structure and composition of the Shigella flexneri "needle complex" a part of its type III secreton. *Mol Microbiol* **39,** 652-663.

59. Journet, L., Agrain, C., Broz, P., and Cornelis, G. R. (2003) The Needle Length of Bacterial Injectisomes Is Determined by a Molecular Ruler. *Science* **302,** 1757-1760.

60. Aizawa, S.-I. (2001) Bacterial flagella and type III secretion systems. *FEMS Microbiol Lett* **202,** 157-164.

61. Tampakaki, A. P., Fadouloglou, V. E., Gazi, A. D., Panopoulos, N. J., and Kokkinidis, M. (2004) Conserved features of type III secretion. *Cellullar Microbiology* **6** (9), 805-816.

62. Allaoui, A., Sheen, R., Lambert de Rouvroit, C., and Cornelis, G. R. (1995) VirG, a Yersinia enterocolitica lipoprotein involved in the Ca^{2+} dependency is related to ExsB of pseudomonas aeruginosa. *J Bacteriol* **177,** 4230-4237.

63. Hoiczyk, E., and Blobel, G. (2001) Polymerization of a single protein of the pathogen Yersinia enterocolitica into needles punctures eukaryotic cells. *Proc Natl Acad Sci* USA **98,** 4669-4674.

64. Goure, J., Broz, P., Attree, O., Cornelis, G.R. and Attree, I. (2005) Protective anti-V antibodies inhibit *Pseudomonas* and *Yersinia* translocon assembly within host membranes. *J Infect Dis* **192,** 218-225.

65. Holmstrom, A., Olsson, J. and Cherepanov, P., Maier, E., Nordfelth, R., Pettersson, J., Benz, R., Wolf-Watz, H, and Forsberg, A. (2001) LcrV is a channel size-determining component of the Yop effector translocon of Yersinia. *Mol Microbiol* **39,** 620-632.

66. Wattiau, P., and Cornelis, G. R. (1993) SycE, a chaperone-like protein of *Yersinia enterocolitica* involved in the secretion of YopE. *Mol Microbiol* **8,** 123-131.

67. Boyd, A. P., Lambermont, I., and Cornelis, G. R. (2000) Competition between the Yops of *Yersinia enterocolitica* for delivery into eukaryotic cells: role of the SycE chaperone binding domain of YopE. *J Bacteriol* **182,** 4811-4821.

68. Lloyd, S. A., Norman, M., Rosqvist, R., and Wolf-Watz, H. (2001) *Yersinia* YopE is targeted for type III secretion by N-terminal, not mRNA, signals. *Mol Microbiol* **39,** 520-531.

69. Cheng, L.W., Anderson, D.M. and Schneewind, O. (1997) Two independent type III secretion mechanisms for YopE in Yersinia enterocolitica. *Mol Microbiol* **24,** 757-765.

70. Quinaud, M., Chabert, J., Faudry, E., Neumann, E., Lemaire, D., Pastor, A., Elsen, S., Dessen, A., and Attree, I. (2005) The PscE-PscF-PscG complex controls type III secretion needle biogenesis in *Pseudomonas aeruginosa*. *J Biol Chem* **280,** 36293-36300.

71. Deane, J. E., Cordes, F. S., Roversi, P., Johnson, S., Kenjale, R., Picking, W. D., Picking, W. L., Lea, S. M., and Blocker, A. (2006) Expression, purification, crystallization and preliminary crystallographic analysis of MxiH, a subunit of the *Shigella flexneri* type III secretion system needle. *Acta Cryst* **62,** 302-305.

72. Zhang, L., Wang, Y., Picking, W. L., Picking, W. D. and De Guzman, R. N. (2006) Solution structure of monomeric BsaL, the type III secretion needle protein of *Burkholderia pseudomallei*. *J Mol Biol* **359,** 322-330.

73. Wang, Y., Ouellette, A. N., Egan, C. W., Rathinavelan, T., Im, W., and De Guzman, R. N. (2007) Differences in the electrostatic surfaces of the type III secretion needle proteins PrgI, BsaL, and MxiH. *J Mol Biol* **371**(5), 1304-1314.

74. Kenjale, R., Wilson, J., Zenk, S. F., Saurya, S., Picking, W. L., Picking, W. D., and Blocker, A. (2005) The Needle Component of the Type III Secreton of *Shigella* Regulates the Activity of the Secretion Apparatus. *J Biol Chem* **280,** 42929-42937.

75. Cordes, F. S., Komoriya, K., Larquet, E., Yang, S., Egelman, E. H., Blocker, A., and Lea, S. M. (2003) Helical Structure of the Needle of the Type III Secretion System of *Shigella flexneri*. *J Biol Chem* **278,** 17103-17107.

76. Sun, P., Tropea, J. E., Austin, B. P., Cherry, S., and Waugh, D. S. (2008) Structural characterization of the *Yersinia pestis* type III secretion system needle protein YscF in complex with its heterodimeric chaperone YscE/YscG. *J Mol Biol* **377,** 819-830.

77. Torruellas, J., Jackson, M. W., Pennock, J. W., and Plano, G. V. (2005) The *Yersinia pestis* type III secretion needle plays a role in the regulation of Yop secretion. *Mol Microbiol* **57,** 1719-1733.

78. Plano, G. V., Day, J. B., and Ferracci, F. (2001) Type III export: new uses for an old pathway. *Mol Microbiol* **40,** 1365-2958.

Chapter 2

Structural Analysis of YscF and its *in vitro* Polymerization Examined by Secondary Structure Prediction, Homology Modeling, Electrophoresis, Mutagenesis, Circular Dichroism, and Transmission Electron Microscopy

ABSTRACT

Structural analysis of YscF and its *in vitro* needle assembly studies were performed by a combination of secondary-structure prediction, homology modeling, electrophoresis, mutagenesis, circular dichroism spectroscopy, and transmission electron microscopy. This analysis improves our understanding of YscF, whose structure has not been solved to date. Secondary-structure predictions of YscF show four α-helices while homology modeling results show that the N-terminal region of YscF is unstructured in the monomer. This model presents YscF in the form of an α-helical hairpin centered on the tetrapeptide PDNP. Deletion of the first 19 residues of YscF did not hinder *in vitro* polymerization. This analysis gave more evidence that the N-terminal region of YscF does not control its polymerization into the needle structure. Mutagenesis and circular dichroism spectroscopy show that 7 YscF mutants (Y65A, N66A, K76A, D77A, I82A, Q84A and F86A) mentioned in chapter 1 of this work have a high helical content, but Y65F is a random coil. We use analytical gel filtration to elucidate the role of Y65 in YscF needle assembly. This work uses transmission electron microscopy to study *in vitro* polymerization (needle assembly) of YscF and its mutants listed above. Our results show that mutant N66A is able to prevent YscF needle assembly.

INTRODUCTION

The *Yersinia* needle plays an important role in secretion and translocation of *Yersinia* outer proteins (Yops) into host cells (1-4). It also plays an important role in the cell-contact regulation of type III secretion (1). Cordes *et al.* (5) used X-ray fiber diffraction and EM to demonstrate that the *Shigella flexneri* needle shares an identical helical architecture (5.6 subunits per turn, 24-Å helical pitch) and inner channel diameter (2 nm) with the flagellar rod, hook, and filament. This structural similarity is likely to exist among other T3SS needles that include *Yersinia*.

The *Yersinia* needle structure is assembled through self-oligomerization of an 87-residue protein known as YscF (6, 7). During needle assembly, YscF is secreted, but YscG and YscE prevent it from premature polymerization in the cytosol of the bacterium prior to the assembly of the needle (8). The crystal structure of the YscEFG protein complex (9) shows that YscG binds tightly to the C-terminal half of YscF, implying that it is this region of YscF that controls its polymerization into the needle structure (9). Sun *et al.* (9) showed that the N-terminal 49 residues of YscF are present and disordered in the structure of the heterotrimer YscEFG. The N terminal regions of both MxiH and BsaL (10, 11) are also shown to be disordered in the structures and may not be involved in needle assembly. Based on their study, Deane *et al.* (10) suggested that either the five C-terminal residues are essential for N-terminal helix formation or the N-terminal region becomes folded only within the intact needle, as it is thought to occur for flagellin (12-14). This suggestion was based on the fact that polymerization was

blocked following truncation of the last 5 residues of MxiH (10). The unfolded N-terminus is thought to facilitate easy movement through the central channel of the needle because the size of the channel in the center of the assembly is likely to allow secretion of only single helices and random-coil proteins, rather than fully folded structures (10).

In their study, Torruellas *et al.* (15) examined the effect of individual amino acid substitutions on the regulation of type III secretion by YscF. By targeting conserved residues for replacement by alanine, they showed that substitution of a single amino acid can totally alter/interfere with the function of YscF. Deane *et al.* (10) generated a model of the *Shigella* T3SS needle by docking the crystal structure for MxiH into the 16 Å density map from their earlier three-dimensional EM reconstruction of the needle (5). The model shows that the C-terminal helix of MxiH forms the outer shell of the needle core, whereas the PSNP loop directs the N-terminal helix to line the inner wall of the needle channel. Their model shows that the C terminal region of MxiH is involved in extensive inter-subunit contacts. They suggest that this interaction is important for needle stability because polymerization was blocked following truncation of the last 5 residues of MxiH.

Mutational studies of MxiH (16) and YscF (15) have shown that these needle proteins determine induction of their secretion systems. Previous secondary structure predictions of the three YscF homologs, PrgI (*Salmonella typhimurium*), MxiH, and BsaL revealed α-helical structures (16) that were confirmed by circular dichroism spectroscopy (17). The three YscF homologs also show a big difference in thermal stabilities (17) in contrast with their

sequence conservation. Moreover, the electrostatic surfaces of PrgI were shown to differ radically from those of BsaL or MxiH (18). In all three needle proteins, deletion of the last five residues stopped self-polymerization resulting into respective monomers (17, 11, 18) whose structures were solved. Although the structures of three T3SS proteins (MxiH, BsaL and PrgI) have been solved, many questions remain concerning the structure and protein-protein interactions in type III secretion needle proteins. The sequences of these needle proteins suggest that electrostatic contacts are important in needle assembly (18).

Wang *et al.* (18) suggested that needle packing interactions may be different among *Shigella, Salmonella* and *Burkholderia*. In the structure of PrgI (18), the surface of the two helix bundle is polar due to residues on: helix α1 (N22, D21, Q24, T25, Q26, E29, K33, and D32), helix α2 (Q48, S49, K50, S52, E53, N55, R58, N59, and S62), and the PxxP region (K27, S39, and D40). They also showed that most of these polar residues are pointed away from the two helix bundle and therefore are not needed in stabilizing the hydrophobic core of the two helix bundle. Their work shows that several polar residues are identical (Q48, N59, and S62) or conserved (Q24, E53, N55, and R58) among needle proteins, suggesting that they are important for function other than stabilizing the core domain. They also concluded that the polar surface of the needle protein is most likely important in pathogenesis.

Kenjale *et al.* (16) performed point mutations on MxiH to analyze needle assembly and effector secretion. Their study shows that in *S. flexneri* MxiH, the L54A or Y57A mutation prevents needle polymerization and secretion of effector

proteins. These mutations disrupt the hydrophobic interactions at the helix α1-α2 interface, thereby destabilizing the two helix bundle. A similar effect is reported in PrgI (18), another YscF homologue. The same effect is likely to exist in YscF due to the conservation of these residues among the needle proteins. These findings suggest that needle assembly depends on proper folding of the two-helix bundle.

It has been shown that the last five residues of PrgI, BsaL, and MxiH are important in needle monomer-monomer interaction (16, 17). In addition, Wang *et al.* (18) demonstrated that electrostatic interaction is an important component of needle assembly. Their suggestion is based on the presence of distinct areas of positively and negatively charged surface potentials on PrgI, MxiH, and BsaL. They concluded that the most significant difference among these needle proteins is in the arrangement of their electrostatic surfaces, and that despite primary sequence conservation, protein-protein interaction maybe different among these needle proteins (18).

Factors like ionic strength and electrostatic interaction affect needle assembly (18). By adjusting the pH from 8 to 10.5, Marlovits *et al.* (19) were able to dissociate the needle, but not the basal structure of the *S. typhimurium* needle apparatus. Their study showed the effect of pH on needle assembly. Wang *et al.* (18) have shown that the polar surface of the two-helix bundle is a common feature among needle proteins. They also demonstrated that conserved tyrosines contribute to surface polarity. In comparing PrgI to BsaL, and MxiH, their study confirmed that the three structures do not show a particular need for tyrosines in position Y47 and Y54 because phenylalanine would have maintained similar

hydrophobic contacts and the overall fold of the two-helix bundle. Owing to the fact that Y47 and Y54 are identical among PrgI, BsaL, and MxiH, they hypothesized that the tyrosyl hydroxyl groups of these conserved residues are important in protein-protein interactions with other needle monomers or with the tip complex (20). Based on our homology model of YscF, Y65 is likely to be involved in similar protein-protein interactions with other needle monomers or with the base proteins because it appears pointed away from the two-helix bundle and does not appear to contribute in stabilizing the core structure of the needle protein. Kenjale *et al.* (16) also developed a model to show that signaling of host-cell contact is relayed through the needle via intersubunit contacts.

Here, we predict the YscF secondary structure (Figure 2.1) by submitting the sequence to four different programs, namely PsiPRED (21, 22), SAM (23), PROFsec and SABLE2 (24). Furthermore, we use homology modeling to build the YscF homology model (Figure 2.2) based on the existing structures of YscF homologs. We also show that cleavage of the first 19 residues of YscF does not hinder *in vitro* needle assembly. Using circular dichroism spectroscopy, we determine the secondary structure of YscF, YscFΔ4 (YscF with C-terminal truncation) and its mutants. We use analytical gel filtration to elucidate the role of Y65 in YscF polymerization. In MxiH, many single mutations (W10A, Y57A, K69A, K72A, and R83A) are capable of severely altering needle polymerization (16). We use single mutations and transmission electron microscopy to study *in vitro* YscF needle assembly and investigate the role of 7 YscF conserved

residues in needle assembly. We use this study to identify YscF conserved residues that don't necessarily affect *in vitro* needle assembly.

EXPERIMENTAL PROCEDURES

Multiple sequence alignment. The YscF sequence was submitted to the NCBI BLAST server (25, 15) to identify homologous sequences; using a cutoff E-value of 10^{-6}, forty-six sequences were identified. However, many of these homologs were redundant, e.g., several versions within the genus *Yersinia* or closely related genera. Therefore, the redundant sequences were eliminated to obtain a set of 21 sequences with no more than 75% sequence identity among them. These 21 species were submitted to the T-Coffee server (27) for multiple sequence alignment, the best-validated algorithm. The results were visualized by the publicly available server ESPript (28), and analyzed numerically to rank the residues by their degree of conservation (data not shown here).

YscF structure prediction. The YscF secondary-structure prediction (Figure 2.1) was done by submitting the sequence to four different programs, namely PsiPRED (21, 22), SAM (23), PROFsec and SABLE2 (24). The results were visualized using our web-server:http://proteins.msu.edu/Servers/Secondary_Structure/visualize_secondary_structure_predictions.html. To get the homology model (Figure 2.2), the YscF sequence was submitted to http://bioinfo.pl/Meta/, a well-validated and publicly available server for consensus fold recognition. The server easily identified the two available structures of type III pilins (2G0U and 2CA5) as the best parent structures. For each of these two structures, the best alignment to the YscF sequence was identified and converted into a backbone homology model for YscF using in-house laboratory software. The conformation of a side chain was

preserved if it was identical to its counterpart in the parent structures; otherwise, the side chain was added using the publicly available SCWRL program. Due to their high sequence similarity, few if any insertions or deletions are needed to align the sequences; the YscF sequence and those of the parent structures match almost over their entire lengths. The resulting homology models were visualized using MOLMOL.

Comparison of de novo protein structure predictions for YscF with experimental structures of its homologs and the YscEFG complex.

The YscF sequence was subjected to the ROSETTA protocol for de novo folding (29), which produces predictions of protein conformations by gradually minimizing a statistical potential energy that measures how plausible a given conformation is for a given protein sequence. In the process, 30,000 such predictions were made for the YscF structure by my thesis advisor, Prof. William Wedemeyer. All predictions were independent of one another and were clustered structurally into families with similar conformations. As shown in Figure 2.3, the three largest clusters (denoted as clusters 0, 1 and 2) account for most of the predictions, meaning that the other clusters could be viewed as structurally similar to these three.

Cloning, protein expression and purification. The YscFΔ4 construct involved C-terminal modifications of *yscF* gene by removal of the three C-terminal amino acid residues (KFP), Q84E single mutation and introduction of a C-terminal His-tag as indicated in the underlined sequence below:

MSNFSGFTKGTDIADLDAVAQTLKKPADDANKAVNDSIAALKDKPDNPALLADL
QHSINKWSVIYNINSTIVRSMKDLMQGILQKFP (YscF).

MSNFSGFTKGTDIADLDAVAQTLKKPADDANKAVNDSIAALKDKPDNPALLADL QHSINKWSVIYNINSTIVRSMKDLMQGILEHHHHHH (YscFΔ4).

This modification was done based on results from other YscF homologs (10, 11) in which it prevented self-association of monomeric MxiH and BsaL. The YscF coding sequence was PCR-amplified (30 cycles of 40 s at 95 °C, 40 s at 55 °C and 1 min 30 s at 68 °C) from a plasmid (pMMB 867) containing the YscEFG construct obtained from Dr. Michael Bagdasarian (Michigan State University-Microbiology and Molecular Genetics) using primers 5′- GGA ATT C**CA TAT G**AG TAA ATT CTC TGG ATT TAC GAA AGG -3′ (forward) and 5′- CCG G**CT CGA G**GA TGC CTT GCA TTA AGT CTT TCA TG -3′ (reverse). We designed a second set of primers, 5′- GGA ATT C**CA TAT G**GCT CAA ACG CTC AAG AAG CCA GCA GA-3′ (forward) and 5′- CCG G**CT CGA G**GA TGC CTT GCA TTA AGT CTT TCA TG -3′ (reverse) to truncate the first N-terminal 19 residues of YscFΔ4. This second construct was named Δ19YscFΔ4 and was used to study the role played by the N-terminal region in YscF needle formation. Both sets of forward and reverse primers were designed with NdeI and XhoI restriction sites (underlined) respectively. The resulting PCR products were digested with NdeI and XhoI then ligated (30) into similarly digested pET22b vector. The correct sequences were verified by DNA sequencing then the expression plasmids containing YscFΔ4 and Δ19YscFΔ4 were transformed into *E. coli* DH5α for replication. The plasmids were isolated using the Qiagen plasmid isolation kit (Qiagen Inc.) then transformed into *E.coli* BL21(DE3) for protein production.

Cell cultures were grown in LB containing 100 μg/mL ampicilin. In each case a single colony was picked from the plate and used to inoculate 5 mL of liquid LB medium containing 100 μg/mL ampicilin. The culture was incubated at 37°C for 6 hours with shaking at 250 rpm. This culture was added to 1.0 L of LB medium as a starter culture. The 1.0 L culture was then incubated at 37°C with shaking to an OD_{600} of approximately 0.9. Protein expression was induced by addition of filter-sterilized isopropyl-β-D-thiogalactopyranoside (IPTG) to a final concentration of 1.0 mM and grown for 4 more hours with shaking (250 rpm) at 37°C. The culture was pelleted by centrifugation (8000g) at 4°C for 20 minutes then pellet resuspended in nickel-A buffer (50 mM NaH_2PO_4, pH 8.0, 300 mM NaCl, 20 mM Imidazole, 5 mM β-Mercaptoethanol and EDTA-free Protease Inhibitor tablet) containing 6 M guanidine hydrochloride. Following sonication, the extract was incubated at room temperature with gentle shaking for 30 minutes. The extract was centrifuged at 20,000g for 20 min to remove insoluble debris. The protein was purified via the C-terminal His tag by nickel-chelation chromatography. The unbound protein was washed off by 3 column volumes of nickel-A buffer followed by 3 column volumes of wash buffer (nickel-A buffer plus 600 mM NaCl). The protein was eluted using nickel-B buffer (50 mM NaH_2PO_4, pH 8.0, 300 mM NaCl, 300 mM Imidazole, 5 mM β-Mercaptoethanol and EDTA-free Protease Inhibitor tablet) (31). The purified protein was verified by protein N-terminal sequencing, Western blot and MALDI-TOF mass spectrometry.

Site-directed mutagenesis. The following six point mutations were each introduced on plasmid pYscFΔ4 (pET22b containing the YscFΔ4 gene) using the

QuikChange XL Site-Directed Mutagenesis Kit (Stratagene): Y65A, Y65F, N66A, K76A, D77A and I82A. Each of the listed forward primers (Table 2.1) was used in a PCR reaction (18 cycles of 50 s at 95 °C, 50 S at 50 °C and 8 min at 72 °C) with its complement that is not listed (mutated codons are underlined). The *PfuTurbo*® master mix (Stratagene) was used in the PCR reaction. After each PCR reaction, *DpnI* was added then sample incubated at 37 °C for 1 h to digest the template plasmid. Each sample was used to transform *E. coli* DH5α cells for plasmid replication according to the mutagenesis kit instructions. Replicated plasmids were isolated using the Qiagen plasmid isolation kit (Qiagen Inc.) before submitting samples for DNA sequencing. Each mutant plasmid was used to transform *E.coli* BL21(DE3) for protein production and purification following the same method described above for YscFΔ4 (the wild type in this case). Analysis of protein expression and purification was done by denaturing gel electrophoresis (32) and standard protein assays (33) respectively.

Analytical gel filtration chromatography. The hydrodynamic radius assay of the Y65AYscFΔ4 mutant was carried out by analytical gel filtration chromatography at pH 5.5 and pH 8.0 on a HiPrep 26/60 S-100 HR sephacryl column (Amersham Biosciences). This enabled us to determine the effective molecular weight of this mutant at both pH values. The column had been calibrated with bovine pancreatic ribonuclease A, chymotrypsinogen A, ovalbumin, and albumin by plotting the logarithm of molecular weight versus elution volume. The effective molecular weight of the protein was determined from the following equation:

$$V_e - V_o = -43.9 \ln (\text{mol. wt.}) + 208.25$$

where V_e is the elution volume and V_o is the void volume.

Circular dichroism (CD) spectroscopy. Circular dichroism experiments were done at protein concentrations ranging between 10 μM to 40 μM using a 1 cm path-length cell. The protein was prepared in 10 mM NaH_2PO_4, pH 7.5, 10 mM NaF. The acquisition of CD spectra was done at 24°C over the far-UV range of 190 nm - 250 nm on a Chirascan CD spectrophotometer (Applied Photophysics) in continuous scanning mode at 15-20 nm/min. Spectra were acquired in triplicate and averaged. The temperature was controlled by a circulating water bath and the data analyzed with DICHROWEB server (34).

Needle formation in vitro and electron microscopy. For each protein, needle assembly was induced through concentration by ultrafiltration to 10 mg/mL in 50 mM NaH_2PO_4, pH 7.5, 300 mM NaF. In case of Y65AYscFΔ4, we went a step further to analyze the effect of pH on its needle assembly process. For this protein, we also used 50 mM NaH_2PO_4, pH 5.5, 300 mM NaF to compare needle assembly at pH 8.0 and 5.5. All samples were frozen at -20°C for a minimum of 24 hours and thawed at 4°C for 12 hours before transmission electron microscopy (TEM) studies. A 2% uranyl acetate solution in 50% ethanol was used for negative staining. The pictures were taken between 80000x and 140000x magnification on a JEOL (Japan Electron Optics Laboratories) 100CXII microscope.

RESULTS

Multiple sequence alignment. The YscF conserved residues targeted for site-directed mutagenesis were chosen based on atomic structures of three YscF homologs, MxiH (Figure 1.2, chapter 1) (10), BsaL (Figure 1.3, chapter 1) (11), and PrgI (Figure 1.4, chapter 1) (18). These three present the only available T3SS needle protein structures and show high sequence identity to YscF. More information was also deduced from the structure of YscEFG complex (Figure 1.5, chapter 1) (9). The multiple-sequence alignment results show a high degree of conservation in the C-terminal region.

YscF structure prediction. Results from all four secondary structure prediction programs show that YscF has high helical content with four α-helices (Figure 2.1) labeled α1 (residue 13-24), α2 (residue 30-42), α3 (residue 48-57) and α4 (residue 69-85). These results are consistent with the four helices observed in the BsaL structure although they vary slightly from the MxiH structure, which had only 3 helices. A portion of the N-terminal region was not solved in the MxiH structure probably because the fourth helix was not stable enough to be solved by X-ray crystallography. As shown in the secondary-structure predictions, the YscF structure might also have the two helix bundle fold around the PDNP coil. This suggestion is further confirmed by our YscF homology model (Figure 2.2) that confirms atleast 3 of the predicted four α-helices. During our homology modeling of YscF, MxiH was picked by the server as the best parent structure due to the high sequence similarity between them. Since the MxiH structure shows only three α helices, it limits the YscF model to

three α helices (α2, α3 and α4). We would have probably seen 4 helices in our YscF model if BsaL was used as the best parent structure. In this study, all the mutated residues except Y65 are located in the region corresponding to predicted helix 4 (C-terminal region). The conserved residue, Y65 is located in the hinge region between α3 and α4. Comparing the YscF homology model to both MxiH and BsaL structures show that all the seven conserved residues in this study (Y65, N66, K76, D77, I82, Q84 and F86) are exposed on the surface of the YscF monomer because they all point away from the two-helix bundle.

Comparison of de novo protein structure predictions for YscF with experimental structures of its homologs and the YscEFG complex. The predicted tertiary structures fell into three main families, which were denoted as cluster 0, cluster 1 and cluster 2 (Figure 2.3). All three families have the 4 helices (α_1, α_2, α_3, and α_4) (Figure 2.4) found in the secondary-structure predictions (Figure 2.1). All three families of predicted structures also form a hairpin between α_2 and α_3. The N-terminal region of α_1 (roughly residues 1-15) appears to be unstructured in all three clusters. In clusters 0 and 2, α_4 forms a three-helix bundle with the α_2-α_3 hairpin. Specifically, in cluster 2, the N-terminal α_1 joins with α_2 to form one long initial α-helix, whereas in cluster 0, α_1 is roughly perpendicular to the bundle, running parallel to the loop connecting α_3 and α_4. By contrast, in cluster 1, α_1 is positioned between α_4 and the α_2-α_3 hairpin; in this case, the α-helices are short and often bent.

When the predicted structures are compared to the experimentally determined structures of three T3SS proteins BsaL (11), MxiH (10) and PrgI (18) (Figure 2.5), they show a common feature, the predicted α_2-α_3 hairpin structure.

In all three experimental T3SS protein structures, α_4 does not form a bundle with the α_2-α_3 hairpin; rather, it projects away, but not in a straight line with α_3. Both MxiH and PrgI structures (Figure 2.5) lack α_1, whereas BsaL (Figure 2.5) has a partially unstructured α_1 forming a bundle with the α_2-α_3 hairpin. Finally, the YscEFG complex (Figure 2.5) shows YscF having an α_3-α_4 hairpin, as predicted in clusters 0 and 2. The positions of the YscF helices α_2 and α_3 agree across the T3SS protein structures (Table 2.2), suggesting that the α_2-α_3 hairpin forms the folding core of the T3SS pilin. The α_3-α_4 hairpin found in the YscEFG complex may also occur in YscF when it folds to form a pilus. Alternatively, given the minimal hydrophobic core of the predicted YscF structures (Figure 2.4), YscF could refold (including the possibility of domain swapping) when it assembles to form pili.

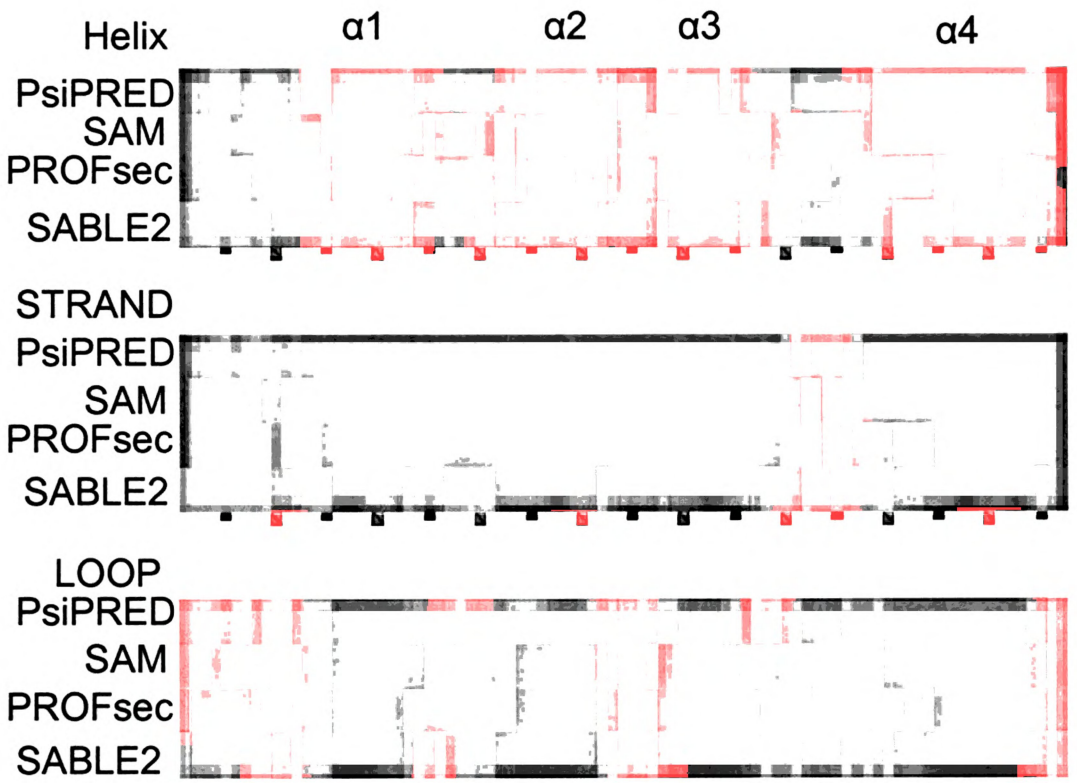

Figure 2.1. Secondary structure predictions for YscF by four different methods, PsiPRED, SAM, PROFsec and SABLE2. Four helices are predicted (structured regions of the sequence are highlighted in red.

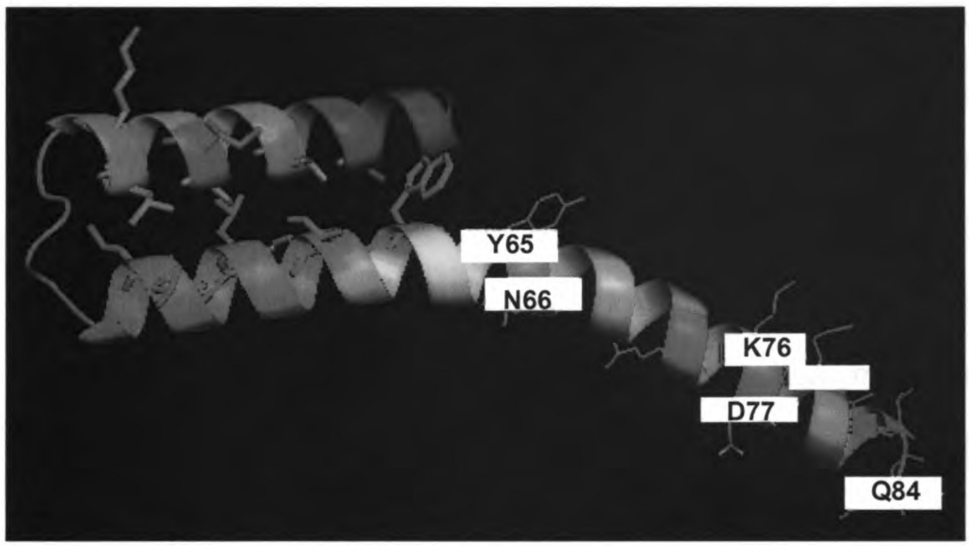

Figure 2.2. YscF homology model based on the MxiH crystal structure. Some of the selected conserved residues are shown on predicted α_2 and α3-α4 helices. Blue represents N terminus while red represents C terminus. Some of the residues are involved in $\alpha_2 - \alpha_3$ hydrophobic interactions to keep the two core helices close to each other.

Site-directed mutagenesis. To demonstrate the effect of some conserved residues on the YscFΔ4 secondary structure and *in vitro* needle assembly, the corresponding codons were each altered to alanine. The expression of all the mutant proteins was comparable to YscFΔ4 (Figure 2.6) except Y65AYscFΔ4 (Figure 2.7) and I82AYscFΔ4 (some of the data not shown here). Expression of Y65AYscFΔ4 was much more than YscFΔ4, while I82AYscFΔ4 was much less than YscFΔ4. There was a noticeable variation in solubility of the mutants compared to the wild type, with Y65AYscFΔ4 being the most soluble.

Protein expression and purification. The 6 M GnHCl was added to the extraction buffer because YscFΔ4 and all its mutants (except Y65AYscFΔ4) did not bind onto the nickel column without the denaturant. This is probably due to

polymerization that occurs at high protein concentrations thereby shielding the His_6-tag. However, the Y65A mutant binds to the nickel column in absence of the denaturant (Figure 2.8). Native gel analysis (Figure 2.9) shows polymerization of Δ19YscFΔ4 confirming that the N-terminal region does not affect YscF polymerization. The gel shows a higher molecular weight band (~1040 kDa) yet the corresponding MALDI-TOF-MS results show the molecular weight of Δ19YscFΔ4 (7.7 kDa). In their work, Matson *et al.* (35) also observed higher molecular weight bands representing multimers of YscF.

Analytical gel filtration chromatography. Unlike purification of YscFΔ4 and other mutants that require a denaturant, Y65A binds onto the nickel column without 6 M GnHCl (Figure 2.8). These results prompted us to analyze Y65AYscFΔ4 further by analytical gel filtration chromatography. We monitored the protein at pH 5.5 and 8.0 to analyze the effect of pH on its polymerization. Each buffer resulted in a different elution volume for the same protein as depicted by the two peaks (Figure 2.10) representing a shift in elution volume. At pH 8.0 the effective molecular weight is ~ 70 kDa while the same protein has an effective molecular weight of 22 kDa at pH 5.5. The protein elutes as a dimer at the lower pH, but it polymerizes further (7-mer) at a higher pH.

Circular dichroism spectroscopy. The CD spectra for YscFΔ4, Δ19YscFΔ4 and all the mutant proteins analyzed except Y65FYscFΔ4 show a high helical content with a double minimum (ellipticity) at around 208 nm and 222 nm corresponding to the α-helix (Figure 2.11) (some data not shown here). We used the Y65FYscFΔ4 mutant to further understand the characteristics of

Y65AYscFΔ4. It gave a spectrum with a single minimum at around 204 (Figure 2.12) corresponding to a random coil. The DICHROWEB server (34) was used for deconvolution and analysis of all the spectra and the results were tabulated (Table 2.3). The helical content is comparable in YscF and YscFΔ4 (61% and 60% respectively). All the mutants have a high helical content except Y65FYscFΔ4 that has 55% random coils. All proteins analyzed had low ß-strand content except Y65FYscFΔ4 that had 19%. Residue Y65 seems to be important for YscF folding.

Needle formation in vitro. In vitro needle formation was induced in YscFΔ4, Δ19YscFΔ4 and in all the mutants except N66AYscFΔ4 and Y65FYscFΔ4 (Figure 2.13). The N66AYscFΔ4 mutant did not form needles probably due to the importance of the N66 residue in needle assembly. However, the inability of Y65FYscFΔ4 to form needles may indicate the importance of the hydroxyl group of Y65 in needle assembly. The Δ19YscFΔ4 protein formed needles (Figure 2.13) even though it lacks the first 19 residues. This supports earlier results in YscF/YscG system (9) or in the MxiH system (10), showing that the N-terminal region does not affect polymerization (needle assembly). In all the cases where needles formed, the process took 24 hours or less. This trend was not observed in Y65AYscFΔ4 because the formation of detectable needles took almost 10 days. We analyzed Y65AYscFΔ4 needle formation at pH 5.5 and pH 8.0 and the two results were different. At pH 5.5, the protein did not form needles even after 14 days. At pH 8.0, the needle-formation process was much slower than in YscFΔ4, but needles were eventually formed (Figure 2.14). Lowering the

pH from 8.0 to 5.5 had an effect of completely hindering needle assembly in Y65AYscFΔ4. This result complements the analytical gel filtration results that showed Y65AYscFΔ4 as a dimer at pH 5.5, and a 7-mer at pH 8.0.

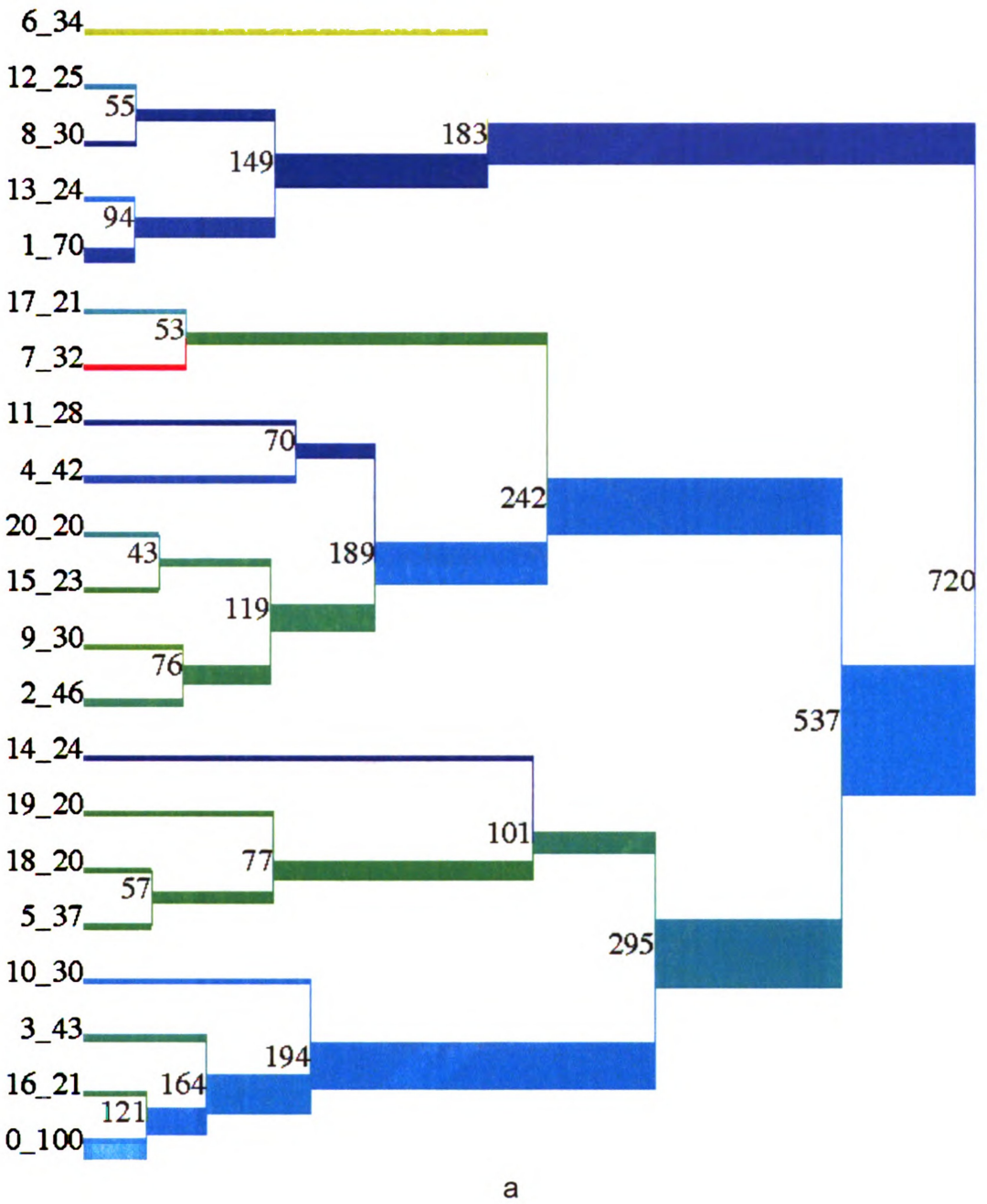

Figure 2.3. YscF structural families from de novo predictions. (a) Each family has similar conformations resulting in three main families (cluster 0, cluster 1, and cluster 2). (b) Cluster 0, showing contacts between α_2 and α_3 and between α_3 and α_4. (c) Cluster 1, showing contact between α_2 and α_3. (d) Cluster 2, showing contact between α_2 and α_3 and between α_3 and α_4.

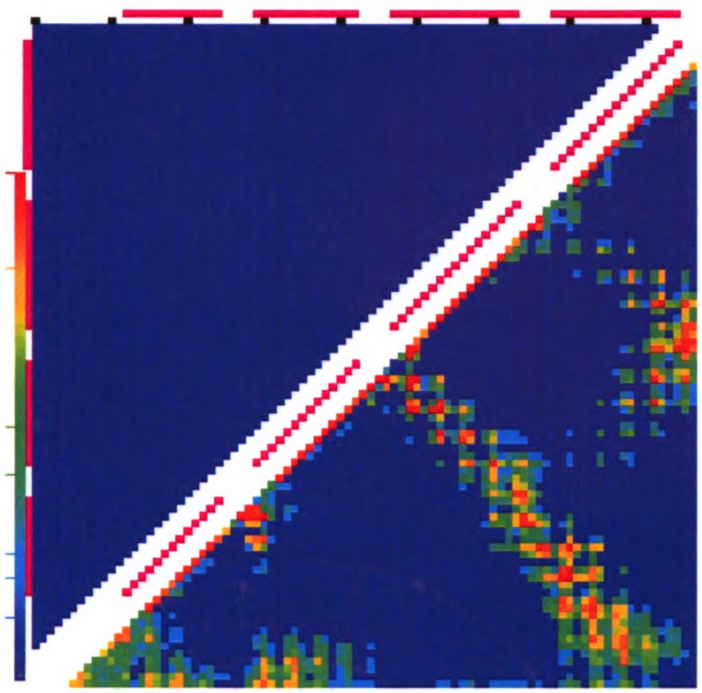

b

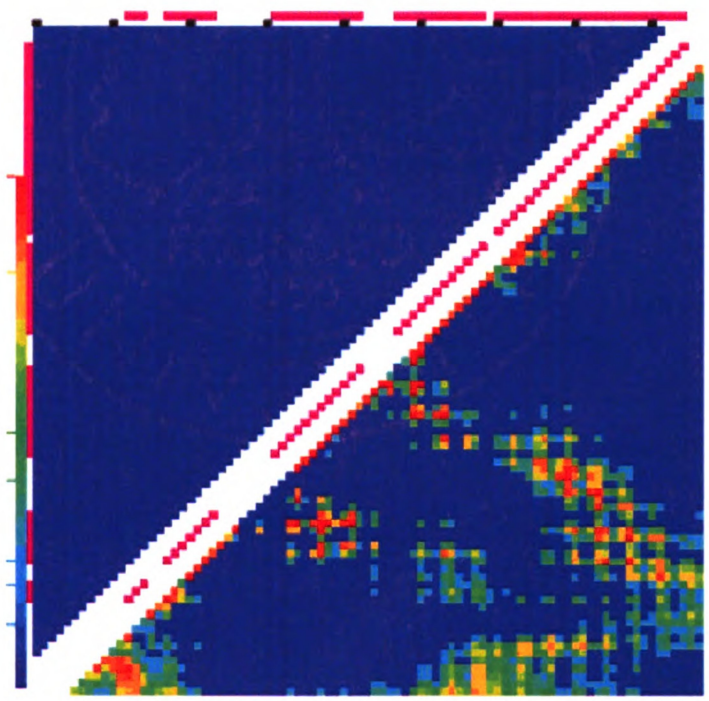

c

Figure 2.3 (cont'd)

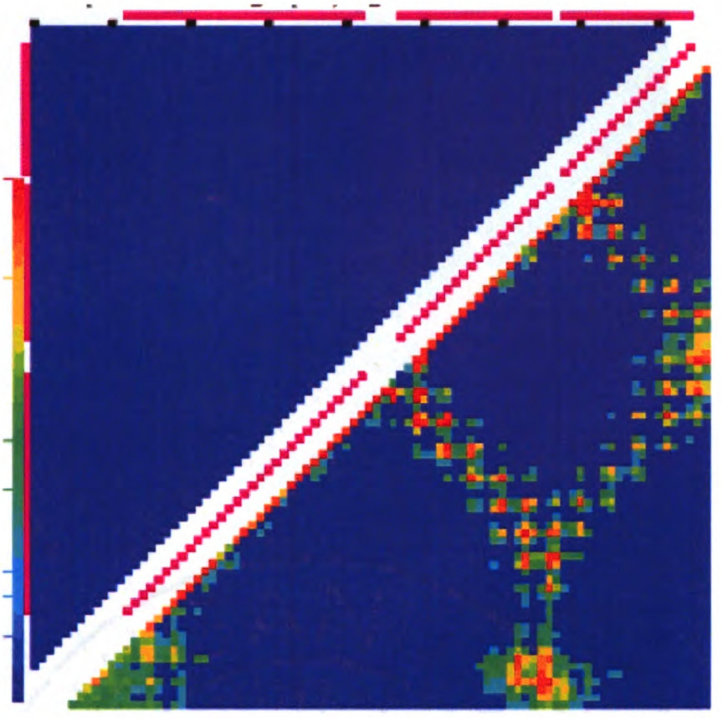

d

Figure 2.3 (cont'd)

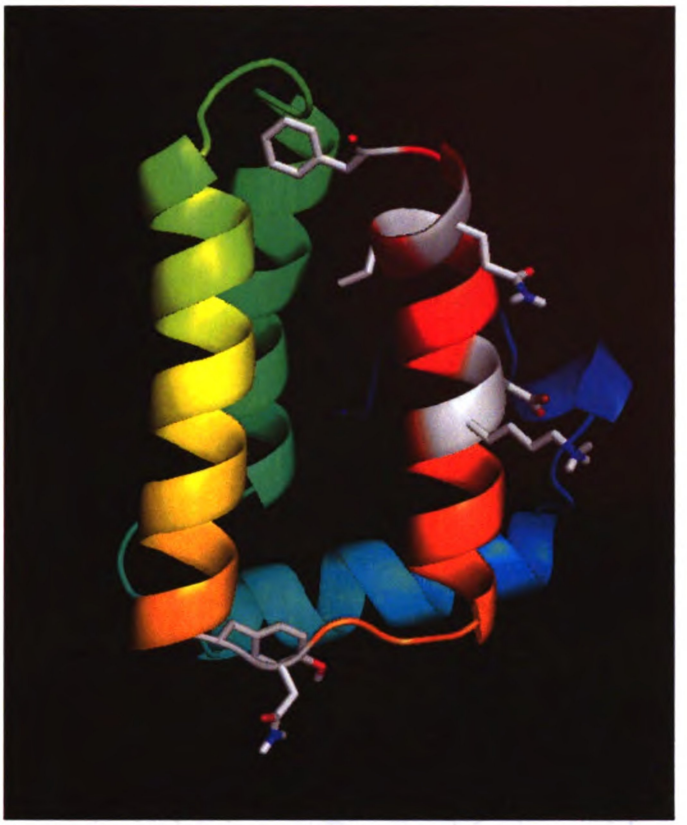

a

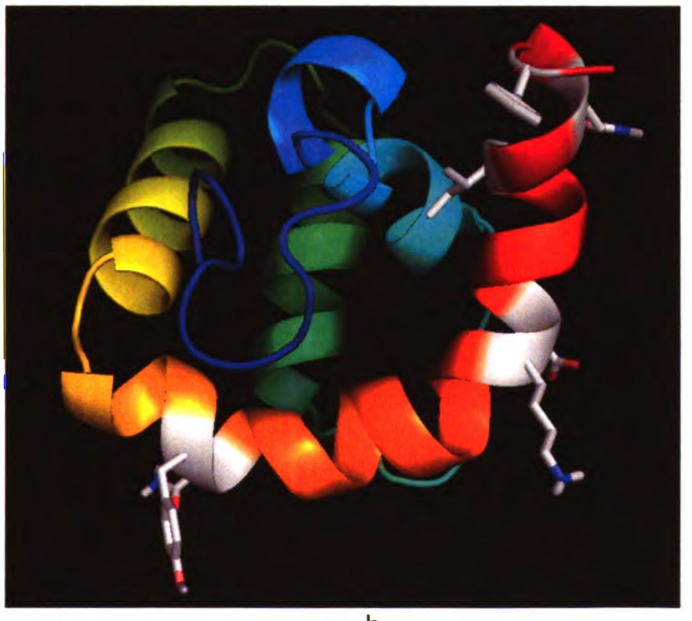

b

Figure 2.4. De novo YscF structure predictions showing the side chains for Y65, N66, K76, D77, I82, Q84 and F86 in: (a) cluster 0, (b) cluster 1, and (c) cluster 2. The coloring of the main-chain ribbons is as follows: blue - α_1, green - α_2, yellow - α_3 and red - α_4.

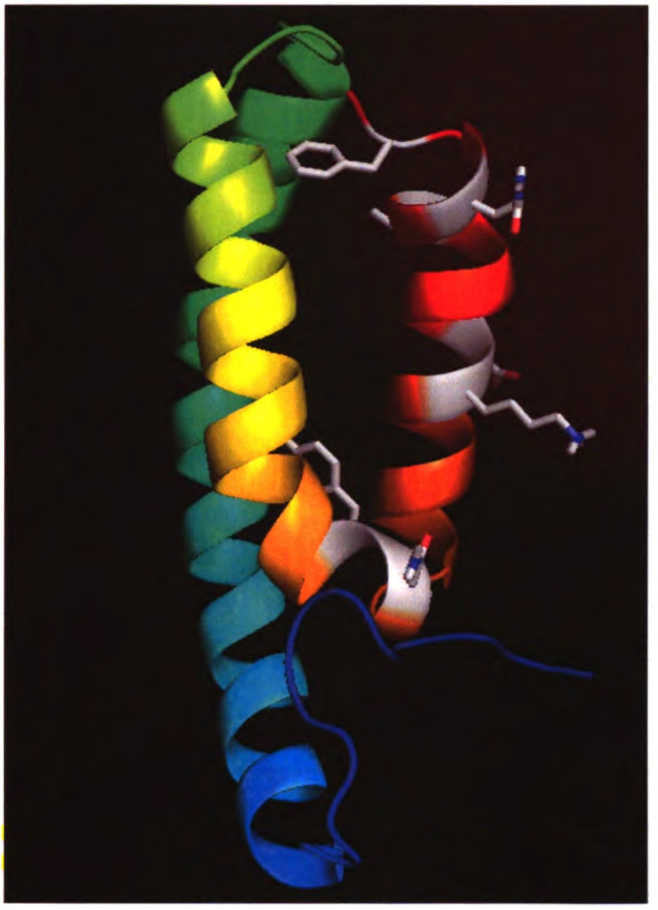

c

Figure 2.4 (cont'd)

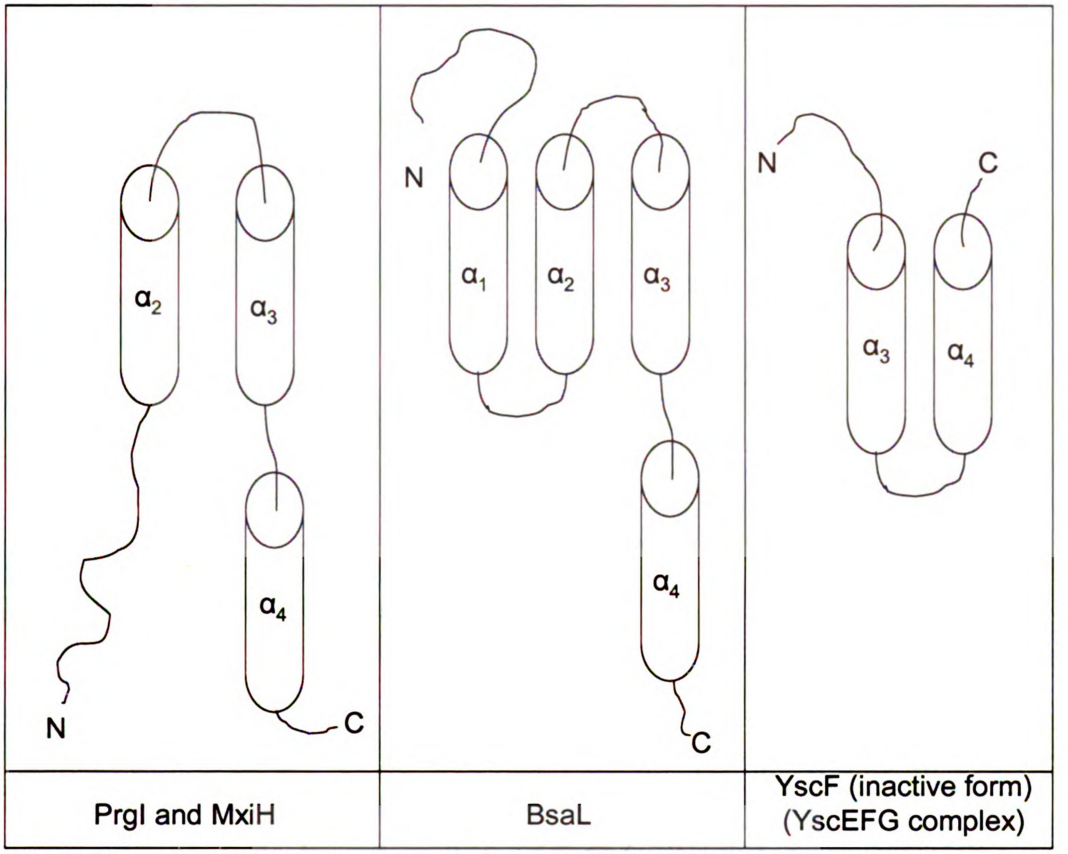

Figure 2.5. T3SS secondary structure models based on the atomic structures of PrgI (18) (PDB ID: 2JOW), MxiH (10) (PDB ID: 2CA5), BsaL (11) (PDB ID: 2G0U) and the inactive form of YscF in the YscEFG complex (9) (PDB ID: 2P58).

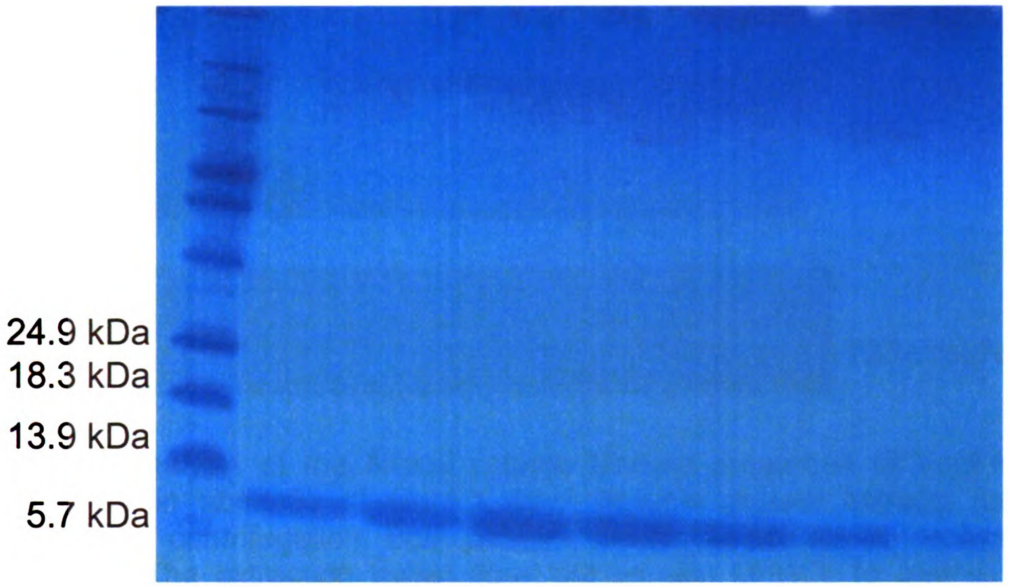

Figure 2.6. 12% SDS-PAGE gel of purified YscFΔ4.

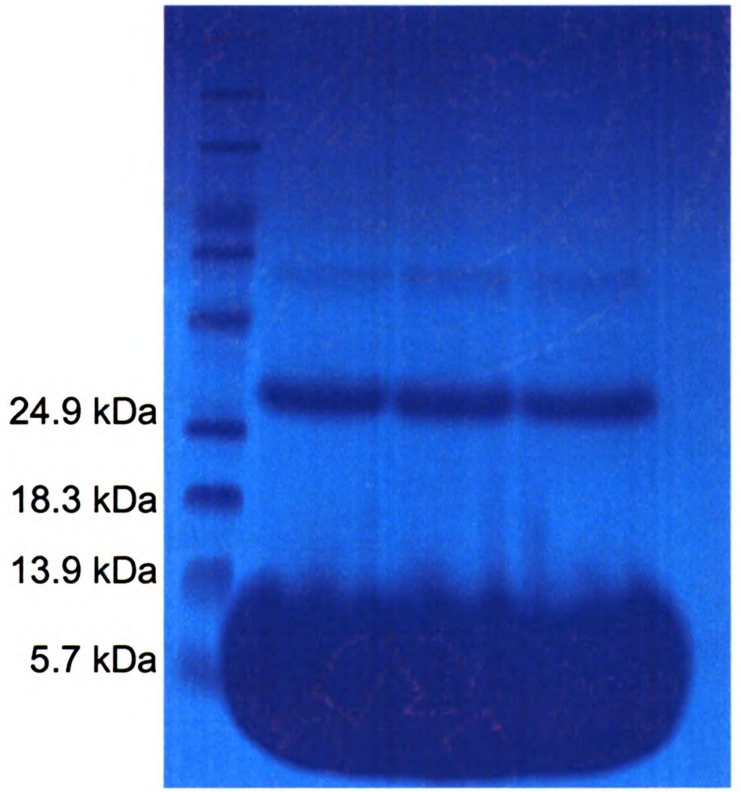

Figure 2.7. (a) 12% SDS-PAGE gel of purified Y65AYscFΔ4 ~ 10 kDa. Note: small amounts of trimer visible ~ 30 kDa.

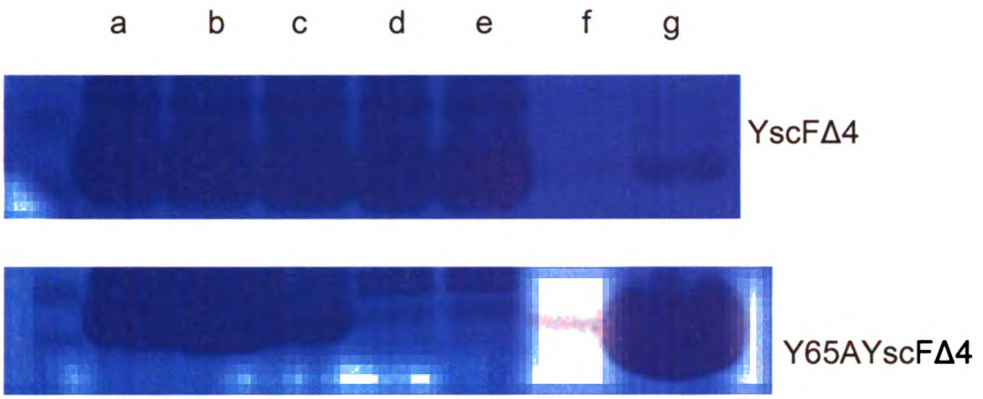

Figure 2.8. Analysis of the Nickel column binding properties of YscFΔ4 and Y65AYscFΔ4 in absence of GnHCl. (a-c) Soluble protein extracts following sonication and centrifugation. Both proteins are highly soluble in the extraction buffer. Note: The extraction buffer does not contain GnHCl. (d and e) Nickel column loading flow through. Note: YscFΔ4 flows through without binding, while Y65AYscFΔ4 binds. (f) Column wash. (g) Protein elution. Note: Y65AYscFΔ4 binds onto the column even in absence of the denaturant.

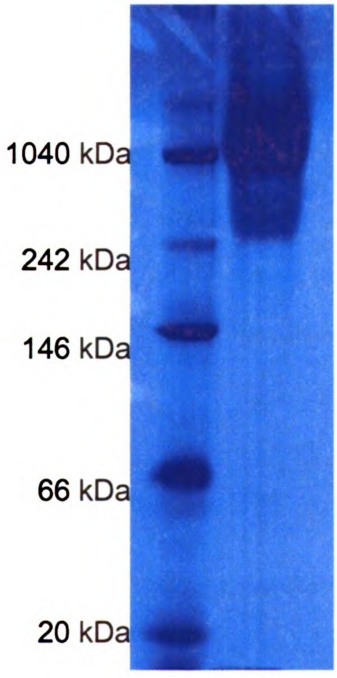

Figure 2.9. Polymerization of Δ19YscFΔ4. Native gel electrophoresis results showing polymerization in absence of residues 1-19 of YscF.

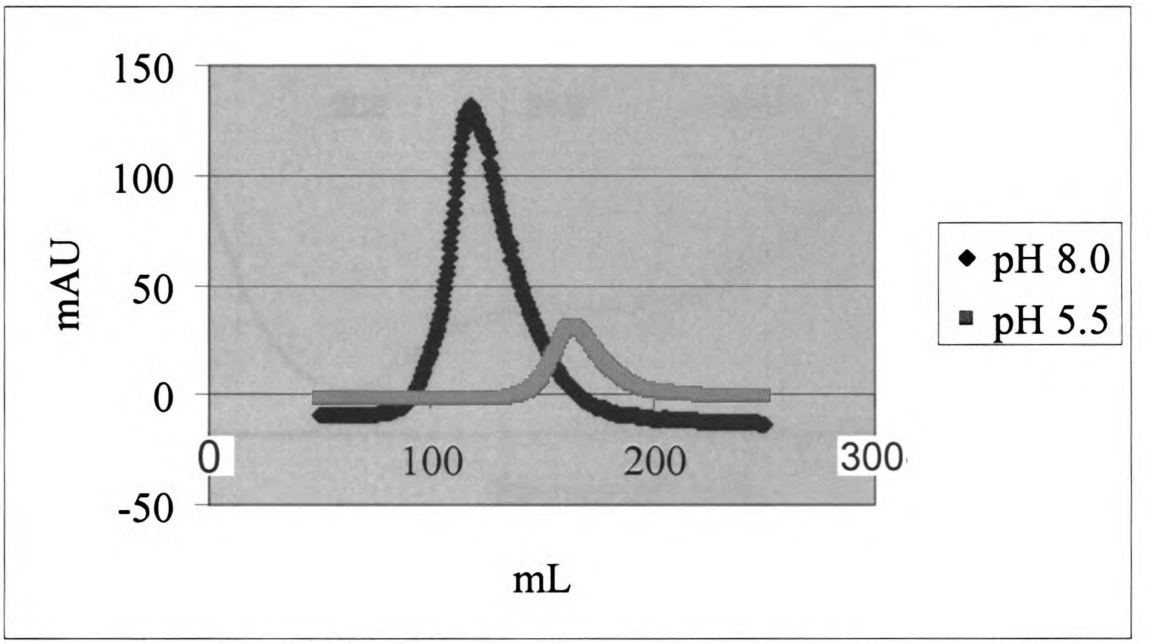

$$V_e - V_o = - 43.9 \ln (\text{mol. wt.}) + 208.25$$

Figure 2.10. Analytical gel filtration of Y65AYscFΔ4 under two different pH conditions. The protein elutes as a dimer at pH 5.5 while it elutes as a multimer at pH 8.0.

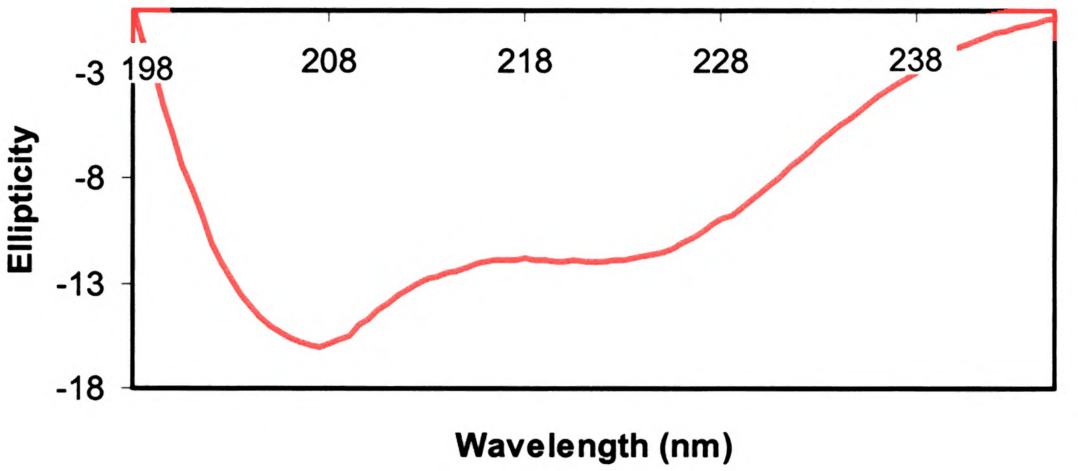

a

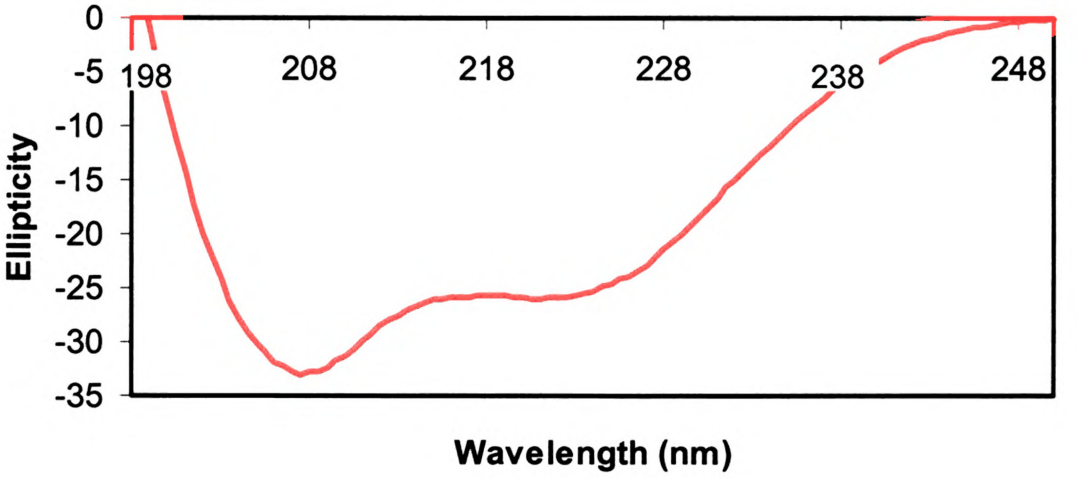

b

Figure 2.11. CD spectra showing α-helical structures: (a) YscF, (b) YscFΔ4, and (c) N66AYscFΔ4.

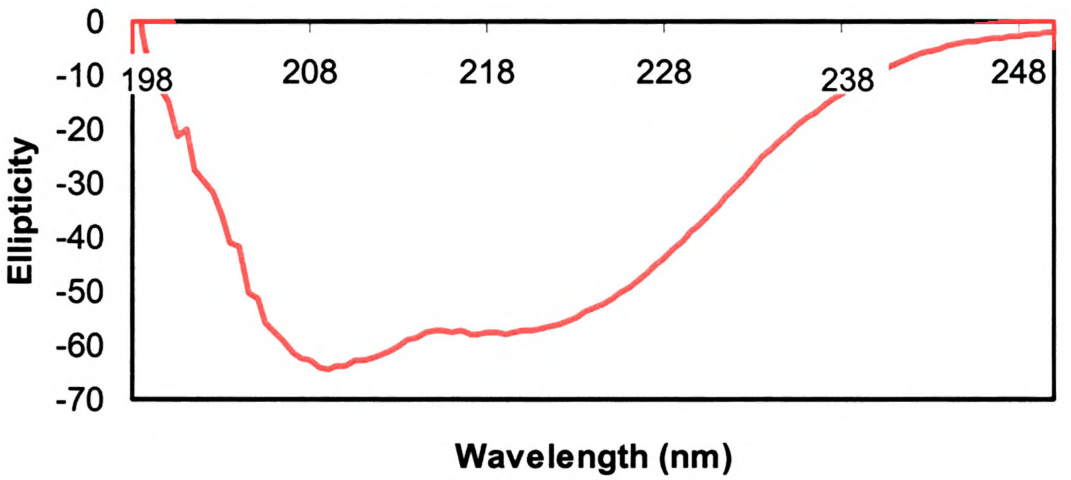

c

Figure 2.11 (cont'd)

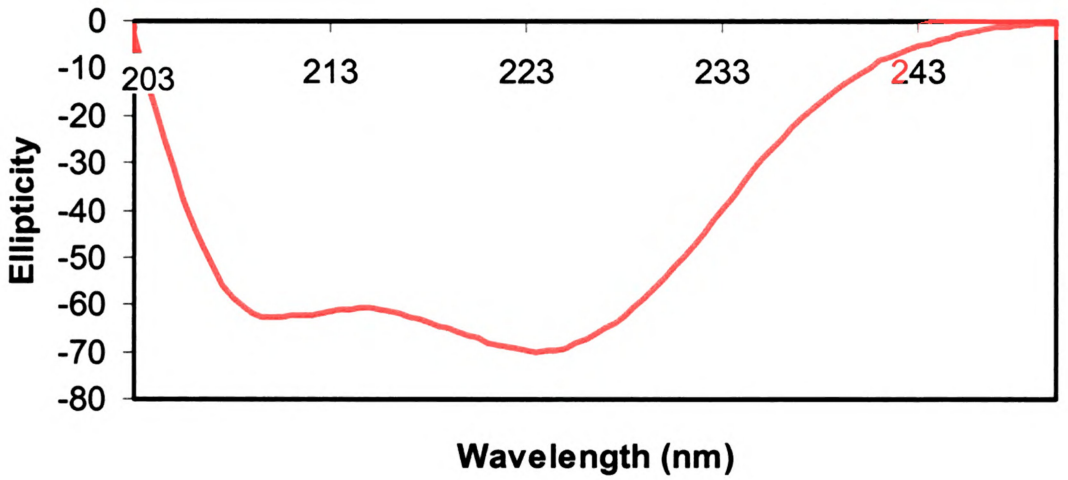

a

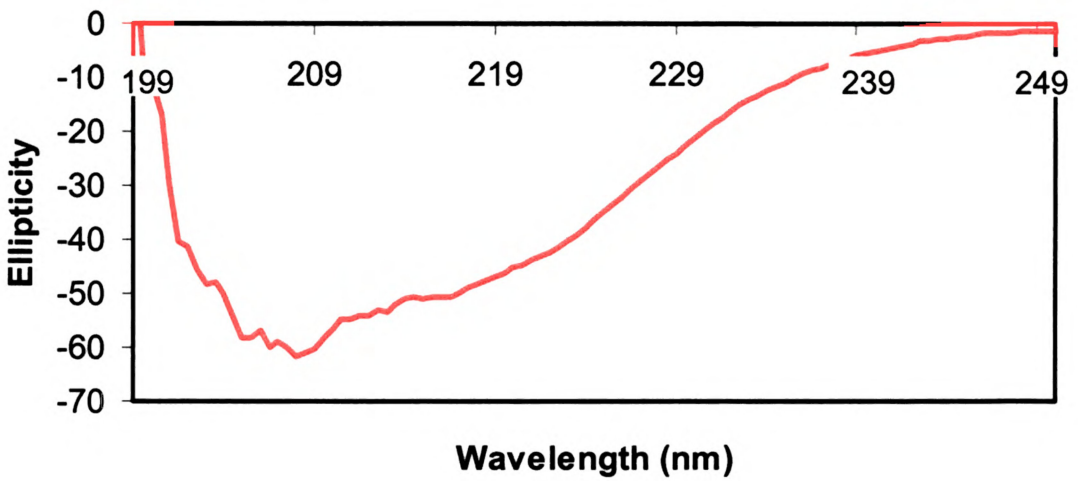

b

Figure 2.12. CD spectra comparing Y65AYscFΔ4 and Y65FYscFΔ4: (a) Y65AYscFΔ4 showing α-helical structure, and (b) Y65FYscFΔ4 showing a random coil structure.

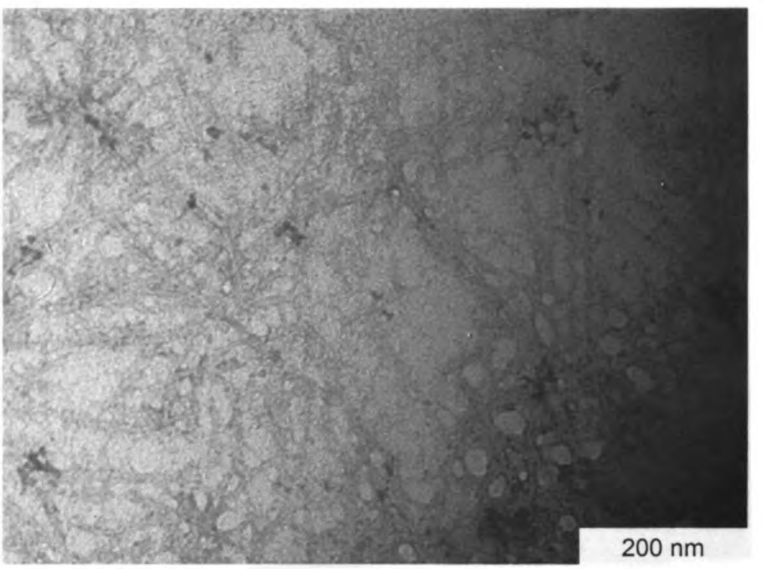

a

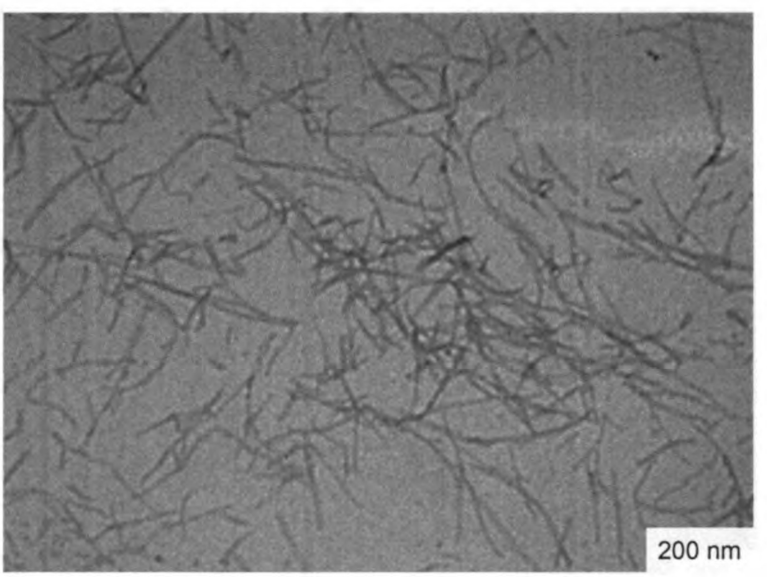

b

Figure 2.13. *In vitro* needle formation: (a) YscFΔ4 formed needles, (b) Δ19YscFΔ4 formed needles even with the N-terminal truncation, (c) N66AYscFΔ4, and (d) Y65FYscFΔ4 did not form needles.

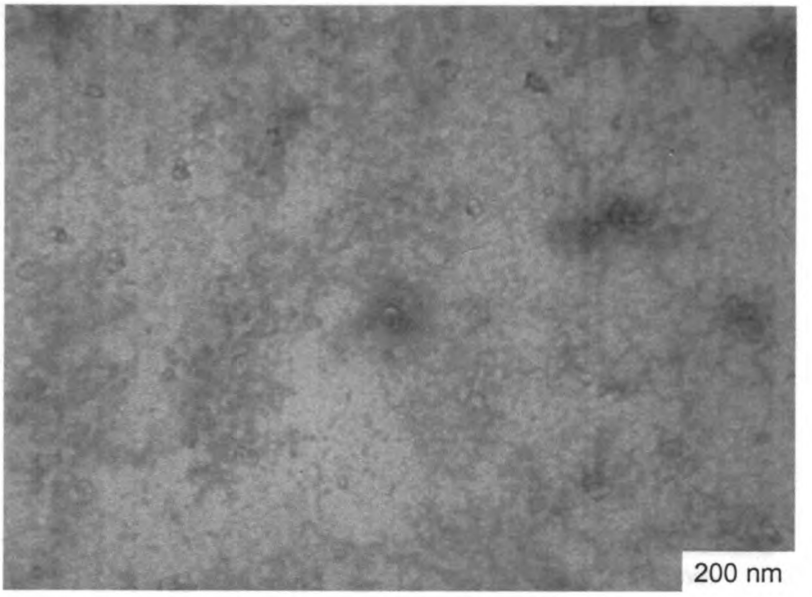

c

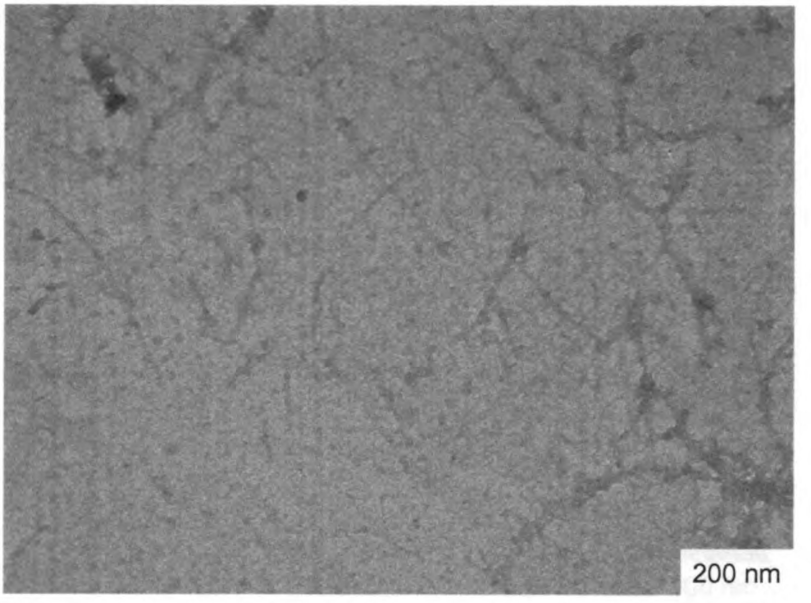

d

Figure 2.13 (cont'd)

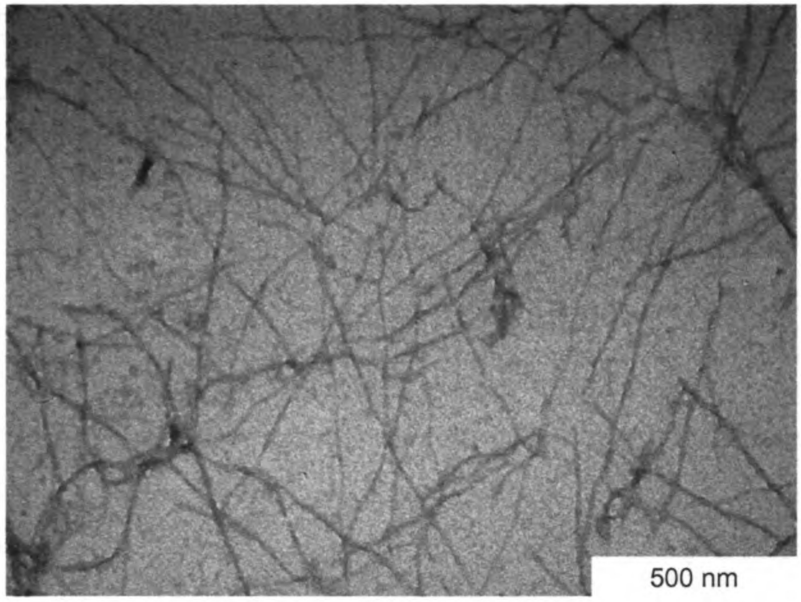

a

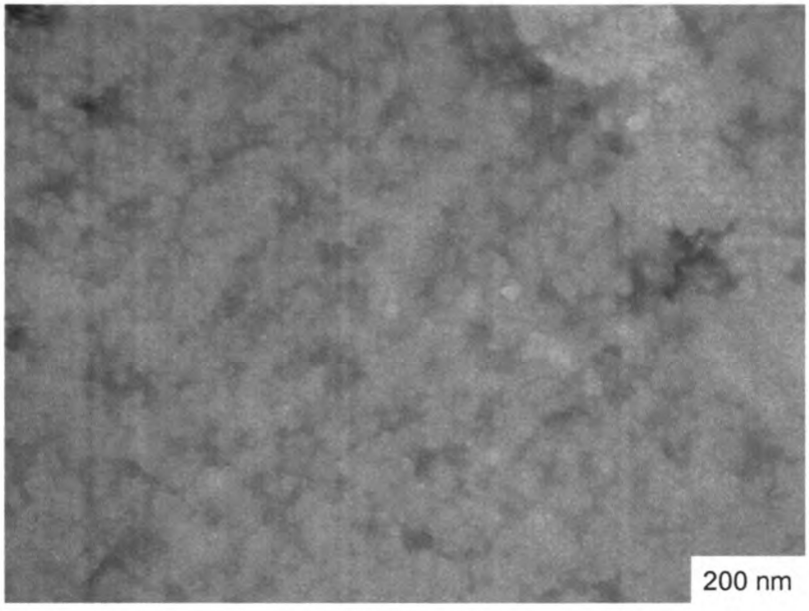

b

Figure 2.14. *In vitro* needle formation for Y65AYscFΔ4 in different buffers: (a) At pH 8.0 needles formed, and (b) at pH 5.5, Y65AYscFΔ4 does not form needles.

Table 2.1. Oligonucleotides used to generate YscF mutants. Mutated codons are underlined.

Y65A	5′- AATAAATGGTCGGTAATTGCCAATATAAACTCAACCATA -3′
Y65F	5′- AATAAATGGTCGGTAATTGCCAATATAAACTCAACCATA -3′
N66A	5′- AAATGGTCGGTAATTTACGCTATAAACTCAACCATAGTT -3′
K76A	5′- ACCATAGTTCGTAGCATGGCAGACTTAATGCAAGGCATC-3′
D77A	5′- ATAGTTCGTAGCATGAAAGCCTTAATGCAAGGCATCCTA -3′
I82A	5′- AAAGACTTAATGCAAGGCGCCCTACAGAAGTTCCCATAA -3′
Q84A	5′- TTAATGCAAGGCATCCTAGCGAAGTTCCCATAATATGAA -3′
F86A	5′- CAAGGCATCCTACAGAAGGCCCCATAATATGAAATATAA -3′

Table 2.2. Comparing positions of the predicted YscF helices α_1, α_2, α_3 and α_4 in relation to the atomic structures of PrgI (18) (PDB ID: 2JOW), MxiH (10) (PDB ID: 2CA5), BsaL (11) (PDB ID: 2G0U) and the inactive form of YscF in the YscEFG complex (9) (PDB ID: 2P58). Note: All the residues are numbered according to the YscF sequence in the multiple sequence alignment (Figure 1.6, chapter 1).

Helix	α_1	α_2	α_3	α_4
YscF (proposed)	I13 – L24	A30 – K44	P48 – I64	T70 – K85
YscF (YscEFG complex)	–	–	L50 – I64	N68 – P87
MxiH	–	K24 – K44	A49 – W61	S62 – Q84
PrgI	–	A27 – K42	P48 – S69	D77 – Q84
BsaL	K9 – P26	D28 – K44	A49 – N66	S69 – I82

Table 2.3. Summary of results from the deconvoluted far-UV CD spectra into various components of secondary structure in YscF, YscFΔ4 and its mutants. Note: All experiments were done at 24°C. Reported values are percentages of the total structure.

Protein	Helix	Strand	Random
YscF	61	8	30
YscFΔ4	60	7	32
Y65A YscFΔ4	73	2	25
N66A YscFΔ4	65	5	29
Y65F YscFΔ4	26	19	55
K76A YscFΔ4	62	6	32
D77A YscFΔ4	68	4	27
I82A YscFΔ4	59	7	34

DISCUSSION

Our work has used circular dichroism to show that YscF secondary structure has a high α-helical content similar to MxiH and BsaL. We confirmed that the N-terminal region of YscF does not affect needle assembly, just as previously hypothesized in YscF/YscG complex (9) and MxiH (10). Protein bands corresponding to oligomers are evident through native gel electrophoresis even after cleaving off the first 19 residues. This was further confirmed by observation of needle formation in solution. Despite the high sequence identity among YscF and its two homologs, MxiH and BsaL, there is a significant difference. The two atomic structures were solved after deletion of five C-terminal residues and introduction of a His_6-tag (16) because this modification totally prevented polymerization in BsaL and MxiH, thereby improving the solubility of the protein. In our work, the same modification (YscFΔ4) significantly reduced polymerization in YscF and improved its solubility. However, we noticed polymerization in YscFΔ4 especially at higher protein concentrations. Generally, we were able to extract and purify YscFΔ4, Δ19YscFΔ4 and all the mutant proteins mainly because of this modification. It was also noticeable that polymerization rate was much slower in Y65A. Results from this work confirm a previous hypothesis (18) that differences exist in the electrostatic surfaces of the type III secretion needle proteins PrgI, BsaL, MxiH and YscF. Indeed YscF has a much higher theoretical pI (~7.77) compared to PrgI (4.76), BsaL (4.76) and MxiH (4.47). These three homologs are acidic and their electrostatic maps show large areas of negatively charged surfaces (18). The locations of negatively charged surfaces are reported

to be radically different among PrgI, BsaL, and MxiH (18). All these differences indicate that YscF needles might have a unique pattern of assembly. Despite the 30% sequence identity between YscF and both MxiH and BsaL, YscF might have some different polymerization characteristics. This opinion is also supported by Sun *et al.* (9) based on their reported YscEFG structure.

The CD spectrum shows that Y65FYscFΔ4 is a random coil and therefore not expected to form needles because it does not form α-helices that are essential for needle assembly. Most of the proteins we looked at show a high helical content. This is in line with the findings of Kenjale *et al.* (16) that show the importance of α-helix in T3SS needle formation. The high helical content is a common characteristic among the T3SS needle proteins like MxiH (50%) and PrgI (59%) (17). These values represent a significant loss in helical content because the studies were done at 25°C as opposed to 10°C that gave 53% (MxiH) and 69% (PrgI) (17). Such results show that lower temperatures promote/stabilize formation of α-helical structures. It may also mean that these proteins are relatively unstable especially at higher temperatures (17). We apply this principle (low temperatures) to induce *in vitro* needle formation because proper needle assembly requires α-helical structures.

Although the CD spectrum for N66AYscFΔ4 shows α-helical structures, the protein does not form needles *in vitro* like YscFΔ4 and other mutants. This mutant might be a monomer since it prevents needle assembly completely. Our YscF model shows these conserved residues (Y65, N66, K76, D77, I82, Q84 and F86) pointed away from the two helix bundle. We propose that these residues

are not needed in stabilizing the hydrophobic core of the two helix bundle because mutating them to alanine does not disrupt the α-helical structures. Needle assembly results also show that mutating these residues (K76A, D77A, I82A, Q84A and F86A) does not interfere with needle assembly. We propose that these conserved residues don't participate in needle monomer-monomer contact, but rather play a role in the interaction at the needle-base interface. Although Y65AYscFΔ4 forms needles, it slows down the process significantly.

One of our mutants, Y65AYscFΔ4 has tremendously slowed down the rate of polymerization. A combination of this mutation and lowering the pH to 5.5 has abolished oligomerization and prevented needle assembly by maintaining it as a dimer. The hydroxyl group of Y65 might be involved in hydrogen bonding that is destroyed in the mutant, thereby interfering with needle monomer-monomer contact. This is supported by evidence from another mutant, Y65FYscFΔ4 that we analyzed for more evidence. The resulting protein has much lower solubility and gives a CD spectrum corresponding to a random coil. The CD spectrum for this mutant supports the corresponding results from electron microscopy because a random coil structure cannot support needle formation. This highlights the importance of the hydroxyl group as opposed to just hydrophobic interaction. Residues Y65 and N66 might not be the only factors behind YscF oligomerization, but they seem to play an important role. Based on these results, it is possible that YscF needle formation depends on the electrostatic interaction between protein surfaces (YscF-YscF interactions), N66 and the hydroxyl group of Y65.

REFERENCES

1. Tamano, K., Aizawa, S., Katayama, E., Nonaka, T., Imajoh-Ohmi, S., Kuwae, A., Nagai, S. and Sasakawa, C. (2000) Supramolecular structure of the *Shigella* type III secretion machinery: the needle part is changeable in length and essential for delivery of effectors. *EMBO J* **19,** 3876-3887.

2. Blocker, A., Jouihri, N., Larquet, E., Gounon, P., Ebel, F., Parsot, C., Sansonetti, P. and Allaoui, A. (2001) Structure and composition of the *Shigella flexneri* "needle complex", a part of its type III secreton. *Mol Microbiol* **39,** 652-663.

3. Kimbrough, T. G. and Miller, S. I. (2000) Contribution of *Salmonella typhimurium* type III secretion components to needle complex formation. *Proc Natl Acad Sci USA* **97,** 11008-11013.

4. Kubori, T., Sukhan, A., Aizawa, S. and Galan, J. E. (2000) Molecular characterization and assembly of the needle complex of the *Salmonella typhimurium* type III protein secretion system. *Proc Natl Acad Sci USA* **97,** 10225-10230.

5. Cordes, F. S., Komoriya, K., Larquet, E., Yang, S., Egelman, E. H., Blocker, A. and Lea, S. M. (2003) Helical structure of the needle of the type III secretion system of *Shigella flexneri. J Biol Chem* **278,** 17103-17107.

6. Hoiczyk, E., and Blobel, G. (2001) Polymerization of a single protein of the pathogen *Yersinia enterocolitica* into needles punctures eukaryotic cells. *Proc Natl Acad Sci USA* **98,** 4669-4674.

7. Journet, L., Agrain, C., Broz, P., and Cornelis, G. R. (2003) The needle length of bacterial injectisomes is determined by a molecular ruler. *Science* **302,** 1757-1760.

8. Quinaud, M., Chabert, J., Faudry, E., Neumann, E., Lemaire, D., Pastor, A., Elsen, S., Dessen, A., and Attree, I. (2005) The PscE-PscF-PscG complex controls type III secretion needle biogenesis in *Pseudomonas aeruginosa*. *J Biol Chem* **280,** 36293-36300.

9. Sun, P., Tropea, J. E., Austin, B. P., Cherry, S., and Waugh, D. S. (2008) Structural characterization of the *Yersinia pestis* type III secretion system needle protein YscF in complex with its heterodimeric chaperone YscE/YscG. *J Mol Biol* **377,** 819-830.

10. Deane, J. E., Cordes, F. S., Roversi, P., Johnson, S., Kenjale, R., Picking, W. D., Picking, W. L., Lea, S. M., and Blocker, A. (2006) Expression, purification, crystallization and preliminary crystallographic analysis of MxiH, a subunit of the *Shigella flexneri* type III secretion system needle. *Acta Cryst* **62,** 302-305.

11. Zhang, L., Wang, Y., Picking, W. L., Picking, W. D. and De Guzman, R. N. (2006) Solution structure of monomeric BsaL, the type III secretion needle protein of *Burkholderia pseudomallei*. *J Mol Biol* **359,** 322-330.

12. Vonderviszt, F., Kanto, S., Aizawa, S. and Namba, K. (1989) Terminal regions of flagellin are disordered in solution. *J Mol Biol* **209,** 127-133.

13. Aizawa, S. I., Vonderviszt, F., Ishima, R. and Akasaka, K. (1990) Termini of *Salmonella* flagellin are disordered and become organized upon polymerization into flagellar filament. *J Mol Biol* **211,** 673-677.

14. Namba, K. (2001) Roles of partly unfolded conformations in macromolecular self-assembly. *Genes Cells* **6,** 1-12.

15. Torruellas, J., Jackson, M. W., Pennock, J. W., and Plano, G. V. (2005) The *Yersinia pestis* type III secretion needle plays a role in the regulation of Yop secretion. *Mol Microbiol* **57,** 1719-1733.

16. Kenjale, R., Wilson, J., Zenk, S. F., Saurya, S., Picking, W. L., Picking, W. D., and Blocker, A. (2005) The needle component of the type III secreton of *Shigella* regulates the activity of the secretion apparatus. *J Biol Chem* **280,** 42929-42937.

17. Darboe, N., Kenjale, R., Picking, W. L., Picking, W. D., and Middaugh, C. R. (2006) Physical characterization of MxiH and PrgI, the needle component of the type III secretion apparatus from *Shigella* and *Salmonella*. *Protein Science* **15,** 543-552.

18. Wang, Y., Ouellette, A. N., Egan, C. W., Rathinavelan, T., Im, W., and De Guzman, R. N. (2007) Differences in the electrostatic surfaces of the type III secretion needle proteins PrgI, BsaL, and MxiH. *J Mol Biol* **371**(5), 1304-1314.

19. Marlovits, T. C., Kubori, T., Sukhan, A., Thomas, D. R., Galan, J. E., and Unger, V. M. (2004) Structural insights into the assembly of the type III secretion needle complex. *Science* **306,** 1040-1042.

20. Espina, M., Olive, A. J., Kenjale, R., Moore, D. S., Ausar, S. F., Kaminski, R. W., Oaks, E. V., Middaugh, C. R., Picking, W. D., Picking, W. L. (2006)

IpaD localizes to the tip of the type III secretion system needle of *Shigella flexneri*. *Infect Immun* **74,** 4391-4400.

21. Jones, D. T. (1999) Protein secondary structure prediction based on position-specific scoring matrices. *J Mol Biol* **292,** 195-202.

22. McGuffin, L. J., Bryson, K., and Jones, D. T. (2000) The PSIPRED protein structure prediction server. *Bioinformatics* **16,** 404-405.

23. Karplus, K., Karchin, R., Barrett, C., Tu, S., Cline, M., Diekhans, M., Grate, L., Casper, J. and Hughey, R. (2001) What is the value added by humen intervention in protein structure prediction? *Proteins: Struct Funct Genet Suppl* **5,** 86-91.

24. Adamczak, R., Porollo, A., and Meller, J. (2005) Combining prediction of secondary structure and solvent accessibility in proteins. *Proteins: Struct Funct Genet* **59,** 467-475.

25. Altschul, S. F., Gish, W., Miller, W., Myers, E. W., and Lipman, D. J. (1990) Basic Local Alignment Search Tool. *J Mol Biol* **215,** 403-410.

26. Altschul, S. F., Madden, T. L., Schaffer, A. A., Zhang, J. H., Zhang, Z., Miller, W., and Lipman, D. J. (1997) Gapped BLAST and PSI-BLAST: a new generation of protein database search algorithms. *Nucl Acids Res* **25,** 3389-3402.

27. Notredame, C., Higgins, D. G., and Heringa, J. (2000) T-Coffee: a novel method for fast and accurate multiple sequence alignment. *J Mol Biol* **302,** 205-217.

28. Gouet, P., Robert, X., and Courcelle, E. (2003) ESPript/ENDscript: extracting and rendering seqeuence and 3D information from atomic structures of proteins. *Nucl Acids Res* **31,** 3320-3323.

29. Bradley, P., Chivian, D., Meiler, J., Misura, K. M., Rohl, C. A., Schief, W. R., Wedemeyer, W. J., Schueler-Furman, O., Murphy, P., Schonbrun, J., Strauss, C. E., and Baker, D. (2003) Rosetta predictions in CASP5: successes, failures, and prospects for complete automation. *Proteins* 53 Suppl **6,** 457-68.

30. Sambrook, J., Fritsch, E. F. and Maniatis, T. (1989) Molecular cloning. A laboratory manual. *Cold Spring Harbor Laboratory Press*, New York

31. Picking, W. L., Mertz, J. A., Marquart, M. E., and Picking, W. D. (1996) Cloning, expression, and affinity purification of recombinant *Shigella flexneri* invasion plasmid antigens IpaB and IpaC. *Protein Expr Purif* **8,** 401-408.

32. Laemmli, U. K. (1970) Cleavage of structural proteins during the assembly of the head of bacteriophage T4, *Nature (London)* **227,** 680-685.

33. Bradford, M. M. (1976) A rapid and sensitive method for the quantitation of microgram quantities of protein utilizing the principle of protein-dye binding. *Ana Biochem* **72,** 248-254.

34. Whitmore, L., and Wallace, B. A. (2004) DICHROWEB, an online server for protein secondary structure analyses from circular dichroism spectroscopic data. *Nucl Acids Res* **32,** W668-673.

35. Matson, J. S., Durick, K. A., Bradley, D. S., and Nilles, M. L. (2005) Immunization of mice with YscF provides protection from *Yersinia pestis* infections. *BMC Microbiology* **5,** 38.

CHAPTER 3

In vivo Analysis of the Functions of YscF Variant Proteins

ABSTRACT

The effect of YscF protein variants on YopQ secretion in *Yersinia pseudotuberculosis* was analyzed using GFP-YopQ18 and GFP-YopQ53 hybrid proteins. We transformed wild-type *Y. pseudotuberculosis* cells with a parent plasmid pYscF (YscF in pET22b) and each of 8 pYscF mutants to determine their effect on wild-type YopQ secretion. We used λ red recombinase, a helper plasmid to knock out the *yscF* gene from *Y. pseudotuberculosis* virulence plasmid pYV. The *yscF* $^{-}$ model resulting from complete deletion of the gene was used to analyze secretion. We used the same plasmids and mutants as described above to transform the YscF knockout model and analyze their effect on GFP-YopQ53 secretion. We detected and analyzed the secreted GFP-YopQ53 by Western blot using anti-GFP antibodies. Through this method, we have been able to identify anomalous phenotypes in secretion. We have combined results from these assays with those from chapter 2 of this thesis to identify two YscF mutants, Y65A and Y65F that display a dominant negative phenotype in wild-type *Y. pseudotuberculosis*. Based on our findings, we also propose that the conserved residue I82 of YscF may be involved in the interaction at the needle-base interface.

INTRODUCTION

Yersinia pathogens invade the eukaryotic system by binding to host cells (1) using different adhesion factors like invasin (2) and YadA (3). The adhesion factors used may vary depending on environmental conditions such as temperature. Efficient injection of *Yersinia* outer proteins (Yops) such as YopE and YopH into host cells requires the pathogens to properly stick to the target cells (1, 5). These pathogens use toxins to evade oxidative burst, phagocytosis and killing by polymorphonuclear leukocytes (6). In *Yersinia*, these virulence factors are encoded by a 70-kb plasmid called pYV (7, 8). Yops were historically called *Yersinia* outer membrane proteins at the time when they were believed to be strictly membrane proteins, but over time they have been identified as secreted proteins (9). Their secretion involves the use of Ysc (*Yersinia* secretion) structure that is encoded by the same virulence plasmid (9, 10). The Ysc system comprises many proteins including YscF (described in chapter 1 and 2 of this thesis), the needle protein that is essential for Yop secretion. Due to their environmental sensitivity, *Yersinia* can secrete toxins *in vitro* (culture medium) when Ca^{2+} is depleted from the medium at 37°C. *In vivo* (eukaryotic cell culture or mouse model) secretion is also turned on during contact with a eukaryotic cell. Regulation of these secretion genes is controlled mainly by the VirF factor (11).

Yersinia relies on YopE and YopH for evasion of phagocytosis (12) and Rosqvist *et al.* (13) have shown that lack of YopH leads to phagocytosis of pathogens by macrophages. Some secreted toxins have been shown to cause apoptosis in a cell-specific manner *in vitro* (14) whereas others are known to play

a critical role in preventing the oxidative burst of immune cells (15). Some Yops like LcrV, YopM, YopQ/YopK, and YopR are readily soluble in culture medium while others like YopH, YopE, YopO/YpkA, YopB, YopD, YopP/YopJ, and YopN/LcrE are insoluble (9). Under conducive environmental conditions, pathogens can secrete large amounts of toxins which vary in stability; the unstable ones can be broken down by proteases over a short period of time (16, 17). Most Yops including YopQ (9) that we use in this study have a minimum region necessary for secretion and translocation, e.g., the first 15 codons for YopN (18) and the first 17 codons for YopH (19). For this reason, secretion of most of the Yops is controlled by their N-terminal sequences. Another secretion signal based on chaperones has been described (20) in some Yops, although the short N-terminal sequence secretion signal is more important.

Translocation of Yops into target cells is unidirectional (polarized) in such a way that toxins are channeled into the host-cell cytosol (21). YopB and YopD bind host-cell membranes (22) to make the pore at the translocon and are believed to interact with LcrV (23), another regulatory protein involved in calcium response (24, 25). Due to regulation by LcrV, *in vitro* Yop secretion will only occur at 37°C in the absence of Ca^{2+} (Ca^{2+}- dependency) (26). It is believed that secretion and assembly of YopB and YopD at the translocon pore is regulated by LcrV; together, these three proteins play an important role in translocation of toxins to the target cell cytosol (22, 23). In *Yersinia*, YopQ/YopK (*Y. enterocolitica*/*Y. pseudotuberculosis*) control translocation (27) by regulating the pore size at the translocon (28).

Jacobi *et al.* (29) constructed truncated *yopE* (23 kDa cytotoxin) genes fused to *gfp* (encoding the green fluorescent protein) (30, 31) to study *yopE* gene expression and GFP-YopE hybrid protein translocation of *Y. enterocolitica* in cell culture and mouse infection models. Since full-length GFP is required for fluorescence, it was necessary to use only the minimum YopE sequence necessary for secretion and translocation. This enabled them to use a much smaller protein because the secretion and translocation signals of YopE are found within the first 53 residues. They used the low-copy-number plasmid pACYC184 for their GFP-YopE construct.

Their method was successful in applying *gfp* as a reporter gene for the study of protein translocation by protein T3SS and differential virulence gene expression *in vivo*. Other methods have used different reporter-gene technologies for the analysis of virulence gene expression of microorganisms (29). Such methods include the YopK–lacZ fusions (32) and luxAB operon fusions (33). However, these methods assay enzyme activity of the reporter-gene product, thereby limiting their use because they cannot be applied in: (i) live microorganisms or target cells and (ii) single bacterial cells (29). The use of GFP is more advantageous because it is more stable against shifts of pH, ionic strength or temperature (29). They used a conventional fluorescence microscope to detect GFP production. GFP fluorescence detection (unlike other reporter genes, for instance CAT, b-galactosidase or luciferase) does not require additional gene products or secondary substrates and occurs, with a few known exceptions, in a species-independent fashion (29). It has been shown that both

N- and C-terminal protein fusions remain fluorescent just like the native GFP (34).

Induction of *yopE* transcription and translocation was achieved by shifting the bacterial culture from 27°C to 37°C in a Ca^{2+}-depleted medium (29). However, their secretion assays showed that the amount of secreted GFP-YopE hybrid protein is less than that of YopE probably because GFP folds into its mature barrel structure of 24A° by 42A° in the cytosol (35). The formed barrel structure may be too large to pass the secretion pores hence accumulates in the cytoplasm whereas unfolded GFP-YopE may be predominantly secreted (29). They offered another possible explanation that binding of SycE (YopE chaperone) to GFP-YopE may be impaired. This would favor rapid maturation of GFP-YopE followed by degradation of the N-terminal secretion domain of YopE resulting in a secretion-deficient hybrid protein. Additional explanations pointed to the fact that a portion of GFP-YopE, which is not co-translationally secreted (36), will accumulate in the cytosol as protease-resistant GFP (29). Despite the difference in amounts of YopE and GFP-YopE secreted, this method remains the best for *in vivo* assays because the hybrid proteins are secreted in quantities large enough for complete assays.

Trček *et al.* (37) has studied YopQ (18 kDa) expression and secretion in different *Yersinia* strains using a similar method with a GFP-YopQ construct. While some toxins like YopE and YopN have a second chaperone-dependent secretion and translocation signal (38), YopQ secretion and translocation depends on one signal located within the first 53 N-terminal residues. Lack of a

chaperone-dependent signal in YopQ solves one of the problems experienced in the GFP-YopE secretion assays (29). While this construct showed a remarkable improvement, it should also be noted that Trcek *et al.* (37) could not demonstrate translocation of GFP-YopQ fusion protein into eukaryotic cells. This restricts the use of GFP-YopQ fusion protein to secretion assays alone.

Successful *in vivo* secretion assays require gene knockout models and Datsenko and Wanner (39) have developed a simple and highly efficient method to disrupt chromosomal genes in *Escherichia coli* in which PCR primers provide the homology to the targeted gene(s) (Figure 3.1). Unlike yeast and a few naturally competent bacteria, most bacteria are not readily transformable with linear DNA (39) because linear DNA is prone to degradation by intracellular exonucleases (40). In their method (Figure 3.1), a chromosomal sequence is replaced with a selectable antibiotic resistance gene that is generated by PCR using primers with 36- to 50-nt homology extensions (H1 and H2). This process (39) is accomplished by Red-mediated recombination in these flanking homologies. Following the antibiotic-mediated selection, the resistance gene is also eliminated by using a helper plasmid expressing the FLP (flippase) recombinase, which acts on the directly repeated FRT (FLP recognition target) sites flanking the resistance gene. The Red and FLP helper plasmids are cured by growth at 37°C because they are temperature-sensitive replicons (39). The Red system is used in this process because it has three genes: γ, ß, and *exo*, whose products are called Gam, Bet, and Exo, respectively (41). Gam inhibits

the host RecBCD exonuclease V so that Bet and Exo can gain access to DNA ends to promote recombination.

Here, we use GFP-YopQ secretion assays (37) to identify YscF mutants that affect Yop secretion in *Y. pseudotuberculosis*. We examine the effect of Y65A, Y65F, N66A, K76A, D77A, I82A, Q84A and F86A on GFP-YopQ secretion. We use a truncated *yopQ* (*Yersinia* outer protein Q) gene fused to *gfp* (encoding the green fluorescent protein) to study GFP-YopQ protein secretion in *Y. pseudotuberculosis.* Through homologous recombination, we used λ red recombinase to knock out the *yscF* gene from *Y. pseudotuberculosis* virulence plasmid pYV in a method (39) described elsewhere in this work. We used the *yscF*⁻ model resulting from complete deletion of the gene to analyze GFP-YopQ protein secretion. The parent plasmid pYscF (wild type) and each of the pYscF mutants mentioned above were individually transformed into the *yscF*⁻ model to reconstitute Yop secretion. We used this method to look for anomalous phenotypes in secretion, such as non-secreting by detecting GFP-YopQ secretion using Western blot analysis (42).

In this work, we show that introduction of some pYscF (YscF in pET22b) mutants to wild type *Y. pseudotuberculosis* leads to reduced GFP-YopQ53 secretion. We also report that GFP-YopQ53 secretion is not totally eliminated by knocking out the *yscF* gene from *Y. pseudotuberculosis*, but the *yscF*⁻ strain shows decreased secretion instead. Our work shows that some YscF mutants restore normal GFP-YopQ53 secretion in the YscF knockout while other mutants don't show similar restoration.

EXPERIMENTAL PROCEDURES

Site-directed mutagenesis. We used site-directed mutagenesis [QuikChange® XL Site-Directed Mutagenesis Kit (Stratagene)] to introduce the following mutations in the parent plasmid pYscF (*yscF* in pET22b): Y65A, Y65F, N66A, K76A, D77A, I82A, Q84A and F86A. Each of the listed forward primers (Table 3.1) was used in a PCR reaction (18 cycles of 50 s at 95 °C, 50 s at 50 °C and 5 min 30 s at 72 °C) with its complement that is not listed (mutant codons are underlined). The rest of the mutagenesis, DNA replication and plasmid isolation processes were done following the same procedure described in chapter 2 of this thesis. We used *E. coli* DH-5α (43) (Hanahan, 1983) as the primary host organism in mutagenesis. The correct mutants were verified by DNA sequencing (MSU genetics core facility).

Y. pseudotuberculosis Competent Cells and Electroporation. We obtained wild type *Y. pseudotuberculosis* cells (CB2587) from Dr. Michael Bagdasarian (MSU microbiology). The culture was incubated at 37°C overnight with shaking, then 2 mL of this starter culture was used to inoculate 100 mL LB medium. The culture was grown at 37°C to an OD_{600} of ~ 0.6; then it was chilled on ice for 30 minutes. Cells were pelleted at 4000 g for 15 minutes at 4°C and the supernatant discarded. The cells were resuspended in 40 mL sterile ice-cold ddiH_2O, then pelleted as described above. The supernatant was discarded and pellet resuspended in 40 mL of GYT medium (10% glycerol, 0.125% yeast extract and 0.25% tryptone). The cells were centrifuged again as described above, the

supernatant was discarded. The pellet was resuspended in 200 µL of GYT medium and immediately stored at -80°C.

We isolated the helper plasmid pKD119 (containing 3 helper genes, ß, γ and exo) from *E. coli* cells (CB2646 obtained from Dr. Bagdasarian) using the Qiagen (Hilden, Germany) plasmid-isolation kit. Electroporation process was done as follows: A 60 µL aliquot of the competent cells prepared as described above were added to an ice-chilled electroporation cuvette. Approximately 100 ng (1 µL) of the isolated pKD119 plasmid was added and thoroughly mixed with the cells. Electroporation was done on a Gene Pulser™ (BIO-RAD) at a voltage of 2.5 kV, resistance of 200 OHMS and capacitance of 25 µF. Shocked cells were added to 1 mL of LB medium containing 1 mM arabinose, then incubated at 30°C (pKD119 is temperature-sensitive) for 1 h before plating 100 µL onto LB agar containing 10 µg/mL tetracycline and 1 mM arabinose. The plate was incubated at 30°C for 30 h before selecting tetracycline-resistant transformants for preparation of new competent cells (named CB2588).

yscF knockout. The *PfuTurbo*® master mix (Stratagene) was used in the PCR reaction (30 cycles of 15 s at 94 °C, 45 s at 48 °C and 1 min 30 s at 68 °C) to amplify the chloramphenicol-resistance gene from a pKD3 plasmid template. The following primers with 36-nt homology extensions (underlined) (H1 and H2) (Figure 3.1) were used in the amplification process:

5′- <u>CCATTATTCATTATGTAGCAGGAGACCTAAAATAA</u>GTGTAGGCTGGAG

CTGCTTC - 3′ (forward)

5′- CTCTGCTAACAGTACGTTGAGTTTATATTTCATTTATGGGAATTAGCCAT

GGTCC - 3′ (reverse)

The PCR-amplified DNA was purified from the gel using the Qiagen (Hilden, Germany) gel-extraction kit, but DNA was eluted with sterile diH_2O instead of the elution buffer in the kit. Following DNA purification, *Dpn*I was added, then the sample was incubated at 37 °C for 1 h to digest any existing template plasmid that could contaminate the amplified DNA. The DNA was concentrated by ethanol precipitation as follows: Two microliters of pellet paint/co-precipitant was added, then 3 M sodium acetate was added (1/10 - v/v). The sample was mixed before adding cold 100% ethanol (twice the volume) followed by 20 minute centrifugation at 4°C (maximum speed on a microfuge). After the supernatant was discarded, the pellet was resuspended in cold 70% ethanol. After being centrifuged for 10 minutes at room temperature, the supernatant was discarded and the pellet air-dried for 30 minutes. The precipitated DNA was resolved in 10 µL of sterile diH_2O ready for electroporation. The *Y. pseudotuberculosis* strain containing the helper plasmid pKD119 (CB2588) was transformed with the amplified chloramphenicol-resistance gene (described above) following the same electroporation process as described above. The chloramphenicol-resistant transformants (named CB2754) were selected using 25 µg/mL chloramphenicol and made electrocompetent using the method described above. At this point, CB2754 is a *Y. pseudotuberculosis* strain that has lost the *yscF* gene (*yscF*$^-$), but still contains the helper plasmid (pKD119), meaning that this strain is both chloramphenicol- and tetracycline-resistant.

Eliminating the helper plasmid pKD119. After knocking out the *yscF* gene, the helper plasmid was eliminated. The *yscF* ⁻ *Y. pseudotuberculosis* strain (CB2754) containing the helper plasmid was grown in 10 mL LB medium containing 25 µg/mL chloramphenicol at 40°C overnight. Based on the OD_{600}, the cells were diluted by 10^6 before plating to get a good colony spread. The cells were plated on LB agar containing 25 µg/mL chloramphenicol, then incubated at 37°C for 30 h. Approximately 50 colonies were picked from the above plate and each used to patch onto two different plates, one tetracycline- and the other chloramphenicol-resistant. The two plates were labeled to enable matching for identification of colonies that had lost the helper plasmid. We picked strains that grew on the chloramphenicol plate, but did not survive tetracycline because they had lost the helper plasmid. The *yscF* knockout strain was confirmed by PCR in which the new *yscE-chloramphenicol-yscG* gene was amplified. For more confirmation, we did a PCR reaction using primers flanking the *yscF* gene to ensure that the *yscF* gene did not exist in the knockout. To ensure that the virulence plasmid pYV was not lost, another gene, *yopE* on the plasmid was also amplified. In each PCR reaction, a bacterial colony was picked and resuspended in 6 µL of H_2O followed by a 10 min heating at 94°C to provide the virulence plasmid template. Glycerol stock solution of the *yscF* knockout strain was prepared and stored at -80°C. The cells were also made electrocompetent ready for GFP-YopQ secretion studies.

GFP-YopQ secretion studies. The *GFP-yopQ* gene construct was designed in a low-copy-number plasmid pACYC184 that is resistant

chloramphenicol (42). We obtained two GFP-YopQ constructs from Dr. Jürgen Heesemann (Max von Pettenkofer-Institut - Munich, Germany) through Dr. Bagdasarian. The two constructs contain GFPmut2 (45, 46) that was generated by exchanging three amino acids (Ser-65 to Ala; Val-68 to Leu; Ser-72 to Ala) in its chromophore. The first construct, GFP-YopQ18 contains only the first 18 residues of YopQ while the second construct, GFP-YopQ53 has the first 53 residues of YopQ. The former can only be secreted, while the latter can be secreted and translocated into eukaryotic cells by *Y. enterocolitica* (37). Based on our preliminary assays in *Y. pseudotuberculosis*, GFP-YopQ18 secretion is low compared to GFP-YopQ53; hence, we use the former as a control in this study.

We carried out the first assay in wild-type *Y. pseudotuberculosis* strains to compare the secretion of both GFP-YopQ18 and GFP-YopQ53. The two constructs were used to transform wild-type *Y. pseudotuberculosis* cells (CB2587) in separate experiments screened by 25 µg/mL chloramphenicol. In each case, a single colony of the transformants was used to inoculate 20 mL of brain-heart infusion (BHI, Difco) medium with the following additives: 4.0 mM $CaCl_2$, 1.0 mM cysteine, 6.25 µg/mL Biotin (vitamin H), 0.5 mM histidine, 0.2 mM tryptophan and 16.0 mM $MgCl_2$. The cultures were grown at 28°C overnight after which the OD_{600} was determined for each culture. Approximately 500 µL (volumes were adjusted based on the recorded OD_{600} to ensure uniformity) of each sample was pelleted on a microfuge; after discarding the supernatant, the cells were resuspended in 500 µL of PBS buffer (pH 7.2). Each sample was

again pelleted and resuspended in fresh PBS buffer. Cells were plated on cellophane overlaid on BHI agar medium. The BHI medium used in making the plates had a different composition of additives compared to the previous BHI medium described above. The new medium had the following additives: 1.0 mM cysteine, 6.25 µg/mL Biotin (vitamin H), 0.5 mM histidine, 0.2 mM tryptophan and 16.0 mM $MgCl_2$. It was also supplemented with 0.2% glucose and 5 mM EGTA (Ca^{2+} depletion) to induce Yop secretion. The plates were incubated at 37°C for 24 hours. PBS buffer (2 mL) was poured onto each plate to wet the cells for easy scraping using a razor blade. Cells from each plate were resuspended in a total of 5 mL PBS buffer; the OD_{600} was determined for each sample before centrifugation. Each culture (before centrifugation – refered to as pellet) and supernatant was analyzed by SDS-PAGE and Western-blot using anti-GFP antibodies. During SDS-PAGE analysis, the amount of bacterial supernatant or pellet loaded was standardized/normalized based on the recorded OD_{600}. All samples were dissolved in a modified SDS sample buffer (37) consisting of 0.1 M $MgCl_2$, 4% SDS, 10% glycerol, 5% ß-mercaptoethanol, 0.001% bromophenol blue and 100 mM Tris/HCl, pH 9. Addition of $MgCl_2$ was necessary to precipitate DNA of whole-cell lysates (47). It was necessary to change the pH from 6.8 to 9 because this process eliminates hydrolysis of aspartyl-prolyl peptide bonds (48).

We analyzed the effect of each one of the 8 pYscF mutants on GFP-YopQ53 secretion in *Y. pseudotuberculosis* by transforming the cells (CB2587 - wild type) with each of the mutants separately. Cells were also transformed with the parent plasmid, pYscF to form a control for comparison with the mutants. In

each case, cells were grown and GFP-YopQ53 secretion induced as described in the method above. In each case, the pellet and supernatant was analyzed by SDS-PAGE and Western blot using anti-GFP antibodies.

The *yscF* knockout strain (CB2754) was transformed with each of the two constructs (GFP-YopQ18 and GFP-YopQ53) separately, but selection of transformants was more detailed because the knockout and GFP-YopQ constructs are resistant to chloramphenicol. We used SDS-PAGE and Western blot (anti-GFP antibodies) to identify the correct transformants. The two strains were made electrocompetent using the method described earlier in this work. By this point, we have two *yscF* knockout strains, one containing GFP-YopQ18 and the other containing GFP-YopQ53.

yscF reconstitution and the effect of 8 YscF mutants. The two *yscF* knockout strains described above were each transformed with the parent plasmid pYscF (*yscF* in pET22b plasmid) to reconstitute YscF. The GFP-YopQ53 containing strain was also transformed with each of the 8 pYscF mutants (described in site-directed mutagenesis above) separately. The right transformants were selected by 100 µg/mL ampicillin because pET22b is ampicillin-resistant. The aim is to compare each one of the mutant-reconstituted strains to the pYscF-reconstituted one. Cultures were grown for each strain and Yop secretion induced using the same method described earlier in this work. All samples were analyzed by SDS-PAGE and Western blot using anti-GFP antibodies.

Table 3.1. Oligonucleotides used to generate YscF mutants. Mutated codons are underlined.

Y65A	5′- AATAAATGGTCGGTAATTGCCAATATAAACTCAACCATA -3′
Y65F	5′- AATAAATGGTCGGTAATTUUCAATATAAACTCAACCATA -3′
N66A	5′- AAATGGTCGGTAATTTACGCTATAAACTCAACCATAGTT -3′
K76A	5′- ACCATAGTTCGTAGCATGGCAGACTTAATGCAAGGCATC-3′
D77A	5′- ATAGTTCGTAGCATGAAAGCCTTAATGCAAGGCATCCTA -3′
I82A	5′- AAAGACTTAATGCAAGGCGCCCTACAGAAGTTCCCATAA -3′
Q84A	5′- TTAATGCAAGGCATCCTAGCGAAGTTCCCATAATATGAA -3′
F86A	5′- CAAGGCATCCTACAGAAGGCCCCATAATATGAAATATAA -3′

RESULTS

Site-directed mutagenesis. Seven YscF conserved residues were each replaced with alanine in a similar method described in chapter 2. One of the residues, Y65, was also replaced with phenylalanine. However, there is a difference between the two cases because in chapter two the *yscF* gene was modified to *yscF*Δ4 to enable successful purification of the protein. In this chapter, we carry out site-directed mutagenesis on an untruncated *yscF* gene. We also have Q84A and F86A in this chapter, but in chapter 2, Q84 and F86 are cleaved off during the construction of *yscF*Δ4. Each mutant in this chapter has the full length *yscF* gene so that any observable changes in the analysis is due to the respective point mutation. All mutants were verified by DNA sequencing.

Y. pseudotuberculosis competent cells and electroporation. Previous YopQ secretion and translocation studies (29, 37) were performed in *Y. enterocolitica.* Here we present GFP-YopQ secretion study results from *Y. pseudotuberculosis*. We use *Y. pseudotuberculosis* because it shares greater than 90% DNA homology with *Y. pestis* and yet they differ in pathogenicity. They cause different diseases and are transmitted differently. *Y. pestis* is very dangerous and difficult to handle because it causes bubonic plague as mentioned in chapter 1, whereas *Y. pseudotuberculosis* is relatively safer to handle (see chapter 1). *Y. enterocolitica* is slightly more distant from the two species as mentioned in chapter 1. We therefore use *Y. pseudotuberculosis* instead of *Y. enterocolitica* as a good model to investigate secretion in *Y. pestis*.

Using the helper plasmid pKD119 required addition of 1 mM L-arabinose to the growth medium and temperatures had to be maintained at 30°C at all times. This helper plasmid was modified from pKD20 and pKD46 (39) that contain the λ, ß, and *exo* genes from phage λ. Therefore, all three plasmids have optimized ribosome-binding site for efficient translation of λ and they all express λ, ß, and *exo* from the arabinose-inducible *ParaB* promoter (39). The three plasmids are also temperature-sensitive thus, they are eliminated (cured) by growing cells at 40°C.

yscF knockout. We amplified the chloramphenicol-resistance gene by PCR and introduced 36-nt homology extensions (H1 and H2) (Figure 3.1) on both ends of the gene. The PCR product is 1103 bp long including the 72 bp extension. We opted not to eliminate the chloramphenicol-resistance gene after knocking out *yscF* because we use it for selection. It can easily be removed because it is flanked by the two FLP recognition targets (FRT) that are recognized by flippase recombinase (FLP). In such a process, the two target sites are joined together hence eliminating the chloramphenicol-resistance gene.

During the knockout process, chances of contamination by the template plasmid were minimized by extracting the PCR product right from the gel followed by a 1 h 37 °C *Dpn*I treatment. This eliminated possible contaminants and was verified by using *E. coli* strains as control because they lack pYV. The PCR product was concentrated through ethanol precipitation to enhance chances of recombination. Successful *yscF* knockout strains were verified by PCR using primers complementary to genes flanking the knockout region (YscE and YscG)

(Figure 3.2). These PCR analyses were performed alongside the wild type (CB2587) for comparison. Results show that the knockout process was successful because PCR results for the knockouts show the size of DNA corresponding to the new YscE-chloramphenicol-YscG (1570 bp) (Figure 3.2). In contrast, PCR results for the wild type cells show DNA corresponding to YscE-YscF-YscG (810 bp) (Figure 3.3). We tried knocking out *yscF* using both Kanamycin- and chloramphenicol-resistance genes, but the latter worked first, so we ended up with a new problem: The GFP-YopQ constructs were provided to us in a chloramphenicol-resistant plasmid, so we had to distinguish between the two strains during selection. We solved this problem by running an SDS-PAGE of the respective lysate followed by Western blot using anti-GFP antibodies.

Eliminating the helper plasmid pKD119. The helper plasmid was eliminated by growing the cells at 40°C. It is important to ensure that the virulence plasmid, pYV is not lost during the study. To ensure that pYV was not lost, another gene, *yopE* (657 bp) on the virulence plasmid was amplified by PCR (Figure 3.4).

GFP-YopQ secretion studies. We used two different constructs (GFP-YopQ18 and GFP-YopQ53) (Figure 3.5) to study YopQ secretion in *Y. pseudotuberculosis.* We started our preliminary work by comparing the secretion levels of the two constructs and results show that GFP-YopQ18 is secreted in very low (almost negligible) quantities compared to GFP-YopQ53 (Figure 3.6). In subsequent studies, we used GFP-YopQ18 as a control to show that all GFP-YopQ53 released in the medium is a result of secretion and not lysed cells. Both

proteins are well-expressed, as can be seen from the pellet samples analyzed by SDS-PAGE and Western blot (Figure 3.6). Both proteins are present in the pellet, but only YopQ53 is visible in the supernatant. Secretion of GFP-YopQ53 was successfully induced by addition of EGTA (Ca^{2+} depletion) because it is a better chelator of Ca^{2+} than EDTA. The amount of protein loaded during SDS-PAGE was normalized based on the OD_{600} therefore the difference in secretion can be clearly seen. To achieve consistency during SDS-PAGE analysis, we modified the sample buffer by changing the pH (37).

In their study, Jacobi *et al.* (42), monitored YopQ secretion in solution using anti-GFP antibodies. Their method involves concentrating of protein from large amounts of solution and TCA precipitation because the protein is secreted in very small quantities. We have designed an easier way of monitoring secretion in which secretion is enhanced tremendously. Instead of using solution BHI medium, we plate the cells on a cellophane covered agar plate. This approach minimizes the background noise caused by many small peptides found in the BHI medium. Secondly, since secretion is many orders of magnitude higher, concentration by TCA precipitation is unnecessary. The SDS-PAGE results are also clear like a Western blot, meaning that we can analyze with SDS-PAGE alone. Both GFP-YopQ constructs appear at approximately the same mass (Figure 3.6) because they are 28 kDa (GFP-YopQ18) and 32 kDa (GFP-YopQ53) in mass.

Secretion assay results show that introduction of two pYscF mutants, Y65A and Y65F to *Y. pseudotuberculosis* (wild type) leads to reduced GFP-

YopQ53 secretion (Figure 3.7). Each one of these two mutants has a negative impact on wild-type secretion. Other mutants don't show an effect on wild-type secretion. Based on our GFP-YopQ secretion assay results, it is evident that GFP-YopQ53 secretion is not totally eliminated after knocking out the *yscF* gene from *Y. pseudotuberculosis*, the knockout strain shows decreased secretion instead (Figure 3.8). Results also show that normal GFP-YopQ53 secretion is restored in YscF knockout following reconstitution by the pYscF plasmid. Normal secretion was also restored in the knockout by the following pYscF mutants: N66A, K76A, D77A, Q84A, and F86A. However, three pYscF mutants, Y65A, Y65F, and I82A did not restore normal secretion because their level of secretion is similar to the *yscF*$^-$ strain.

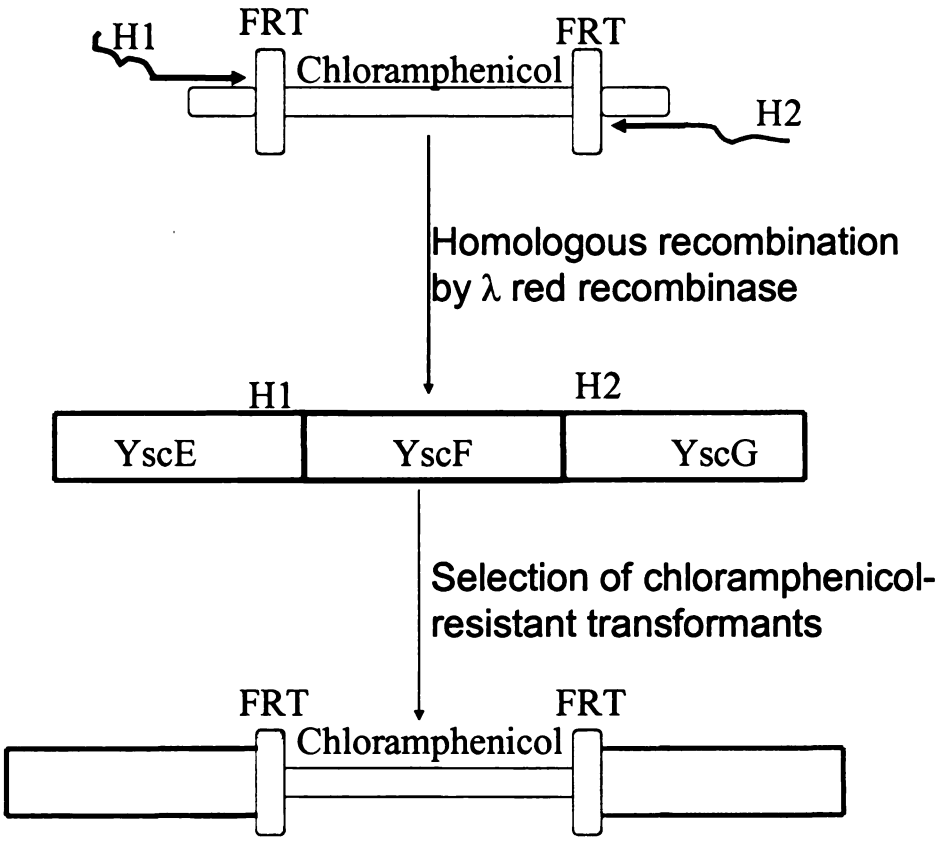

Figure 3.1. A simple gene disruption strategy. H1 and H2 refer to the homology extensions or regions.

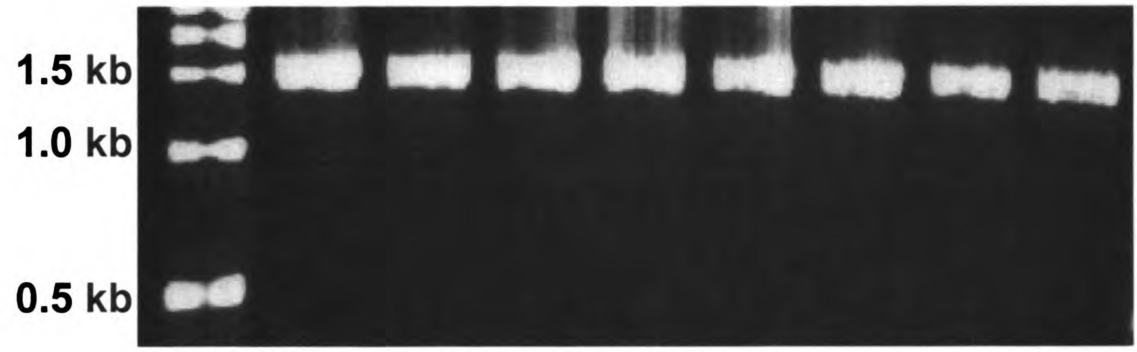

Figure 3.2. Verification of yscF knockout by PCR using primers complementary to genes flanking the knockout region (YscE and YscG). Results show the YscE-Chloramphenicol-YscG gene (1570 bp) from the knockout strain.

Figure 3.3. Verification of yscF knockout by PCR using primers complementary to genes flanking the knockout region (YscE and YscG). Results show the YscEFG gene (810 bp) from wild-type *Y. pseudotuberculosis.*

Figure 3.4. PCR amplification of the *yopE* gene (657 bp) from the *yscF* knockout strain to verify the presence of the virulence plasmid pYV.

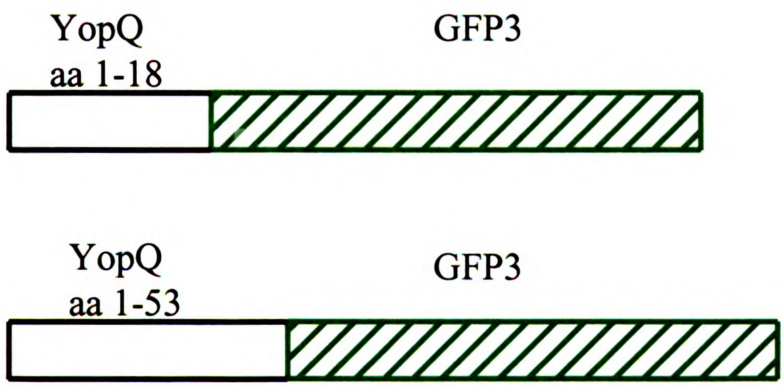

Figure 3.5. GFP-YopQ18 and GFP-YopQ53 constructs for *in vivo* secretion assays.

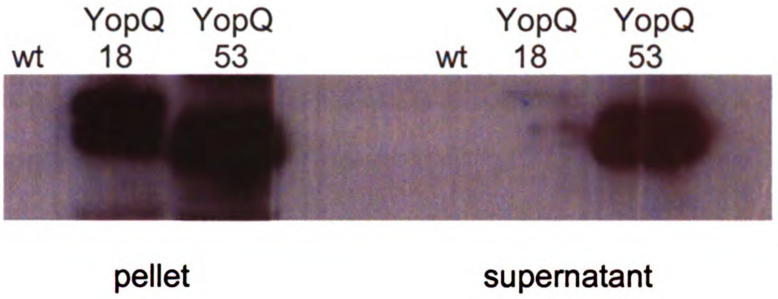

a

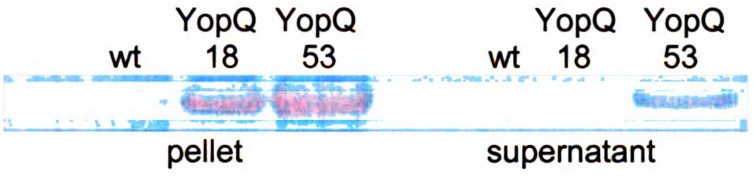

b

Figure 3.6. YopQ-GFP secretion assay results. (a) Western-blot using anti-GFP antibodies. (b) The same secretion assay analyzed by SDS-PAGE. YopQ18 is expressed, but not secreted.

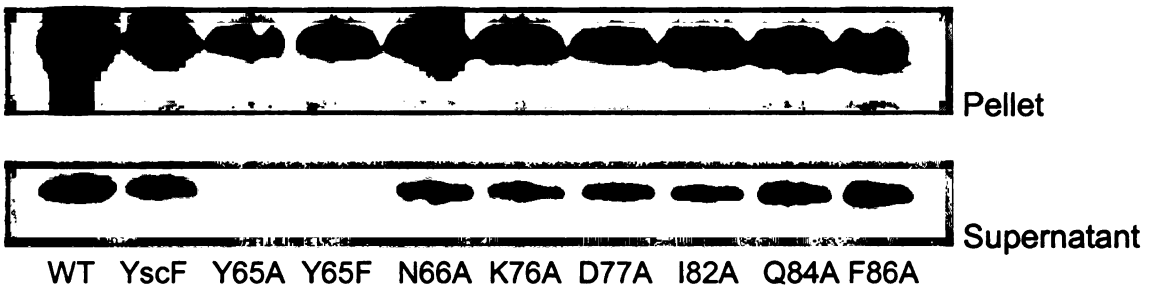

Figure 3.7. Western blot analysis of differential secretion. Secretion assays in the wild-type *Y. pseudotuberculosis.* Results show that introduction of two pYscF mutants, Y65A and Y65F to *Y. pseudotuberculosis* (wild type) leads to markedly reduced GFP-YopQ53 secretion.

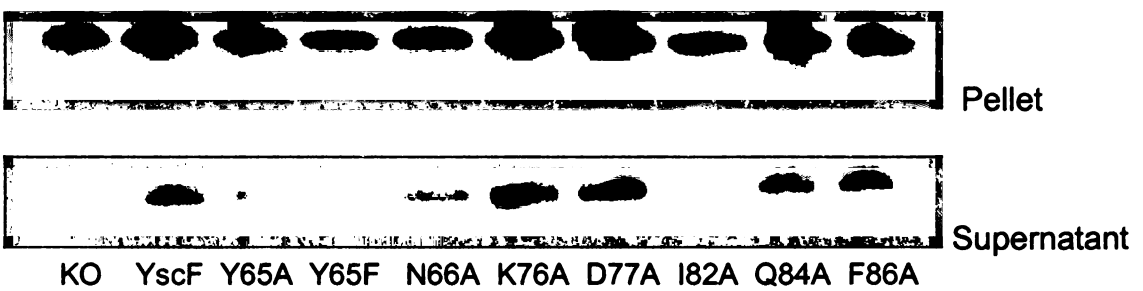

Figure 3.8. Complementation of the *yscF* knockout strain using YscF and different mutants. The knockout strain (lane 1) shows decreased secretion.

DISCUSSION

We have determined that modification of the SDS sample buffer was necessary based on previous studies (37, 42) because both YopQ and YopK have aspartyl-prolyl peptide bonds which are prone to hydrolyse during heating in Laemmli sample buffer due to low pH (48). Other Yop secretion studies (49) have used TCA precipitation to concentrate the secreted toxins because of the minute amounts secreted.

In the original design, Jacobi *et al.* (29) monitored secretion in solution using anti-GFP antibodies. Their method involves concentrating large amounts of solution and TCA precipitation because the protein is secreted in very small quantities. This process involves many steps and may compromise consistency. We have designed an easier way of monitoring secretion in which secretion is enhanced tremendously. Instead of using soluble BHI medium, we plate the cells on a cellophane-covered agar plate. Thus, we prevent background noise caused by many small peptides found in the BHI medium.

Secondly, concentration of secreted YopQ derivatives is higher because the protein remains on the cellophane membrane. It is possible to analyze just by simple SDS-PAGE or native gel electrophoresis. In this modified method, the process of concentrating protein by TCA precipitation is eliminated. By using our method, the protein can be recovered by cutting from the gel for further analysis by (for example) N-terminal sequencing and mass spectrometry. Our method provides a better way of concentrating cells and the secreted proteins. However,

it should be noted that some secretion assays can only be carried out in soluble medium.

Our study shows that GFP-YopQ53 is well secreted by *Y. pseudotuberculosis* in Ca^{2+}-depleted medium, but secretion of GFP-YopQ18 is negligible. This characteristic makes GFP-YopQ18 a good control because it is well-expressed, but not well secreted. Although we used YopQ constructs of *Y. enterocolitica* to assay secretion in *Y. pseudotuberculosis*, it is worth noting that YopK is the corresponding homolog in *Y. pseudotuberculosis.* It would be interesting to compare secretion of both YopQ and YopK in *Y. pseudotuberculosis.*

We have used the *yscF*$^-$ model resulting from complete deletion of *yscF* to analyze GFP-YopQ secretion. The parent strain pYscF (wild type) and each of the pYscF mutants were transformed into the *yscF*$^-$ model to determine their effect on GFP-YopQ secretion. This method enabled us to identify anomalous phenotypes in secretion (reduced secretion) caused by three mutants, Y65A, Y65F, and I82A.

While previous studies have focused mainly on secretion analysis, our study goes a step further by looking at both the *in vitro* and *in vivo* needle formation by YscF variant proteins. If a given mutant is able to form needles *in vitro* but prevents Yop secretion, then we propose that such a residue might participate in linking the needle to the base. Since YscF I82A assembles into needle-like structures *in vitro* but does not support secretion *in vivo*, it must assemble nonfunctional needles that are possibly unable to interact with other

components of injectisome such as the base. Two other mutants, Y65A and Y65F seem to interfere with secretion in the wild type and don't restore normal secretion in the knockout strains following reconstitution. These two mutants display dominant negative phenotypes because they decrease secretion in the wild-type cells. It is not clear whether residue Y65 interacts at the YscF-base interface because the corresponding mutant Y65A slows down *in vitro* needle assembly (chapter 2). This residue might be important for keeping the needle intact.

REFERENCES

1. Bliska, J. B., Guan, K. L., Dixon, J. E., and Falkow, S. (1991) Tyrosine phosphate hydrolysis of host proteins by an essential *Yersinia* virulence determinant. *Proc. Natl Acad Sci* USA **88,** 1187-1191.

2. Isberg, R. R., and Falkow, S. (1985) A single genetic locus encoded by *Yersinia pseudotuberculosis* permits invasion of cultured animal cells by *Escherichia coli* K-12. *Nature* (London) **317,** 262-264.

3. Yang, Y., and Isberg, R. R. (1993) Cellular internalization in the absence of invasin expression is promoted by the *Yersinia pseudotuberculosis yadA* product. *Infect Immun* **61,** 3907-3913.

5. Rosqvist, R., Forsberg, A., Rimpilaninen, M., Bergman, T., and Wolf-Watz, H. (1990) The cytotoxic protein YopE of *Yersinia* obstructs the primary host defence. *Mol Microbiol* **4,** 657-667.

6. Ruckdeschel, K., Roggenkamp, A., Schubert, S., and Heesemann., J. (1996) Differential contribution of *Yersinia enterocolitica* virulence factors to evasion of microbicidal action of neutrophils. *Infect Immun* **64,** 724-733.

7. Laroche, Y., Van Bouchaute, M., and Cornelis, G. (1984) A restriction map of virulence plasmid pVYE439-80 from a serogroup 9 *Yersinia enterocolitica* strain. *Plasmid* **12,** 67-70.

8. Datsenko, K. A., and Wanner, B. L. (2000) One-step inactivation of chromosomal genes in *Escherichia coli* K-12 using PCR products. *PNAS* **97,** 6640-6645.

9. Michiels, T., Wattiau, P., Brasseur, R., Ruysschaert, J. M., and Cornelis, G. (1990) Secretion of Yop proteins by yersiniae. *Infect Immun* **58,** 2840-2849.

10. Michiels, T., Vanooteghem, J. C., Lambert de Rouvroit, C. L., China, B., Gustin, A., Boudry, P., and Cornelis, G. R. (1991) Analysis of *virC*, an operon involved in the secretion of Yop proteins by *Yersinia enterocolitica*. *J Bacteriol* **173,** 4994-5009.

11. Lambert de Rouvroit, C. L., Sluiters, C., and Cornelis, G. R. (1992) Role of the transcriptional activator, VirF, and temperature in the expression of the pYV plasmid genes of *Yersinia enterocolitica*. *Mol Microbiol* **6,** 395-409.

12. Hanski, C., Kutschka, U., Schmoranzer, H. P., Naumann, M., Stallmach, A., Hahn, H., Menge, H., and Riecken, E. O. (1989) Immunohistochemical and electron microscopic study of interaction of *Yersinia enterocolitica* serotype O:8 with intestinal mucosa during experimental enteritis. *Infect Immun* **57,** 673-678.

13. Rosqvist, R., Bölin, I., and Wolf-Watz, H. (1988) Inhibition of phagocytosis in *Yersinia pseudotuberculosis*: a virulence plasmid-encoded ability involving the Yop2b protein. *Infect Immun* **56,** 2139-2143.

14. Mills, S. D., Boland, A., Sory, M. P., Van der Smissen, P., Kerbourch, C., Finlay, B. B., and Cornelis, G. R. (1997) *Yersinia enterocolitica* induces apoptosis in macrophages by a process requiring functional type III secretion and translocation mechanisms and involving YopP, presumably acting as an effector protein. *Proc Natl Acad Sci* USA **94,** 12638-12643.

15. Lian, C. J., and Pai, C. H. (1985) Inhibition of human neutrophil chemiluminescence by plasmid-mediated outer membrane proteins of *Yersinia enterocolitica*. *Infect Immun* **49,** 145-151.

16. Sodeinde, O. A., Sample, A. K., Brubaker, R. R., and Goguen, J. D. (1988) Plasminogen activator/coagulase gene of *Yersinia pestis* is responsible for degradation of plasmid-encoded outer membrane proteins. *Infect Immun* **56,** 2749-2752.

17. Sodeinde, O. A., and Goguen, J. D. (1988) Genetic analysis of the 9.5-kilobase virulence plasmid of *Yersinia pestis*. *Infect Immun* **56,** 2743-2748.

18. Anderson, D. M., and Schneewind, O. (1997) A mRNA signal for the type III secretion of Yop proteins by *Yersinia enterocolitica*. *Science* **278,** 1140-1143.

19. Sory, M. P., Boland, A., Lambermont, I., and Cornelis, G. R. (1995) Identification of the YopE and YopH domains required for secretion and internalization into the cytosol of macrophages, using the *cyaA* gene fusion approach. *Proc Natl Acad Sci* USA **92,** 11998-12002.

20. Cheng, L. W., Anderson, D. M., and Schneewind, O. (1997) Two independent type III secretion mechanisms for YopE in *Yersinia enterocolitica*. *Mol Microbiol* **24,** 757-765.

21. Rosqvist, R., Magnusson, K.-E., and Wolf-Watz, H. (1994) Target cell contact triggers expression and polarized transfer of *Yersinia* YopE cytotoxin into mammalian cells. *EMBO J* **13,** 964-972.

22. Håkansson, S., Bergman, T., Vanooteghem, J. C., Cornelis, G., and Wolf-Watz, H. (1993) YopB and YopD constitute a novel class of *Yersinia* Yop proteins. *Infect Immun* **61,** 71-80.

23. Sarker, M. R., Neyt, C., Stainier, I., and Cornelis, G. R. (1998) The *Yersinia* Yop virulon: LcrV is required for extrusion of the translocators YopB and YopD. *J Bacteriol* **180,** 1207-1214.

24. Bergman, T., Håkansson, S., Forsberg, A., Norlander, L., Macellaro, A., Backman, A., Bolin, I., and Wolf-Watz, H. (1991) Analysis of the V antigen *lcrGVH-yopBD* operon of *Yersinia pseudotuberculosis*: evidence for a regulatory role of LcrH and LcrV. *J Bacteriol* **173,** 1607-1616.

25. Perry, R. D., Harmon, P. A., Bowmer, W. S., and Straley, S. C. (1986) A low-Ca^{2+} response operon encodes the V antigen of *Yersinia pestis*. *Infect Immun* **54,** 428-434.

26. Brubaker, R. R. (1983) The Vwa1 virulence factor of yersiniae: the molecular basis of the attendant nutritional requirement for Ca11. *Rev Infect* Dis. **5**(Suppl. 4), S748-S758.

27. Holmström, A., Rosqvist, R., Wolf-Watz, H., and Forsberg, A. (1995) Virulence plasmid-encoded YopK is essential for *Yersinia pseudotuberculosis* to cause systemic infection in mice. *Infect Immun* **63,** 2269-2276.

28. Holmström, A., Pettersson, J., Rosqvist, R., Håkansson, S., Tafazoli, F., Fallman, M., Magnusson, K. E., Wolf-Watz, H., and Forsberg, A. (1997) YopK of *Yersinia pseudotuberculosis* controls translocation of Yop effectors across the eukaryotic cell membrane. *Mol Microbiol* **24,** 73-91.

29. Jacobi, C. A., Roggenkamp, A., Rakin, A., Zumbihl, R., Leitritz, L., and Heesemann, J. (1998) *In vitro* and *in vivo* expression studies of yopE from *Yersinia enterocolitica* using the gfp reporter gene. *Molecular Microbiology* **30**(4), 865-882.

30. Prasher, D. C., Eckenrode, V. K., Ward, W. W., Prendergast, F. G., and Cormier, M. J. (1992) Primary structure of the Aequorea victoria green-fluorescent protein. *Gene* **111,** 229-233.

31. Chalfie, M., Tu, Y., Euskirchen, G., Ward, W. W., and Prasher, D.C. (1994) Green fluorescent protein as a marker for gene expression. *Science* **263,** 802-805.

32. Pollack, C., Straley, S. C., and Klempner, M. S. (1986) Probing the phagolysosomal environment of human macrophages with a Ca^{2+}-responsive operon fusion in *Yersinia pestis*. *Nature* **322,** 834-836.

33. Forsberg, A., and Rosqvist, R. (1993) *In vivo* expression of virulence genes of Yersinia pseudotuberculosis. *Infect Agents Dis* **2,** 275-278.

34. Wang, S., and Hazelrigg, T. (1994) Implications for bcd mRNA localization from spatial distribution of exu protein in Drosophila oogenesis. *Nature* **369,** 400-403.

35. Ormö, M., Cubitt, A. B., Kallio, K., Gross, L. A., Tsien, R. Y., and Remington, S. J. (1996) Crystal structure of the Aequorea victoria green fluorescent protein. *Science* **273,** 1392-1395.

36. Anderson, D. M., and Schneewind, O. (1997) A mRNA signal for the type III secretion of Yop proteins by Yersinia enterocolitica. *Science* **278,** 1140-1143.

37. Trcek, J., Wilharm, G., Jacobi, C. A., and Heesemann, J. (2002) *Yersinia enterocolitica* YopQ: strain-dependent cytosolic accumulation and post-translational secretion. *Microbiology* **148,** 1457-1465.

38. Cheng, L. W., Anderson, D. M. & Schneewind, O. (1997). Two independent type III secretion mechanisms for YopE in *Yersinia enterocolitica*. *Mol Microbiol* **24,** 757-765.

39. Datsenko, K. A., and Wanner, B. L. (2000) One-step inactivation of chromosomal genes in Escherichia coli K-12 using PCR products. *PNAS* **97,** 6640-6645.

40. Lorenz, M. G., and Wackernagel, W. (1994) Bacterial gene transfer by natural genetic transformation in the environment. *Microbiol Rev* **58,** 563-602.

41. Murphy, K. C. (1998) Use of Bacteriophage λ Recombination Functions To Promote Gene Replacement in *Escherichia coli J Bacteriol* **180,** 2063-2071.

42. Jacobi, C. A., Roggenkamp, A., Rakin, A., Zumbihl, R., Leitritz, L., and Heesemann, J. (1998) In vitro and in vivo expression studies of yopE from Yersinia enterocolitica using the gfp reporter gene. *Mol Microbiol* **30,** 865-882.

43. Hanahan, D. (1983). Studies on transformation of *Escherichia coli* with plasmids. *J Mol Biol* **166,** 557-580.

44. Davis, R. W., Botstein, D., and Roth, J. R. (1980). *Advanced Bacterial Genetics. A Manual for Genetic Engineering.* Cold Spring Harbor, NY: Cold Spring Harbor Laboratory.

45. Heim, R., Prasher, D. C., and Tsien, R.Y. (1994) Wavelength mutations and posttranslational autoxidation of green fluorescent protein. *Proc Natl Acad Sci USA* **91,** 12501-12504.

46. Cormack, B. P., Valdivia, R. H., and Falkow, S. (1996) FACSoptimized mutants of green fluorescent protein (GFP). *Gene* **173,** 33-38.

47. Chen, M. and Christen, P. (1997) Removal of chromosomalDNA by Mg^{2+} in the lysis buffer: an improved lysis protocol for preparing *Escherichia coli* whole-cell lysates for sodium dodecyl sulfatepolyacrylamide gel electrophoresis. *Anal Biochem* **246,** 263-264.

48. Cannon-Carlson, S. and Tang, J. (1997). Modification of the Laemmli sodium dodecyl sulfate-polyacrylamide gel electrophoresis procedure to eliminate artifacts on reducing and nonreducing gels. *Anal Biochem* **246,** 146-148.

49. Heesemann, J., Gross, U., Schmidt, N., and Laufs, R. (1986). Immunochemical analysis of plasmid-encoded proteins released by enteropathogenic *Yersinia* sp. grown in calcium defficient media. *Infect Immun* **54,** 561-567.

50. Cornelis, G. R., Boland, A., Boyd, A. P., Geuijen, C., Iriarte, M., Neyt, C., Sory, M., and Stainier, I. (1998) The Virulence Plasmid of *Yersinia*, an antihost genome. *Microbiology and Molecular Biology Reviews* **62,** 1315-1352.

Chapter 4

Conclusions and Remaining Questions

CONCLUSIONS AND REMAINING QUESTIONS

The studies presented in this thesis aimed to identify YscF point mutants that affect GFP-YopQ secretion in *Yersinia pseudotuberculosis* without affecting *in vitro* YscF needle assembly. These results were used to identify YscF residues that are likely to be involved in the interactions at the needle-base interface in *Yersinia* type III secretion system. Secretion and translocation of Yops into target cells by the *Yersinia* T3SS requires proper assembly of the needle and the base. The interaction between these two structures of the T3SS depends on residues at the interface.

Previous studies have focused mainly on secretion analysis, but our work went a step further by looking at both the *in vitro* needle assembly and Yop secretion. If a particular YscF mutant is able to form needles *in vitro* but prevents Yop secretion, then we propose that the mutated residue might be involved in the interactions at the needle-base interface. We performed a detailed analysis of YscF sequence conservation, predicted secondary structure and homology modeling based on the published structures of YscEFG complex (1), MxiH (2), BsaL (3), and PrgI (4). From that preliminary analysis, our study focused on seven YscF residues: Y65, N66, K76, D77, I82, Q84 and F86.

In chapter 2, we performed a structural analysis of YscF (YscFΔ4) and its *in vitro* needle assembly studies by a combination of secondary-structure prediction, homology modeling, electrophoresis, mutagenesis, circular dichroism spectroscopy, and transmission electron microscopy. We performed a similar study on 8 YscF point mutants: Y65A, Y65F, N66A, K76A, D77A, I82A, Q84A

and F86A. Results show that all mutants have α-helical secondary structures except Y65F, which appears to be unstructured. Six mutants were able to assemble into needles *in vitro*, but Y65F and N66A did not. The needle-assembly process was much slower for Y65A compared to the rest of the mutants. Lowering the pH from 8.0 to 5.5 prevented needle formation in Y65A. We have also shown that the N-terminal region of YscF does not participate in needle formation. A similar finding had been reported earlier for MxiH and PrgI (2, 4).

Chapter 3 uses GFP-YopQ53 to study secretion in *Y. pseudotuberculosis.* A *yscF*$^-$ knockout model was created through homologous recombination using λ red recombinase to be used for this study. The parent plasmid pYscF (wild type) and each of the pYscF mutants were separately transformed into the *yscF*$^-$ strain to reconstitute secretion and monitor their effect on GFP-YopQ secretion. A similar study was carried out to monitor the effect of pYscF and its mutants on secretion in the wild-type *Y. pseudotuberculosis*.

This method enabled us to identify anomalous phenotypes in secretion (reduced secretion) caused by three mutants, Y65A, Y65F, and I82A. These mutants failed to restore normal secretion in the *yscF*$^-$ strain following reconstitution. Results also show that secretion was not totally abolished in the *yscF*$^-$ strain as some GFP-YopQ53 was detected by Western blot. Two mutants, Y65A and Y65F, showed a semi-dominant negative phenotype because they lead to a significant reduction in secretion when transformed into wild-type *Y. pseudotuberculosis*. Results also show that N66A abolished needle polymerization, but allowed secretion.

By comparing results from chapter 2 and chapter 3, we propose that the YscF residue I82 might be involved in the interaction at the needle-base interface. These results contribute to a better understanding of the structure and assembly of the *Yersinia* T3SS. Such insight is useful because in the T3SS, needles are a good target for vaccine development.

Some questions are still unanswered about YscF, the needle-formation process and *Yersinia* T3SS in general. Here, I propose some experiments that could help in elucidating the YscF structure and understanding T3SS further.

a. Self-polymerization remains the biggest hinderance to solving the YscF atomic structure. Unlike MxiH and PrgI structures that were solved following C-terminal modification, YscF still shows some polymerization after this modification. However, my work has shown that replacing residue Y65 with alanine can stop polymerization of YscFΔ4 at pH 5.5. The lower pH maintains this protein as a dimer based on my results from analytical gel filtration. Since the CD results show that the protein is folded, it might be possible to solve the atomic structure through crystallography or by solution NMR. The homology model shows residue Y65 pointing away from the two-helix bundle, therefore it might not be involved in folding of the monomer, but participates in YscF self-polymerization. This mutant could be useful in solving the YscF structure.

b. Results of this work show that mutant N66A prevented *in vitro* needle formation. This mutant is α-helical based on the CD results. Its quaternary structure should be analyzed by analytical gel filtration with the possibility of using it for structural determination.

c. Secretion studies have shown that both Y65A and Y65F display semi-dominant negative phenotypes. An *in vitro* needle assembly study should be performed by mixing Y65F with the wild type YscF in equal proportions. The i*n vitro* needle assembly process can then be induced to assess the effect it has on YscF needle assembly. This study can confirm the dominant negative characteristics of this mutant if it prevents wild-type YscF needle assembly. We choose not to use Y65A in this study because it formed needles *in vitro* albeit at a very slow rate. An *in vivo* needle assembly assay should also be carried out by separately introducing each mutant plasmid into the wild-type *Y. pseudotuberculosis* as described in chapter 3. However, needle formation in this case should be analyzed by transmission electron microscope instead of assaying for secretion. Thus, formed needles can be visualized.

d. Secretion study results show that knocking out YscF did not completely abolish secretion, as GFP-YopQ53 was detected by Western blot in the *yscF*$^{-}$ knockout model. The detected secretion might be caused by an alternative secretion system or it could be due to leaking of the GFP-YopQ53 protein as it accumulates in the bacterial cytosol following induction (Ca^{2+}-depletion). An *in vivo* needle formation assay should be carried out by inducing secretion in the *yscF*$^{-}$ model. The growth solution should be analyzed for presence of

needles using transmission electron microscopy. Alternatively, presence of YscF can be analyzed by Western blot using anti-YscF antibodies. If needles form and/or YscF is detected, this will mean that an alternative YscF gene exists in addition to the one on the virulence plasmid.

REFERENCES

1. Sun, P., Tropea, J. E., Austin, B. P., Cherry, S., and Waugh, D. S. (2008) Structural characterization of the *Yersinia pestis* type III secretion system needle protein YscF in complex with its heterodimeric chaperone YscE/YscG. *J Mol Biol* **377,** 819-830.

2. Deane, J. E., Cordes, F. S., Roversi, P., Johnson, S., Kenjale, R., Picking, W. D., Picking, W. L., Lea, S. M., and Blocker, A. (2006) Expression, purification, crystallization and preliminary crystallographic analysis of MxiH, a subunit of the *Shigella flexneri* type III secretion system needle. *Acta Cryst* **62,** 302-305.

3. Zhang, L., Wang, Y., Picking, W. L., Picking, W. D. and De Guzman, R. N. (2006) Solution structure of monomeric BsaL, the type III secretion needle protein of *Burkholderia pseudomallei*. *J Mol Biol* **359,** 322-330.

4. Wang, Y., Ouellette, A. N., Egan, C. W., Rathinavelan, T., Im, W., and De Guzman, R. N. (2007) Differences in the electrostatic surfaces of the type III secretion needle proteins PrgI, BsaL, and MxiH. *J Mol Biol* **371**(5), 1304-1314.

5. Matson, J. S., Durick, K. A., Bradley, D. S. and Nilles, M. L. (2005) Immunization of mice with YscF provides protection from *Yersinia pestis* infections. *BMC Microbiology* **5,** 38.